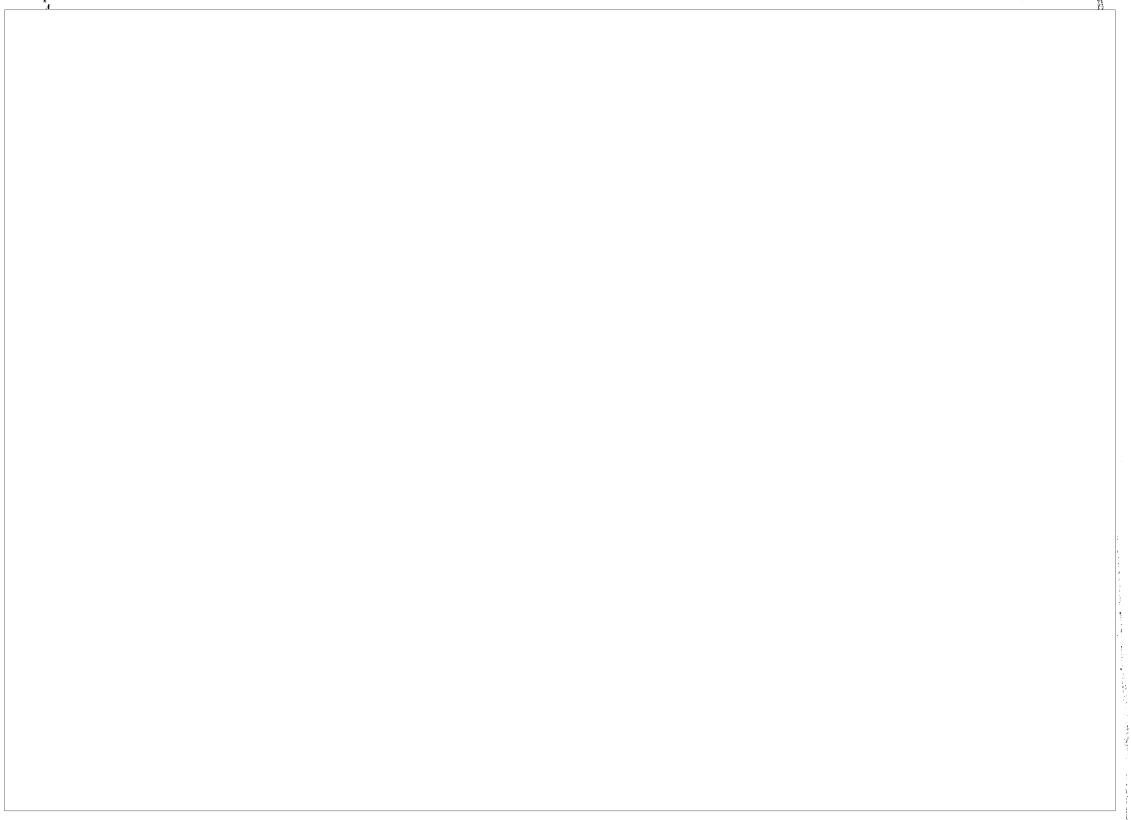

STAT

Generation of Decimeter and Centimeter Waves

By: V. I. Kalinin

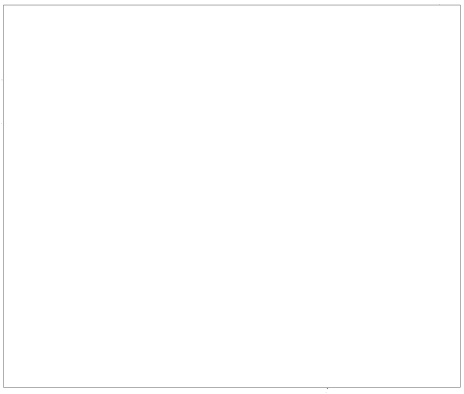

STAT

CHAPTER V

DYNAMICALLY CONTROLLED ELECTRON STREAMS

1. The Principles of Phase Focusing of an Electron Stream

We have already noted (Paragraph 2.3) that the principles of dynamic control of an electron stream consists in the action of a rapidly alternating electric field on electrons possessing a considerable velocity V_o acquired through the action of the accelerating constant potential U_o. The individual electrons or groups of electrons that are subject to the action of the various phases of the alternating field acquire various velocities and form regions of increased electron density in space, owing to the faster electrons overtaking and passing the slower ones. The current or charge densities produced in the stream at the places of "overtaking" may be many times as high as the initial values that characterized the stream on its emission from the cathode. Thus, the dynamic control of the electron stream, which aims at creating considerable densities in the stream by the mutual variation of its individual parts, is subdivided into two basic processes: (a) what is termed "velocity modulation", or the variation of the velocity of individual electron-groups under the influence of a high-frequency alternating field; and (b) "density modulation", or the formation of condensations in the further course of the motion of the stream.

Detailed consideration of the dynamic control of the electron stream from the very interesting and fruitful viewpoint of "phase focusing" was first given by Brüche and Recknagel /1/. By drawing an analogy between the behavior of a pencil of light rays focused

by a lens and an electron stream controlled by a gap with a high-frequency electric field ("phase lens"), the following picture (Figure 5.1) may be imagined. A parallel beam of rays leaving diaphragm D encounters the lens L on its path and at a certain distance from it, at the point F, the rays of the beam meet at a focus (Figure 5.1a). Let us compare Figure 5.1b with this; an electron

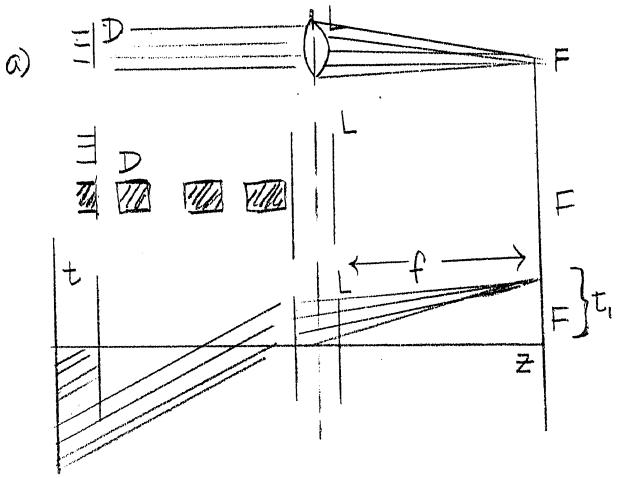

Figure 5.1

beam, consisting of a uniform sequence of electrons with equal velocities, moves from left to right through diaphragm D, which acts like the shutter of a camera to cut out of the stream a series of electron-groups of uniform length ("packets"). The length of each group and the time of its passage past an observer at rest are equivalent to the breadth of the beam in the optical example. This sequence of "electron-packets" passes through the space L -- the "phase lens" -- in which an electric field is concentrated, which varies in time and is parallel to the direction of the electron stream. The field at L varies in such a way that at the mo-

ment the first electrons of any packet reach the field L, that field will be oriented so as to retard these electrons, which will consequently leave the field at somewhat lower velocities than their initial velocities. On the other hand, the last electrons of the packet dall into a field that accelerates them, and therefore will emerge from the field at velocities higher than their initial velocities. The electron packets thus become gradually denser as they travel on, since the electrons moving in the rear overtake those moving in the front, and at a certain distance f a "focusing" occurs: the electron-packet under consideration is transformed into an infinitely thin sheet, and all its constituent electrons then lie in the same plane.

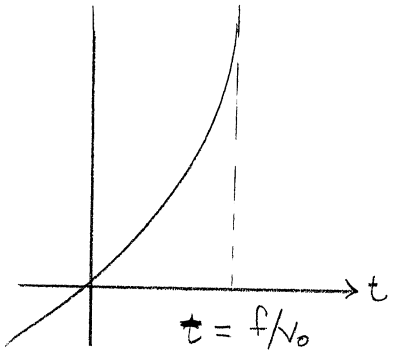

Figure 5.2

This process may be illustrated by the time-distance diagram of electron movement in Figure 5.1b, where the time is laid off along the vertical axis. Up to the "phase lens", a pencil of parallel lines corresponds to the electrons, and the slope of these lines defines the velocity of the electrons. After reaching the

phase lens, the slope of the lines (and consequently also the velocities of the electrons) is varied so that they all intersect at the point F.

The character of phase focusing obviously depends on the law of variation for the electric field in the phase lens. If the electron-packets are very short, then their focusing will occur under a linear law of variation of the field in the phase lens.

If the electron-packets are very long, which case corresponds to a very broad pencil in optics, a field varying by a linear law will not yield good focusing results. In this case the potential of the field should vary according to the law:

$$U = \frac{mv_o^2}{2e}\left[\frac{1}{\left(1 - \frac{v_o t}{f}\right)^2} - 1\right] \qquad (5.1)$$

where v_o is the velocity of the "middle" of the electron packet passing through the "optical center" of the phase lens. The graph U(t), constructed according to equation (5.1) is presented in Figure 5.2. It will be seen that an electron traversing the lens at time $t = 0$ does not experience the influence of the field. An electron traversing it at time $t = f/v_o$ must experience an infinitely great velocity-increment to overtake the other electrons at the focus. For the electrons still farther behind, all consideration is devoid of meaning, since it is impossible to focus electrons that pass through the field only when those that have already traversed it have been focused. It is clear that the longer the focal

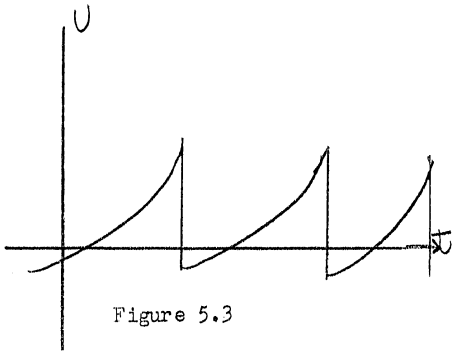

Figure 5.3

length and the lower the electron velocity, the longer the electron-packet that can be focused.

The process of phase focusing of an electron stream thus enables us to transform an uninterrupted electron stream of low intensity into a series of separate pulses of considerably greater intensity. The degree of intensification obviously depends on how well the focusing proceeds. If the course of the potential at the phase lens represented a periodic repitition of the curve defined by equation (5.1) (Figure 5.3), then the electron stream could be transformed almost completely into periodic surges of great density at the focus. However, it is still impossible to obtain the desired course of the potential at UHF, and consequently the attainment of full focusing of the stream cannotbbe expected.

The "incomplete" phase focusing of the electron stream that is obtained with any law of variation in intensity at the phase lens, other than that described by equation (5.1), may be imagined as follows. An uninterrupted electron stream passing through the phase lens may be represented in the form of a sequence of short

electron-packets moving one after the other. The variation in the potential during the passage of each of these packets may be represented as linear (a segment of the tangent to the actual variation in the potential at the given point). The velocity of the "middle" electron of each packet will, of course, vary from packet to packet in accordance with the law of the variation in the potential. We must deal then not with a single focus, but with a whole "caustic", to use an optical term. Each electron packet will be focused at a definite distance from the phase lens, as a result of which there will be a whole sequence of successive foci in space and in time, which may be represented as the displacement of one or more focal condensations /uplotneniya/ along the electron stream, which displacement takes place according to a definite law. For a detailed study of the focusing of the stream in this case, the concepts of the "locus of the foci" and the "trajectory of the foci" must be plotted on time-distance diagrams.

Following the fairly numerous works devoted to the problems of phase focusing, let us analyze this phenomenon more in detail /2-8/. Let us leave in force the usually employed restrictions:

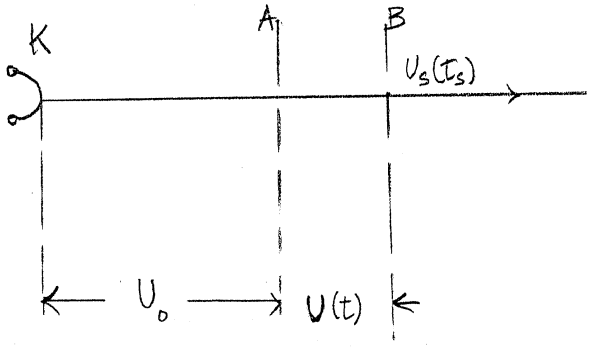

Figure 5.4

(a) We neglect the interaction of the electrons in the stream;

(b) We neglect the statistical distribution of electron velocities;

(c) We consider the time of transit through the field of the velocity modulator (the phase lens) as very small in comparison with the period of variation in the velocity.

Taking these simplifications into account, let us imagine an uninterrupted electron stream that arrives from a uniformly emitting cathode at the zone of acceleration KA (Figure 5.4). The grids A and B, carrying the high accelerating potential U_o, are connected to a source of alternating VHF voltage, so that the difference of potential between them varies according to some law U(t). If the middle electron of any packet passes through the field of the pahse lens (velocity modulator) AB, with velocity v, at the moment of time t = 0, when the alternating potential is equal to zero, then another electron, passing later by the interval dt, will transverse the field under the action of the potential

$$dU = \frac{\partial U}{\partial t}\, dt \tag{5.2}$$

The new velocity v_1 may be found from the law of conservation of energy

$$\frac{mv_1^2}{2} = \frac{mv^2}{2} + \frac{\partial U}{\partial t}\, edt$$

or

$$v_1^2 = v^2 + \frac{\partial U}{\partial t}\,\frac{2e}{m}dt. \tag{5.3}$$

Let

$$D = \frac{\partial U}{\partial t}\frac{e}{m} = v\frac{dv}{dt}$$

Then

$$v_1^2 = v^2 + 2Ddt.$$

Or

$$v_1 = v\left(1 + \frac{2Ddt}{v^2}\right)^{\frac{1}{2}} \approx v\left(1 + \frac{Ddt}{v^2}\right) \tag{5.4}$$

Then the path x, over which the second electron passes up to time t, after leaving the modulator, is equal to

$$x = v_1(t - dt) = v\left(1 + \frac{Ddt}{v^2}\right)t\left(1 - \frac{dt}{t}\right) =$$

$$= vt\left[1 + dt\left(\frac{D}{v^2} - \frac{1}{t}\right)\right]. \tag{5.5}$$

The determination of the focal length x_F reduces down to the determination of that value of x which shall be independent of dt, that is, of the moment of passage of the electron through the modulator. The condition for this is obviously that

$$\frac{D}{v^2} - \frac{1}{t} = 0.$$

Here $t = t_f$, the time when focus is attained, and, consequently, $x_F = vt_f$; consequently

$$\frac{1}{x_F} = \frac{D}{v^2} \tag{5.6}$$

But since $D = v\frac{dv}{dt} = \frac{e}{m} \cdot \frac{dU}{dt}$, then the "focal length x_F" may be expressed as

$$x_F = \frac{v^2}{D} = \frac{v^2}{dv/dt} = \frac{v^3}{\frac{e}{m} \cdot \frac{dU}{dt}} \qquad (5.7)$$

These expressions are true for any law of variation of potential and velocity with the time.

In the subsequent discussion the following notation will be consistently employed: t_s -- the instant or time the electron starts to leave the modulator (in passing through the plane $x = 0$); v_s -- the velocity corresponding to this moment; t -- the current time (instant); t_f -- the instant of focus; $\uparrow t$ the time interval taken to travel any distance, for example, $\uparrow_f$, the time between leaving the modulator and focus, and x -- the distance from the modulator.

5.2 General Relationships

Let us imagine an uninterrupted electron stream, arriving at the modulator (Figure 5.4) with the velocity v_o. At its exit from the modulator, the velocities of the individual electron packets are distributed according to some periodic law $v_s(t_s)$. Taking these simplifications into account, we shall suppose that each of the electron packets carries the same charge dq, and let us follow up the deformation of these packets during their subsequent motion. Each packet is naturally subject to the law of conservation of charge, and consequently

$$dq = \text{constant} \qquad (5.8)$$

for any point on the path and for any time, but the length of the packet, in consequence of the difference in the velocities of the electrons that compose it, changes. The general re-

lationships that characterize this variation of length, may also be used as the foundation of the study of the properties of a velocity-modulated electron-stream. If any given packet dq leaves the modulator during a certain definite time-interval t_s, then by virtue of (5.8) we may write, for unit cross-section area of the stream

$$j_o dt_s = j_x dt_x \tag{5.9}$$

where j_o is the current density produced by the electron packet in question at the instant it leaves the modulator, while j_x and dt_x are respectively the current density and the time interval that characterize the passage of this same packet through a point located at distance x from the modulator. By virtue of assumption (c) the value of j_o may be considered constant and determined by the cathode emission (allowing for that part of the current absorbed by the modulator grids); and the quantity j_x may be expressed as

$$j_x = j_o \left| \frac{1}{\frac{dt_x}{dt_s}} \right| \tag{5.10}$$

If the transit time τ_x from the modulator to the given point be taken so that

$$t_x = t_s + \tau_x,$$

then the current density at any point of the electron stream will be represented in the following manner:

$$j_x = j_o \left| \frac{1}{1 + \frac{d\tau_x}{dt_s}} \right| \tag{5.11}$$

The expressions (5.10) and (5.11) are true for all laws of variation of the modulating field intensity, and no matter what the subsequent fate of the electron stream is to be. The latter is obviously determined by the electrical conditions of the space beyond the modulator.

In the preceding section we assumed that the electrons moved by their inertia after their exit from the modulator. In specific apparatus, however, this is not necessarily the case: on leaving the modulator, the electron stream may impinge on a retarding or accelerating electric field, sometimes in combination with magnetic fields as well.

By using equations (5.10) and (5.11), we may obtain the conditions for focusing, which are formally expressed in the form: $j_x = \infty$. Physically this corresponds to the instant when all the electrons of a given packet are disposed in the single plane $x = x_f$, perpendicular to the direction of stream flow. The condition $j_x = \infty$ reduces down to

$$\frac{dt_x}{dt_s} = 0 \qquad \text{or} \qquad 1 + \frac{d\Theta_x}{dt_s} = 0. \tag{5.12}$$

Equations (5.10) to (5.12) constitute the most general relationships, and enable us to study the general properties of electron stream subjected to phase focusing, independently of the law of variation of electron velocity in the modulator and of the subsequent fate of the electrons.

Let us put some of these general relationships into concrete form, assuming that for any law of variation in the velocity, the

electric field past the modulator is equal to zero, and the further motion of the electrons proceeds by virtue of their inertia, at the velocities they have when they leave the modulator. Then

$$x = v_s(t_s)(t_x - t_s) = v_s(t_s) \tag{5.13}$$

For any value of x it is obviously possible to write

$$\uparrow_x \frac{dv_s}{dt_s} + v_s \frac{d\uparrow_x}{dt_s} = 0$$

whence

$$\frac{d\uparrow_x}{dt_s} = -\frac{\uparrow_x}{v_s} \cdot \frac{dv_s}{dt_s} \tag{5.14}$$

This means that the current density at any point x of the stream moving by inertia may be expressed

$$j_x = j_o \frac{1}{\left|1 + \frac{d\uparrow_x}{dt_s}\right|} = j_o \frac{1}{\left|1 - \frac{\uparrow_x}{v_s} \frac{dv_s}{dt_s}\right|}. \tag{5.15}$$

Inasmuch as $\uparrow_x / v_s = x/v_s^2$, then, remembering that $\dot{v}_s = \frac{dv_s}{dt_s}$, we may obtain the somewhat more convenient expression

$$j_x = j_o \left|\frac{1}{1 - x\frac{\dot{v}_s}{v_s^2}}\right| \tag{5.16}$$

It follows from this equation that the conditions for focusing are

$$1 - x_F \cdot \frac{\dot{v}_s}{v_s^2} = 0 \tag{5.17}$$

from which the value of the focal length x_F may be found:

$$x_F = \frac{v_s^2}{\dot{v}_s} \tag{5.18}$$

This expression, as may readily be seen, coincides with (5.7), which we obtained on energetic considerations. Substituting (5.18) in (5.16), it is possible to express the current density somewhat differently:

$$j_x = j_o \frac{1}{\left| 1 - \frac{x}{x_F} \right|} \tag{5.19}$$

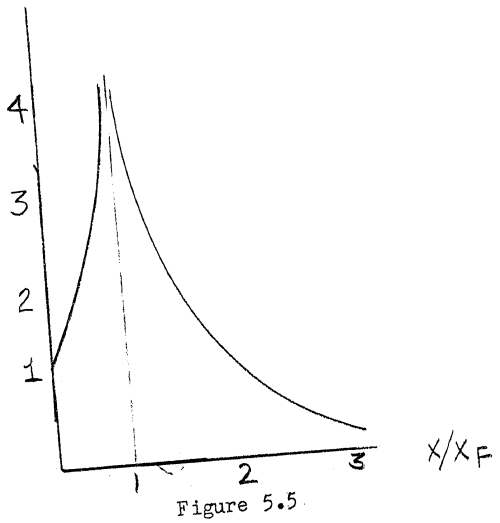

Figure 5.5

This equation makes it possible to represent graphically the course taken by the current density along the electron stream, as is done in Figure 5.5, where the ratio j_x/j_o is represented as a function

of the ratio x/x_F. It must, however, be noted that equations (5.18) and (5.19) have a physical meaning in the case where $\dot{v}_s > 0$, i.e. if the velocity increases with time; but if $\dot{v}_s < 0$, then in the regions where x is positive, and consequently, on the actual path of a modulated stream, no focus is formed, and the current density, falling along the x axis, approaches zero (the electron-packets being dissipated).

We may thus note the following fundamental features in the behavior of a velocity-modulated electron-stream, moving by inertia after it leaves the modulator:

(a) the electron-packets that leave the modulator during the time when their exit velocity is increasing ($\dot{v}_s > 0$), are focused at various distances x_F from the modulator;

(b) the packets that leave the modulator at moments of experimental values for the velocity $v_s(t_s)$, i.e. satisfying the conditions $\dot{v}_s = 0$, proceed further without change.

(c) the packets that leave the modulator during the time that the exit velocities are falling, i.e. when $\dot{v}_s < 0$, are "defocused" and increase their length along the x axis.

5.3 Modulation of the Electron Stream by a Sinusoidal Voltage

The application of the general relationships we have presented to the case of sinusoidal variation of the modulation voltage is of most practical interest, since this is the only method in technical use in the UHF field.

Let us imagine that electrons that have acquired the velocity

v_o under the influence of the constant potential difference U_o between K and A, fall in the modulator M under the influence of the alternating potential difference $U_1 \sin \omega t_s$ (Figure 5.6) Then, under the condition that the transit time through zone AB shall be short in comparison to the period of oscillation, the velocity of v_s of any electron at its exit from the modulator is expressed as

$$v_s = \sqrt{2\frac{e}{m}(U_o + U_1 \sin \omega t_s)} = \sqrt{2\frac{e}{M} U_o (1 + \xi \sin \omega t_s)} =$$

$$= v_o \sqrt{1 + \xi \sin \omega t_s} = v_o \alpha_s .$$

Here $\xi = \frac{U_1}{U_o}$ --"the coefficient of voltage modulation", while $\alpha_s = \sqrt{1 + \xi \sin \omega t_s}$ has been introduced to shorten the writing of the expression. Let us now consider the behavior of the sinusoidally modulated stream under various regimes in the space beyond the modulator -- the "zones of reorganization of the stream".

(A) Electric Field Absent from the Zone of Stream Reorganization

Let the potential of the modulator vary, as has just been said, according to the sinusoidal law. Then, in accordance with the preceding

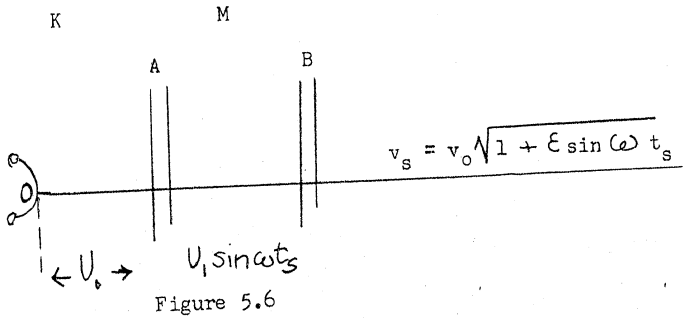

Figure 5.6

each period of variation of the modulation voltage is composed of two equal intervals: the interval of focusing, corresponding to rising potential, i.e. to the half-periods from $\omega t_s = -\frac{\pi}{2}$ to $\omega t_s = +\frac{\pi}{2}$; from $\omega t_s = 3\pi/2$ to $\omega t_s = 5\pi/2$ etc, and the interval of defocusing, embracing the remaining half-periods (from $\omega t_s = \pi/2$ to $\omega t_s = 3\pi/2$; from $\omega t_s = 5\pi/2$ to $\omega t_s = 7\pi/2$, etc) which are half-periods of voltage drop. The behavior of the electrons is thus in the main determined by the moment t_s of their exit from the modulator, or by the corresponding "exit phase" ωt_s. These quantities will in the future discussion play the role of independent variables in many formulae.

For the case under consideration, of course, we shall have:

$$\tau_x = \frac{x}{V_0\sqrt{1 + \xi \sin \omega t_s}} \qquad (5.20)$$

$$\dot{V}_s = \frac{\dot{V}_0\, \omega \xi \cos \omega t_s}{2\sqrt{1 + \xi \sin \omega t_s}} \qquad (5.21)$$

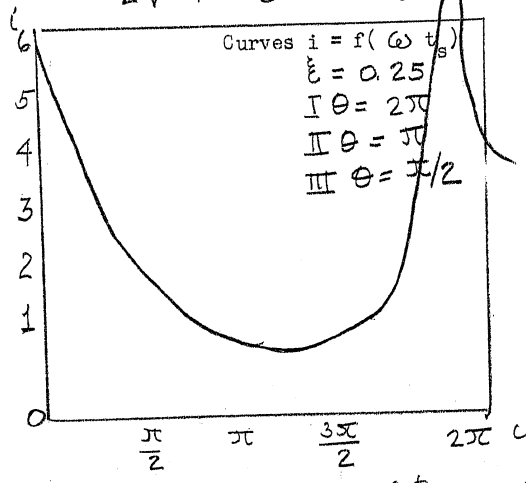

$\omega t_{s\,min} = 201°2'$

$\omega t_{s\,max} = 338°58'$

Figure 5.7

To secure greater generality, let us now introduce the "dimensionless factor of current density" i

$$i = \frac{j_x}{j_o} \tag{5.22}$$

For which we obtain the expression

$$i = \frac{1}{\left| 1 - \frac{x\omega\xi \cos \omega t_s}{2V_o (1+\xi \sin \omega t_s)^{3/2}} \right|} \tag{5.23}$$

Let us introduce also the mean transit angle θ, defined as the angle of transit to the point x of an electron with the constant velocity v_o

$$\theta = \frac{x\omega}{v_o} \tag{5.24}$$

We then obtain

$$i = \frac{1}{\left| 1 - \frac{\xi\theta}{2} \left(\frac{\cos \omega t_s}{1+\xi \sin \omega t_s} \right)^{3/2} \right|} \tag{5.25}$$

This formula may be used to calculate the current density produced along the stream by a certain electron packet defined by the exit-phase ωt_s, and we get a result somewhat recalling Figure 5.5; the formula may likewise be used to calculate the relationship of the current density to the definite distance x (or, more generally, with the corresponding transit angle θ) to the exit-phase ωt_s. For small values of ξ and θ, the denominator is depicted by the curves $i = f(\omega t_s)$, which are of periodic character and have more or less sharply expressed maxima, the height and sharpness of which increases with increasing ξ and θ, as shown

by Figure 5.7, which gives the curves of current density for $\xi = 0.25$, when $\theta = \pi/2, 5\pi$, and $2\,5\pi$. The position of the curves of current density along the axis ωt_s is determined by the condition

$$\frac{d_i}{d(\omega t_s)} = 0,$$

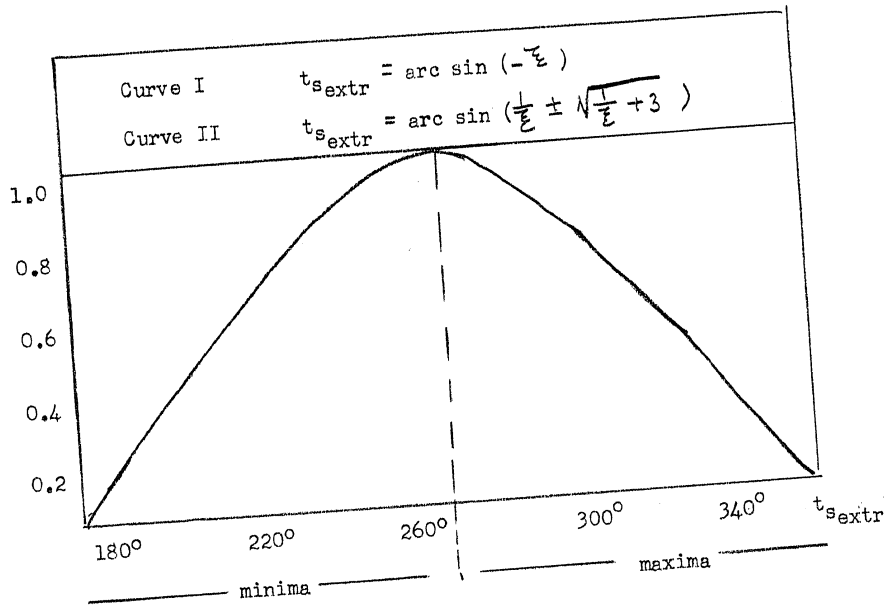

Figure 5.8

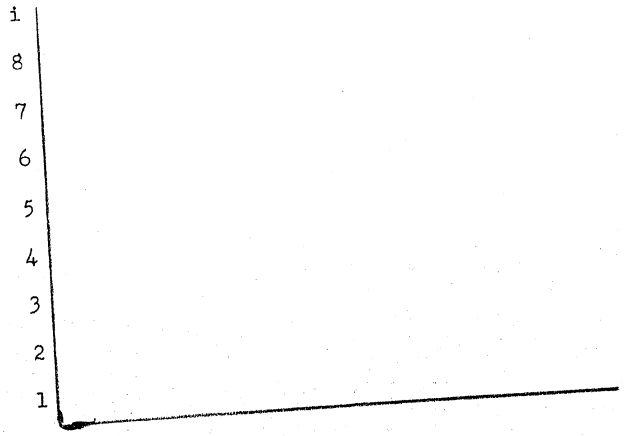

Curves $i = f(\omega t_s)$
$\xi = 0.5$
I $\theta = 2\pi$
II $\theta = \pi$
III $\theta = \pi/2$

Points b_1, b_1', b_2, b_2' correspond to i(t)

Figure 5.9

which leads to the corresponding value for $t_{s_{extr}}$

$$\omega t_{s_{extr}} = \arcsin\left(\frac{1}{\xi} \pm \sqrt{1/\xi^2+3}\right). \qquad (5.26)$$

It should be noted that the phase-angle of exit for the electron-packets, which form amximum and minimum condensations at the given distance, depend only on the modulation coefficient ξ. The dependence of $t_{s_{extr}} = f(\xi)$ is shown in Figure 5.8. The maxima of the current-density curves are obviously formed by packets that condense and focus otherearlier ones.

Figure 5.7 refers to the current-density curves obtained before the focus. At the moment the value i(ωt_s) = ∞ is attained (when the denominator of formula (5.25) becomes equal to zero), a maximum is obtained, exactly for the packet with exit phase $\omega t_{s_{max}}$. In its subsequent path, this packet is "stretched out" more rapidly than the others, and a minimum value for $\omega t_{s_{max}}$ is now obtained on the curve of current density, while its maximum splits into two parts, since the denominator of formula (5.25) vanishes twice during the period. The similar behavior of the "transfocal" curves of current density is shown in Figure 5.9, in which, alongside of the prefocal curve $\theta = \pi/2$, two "transfocal" curves are plotted, which were obtained for the same value of ξ = = 0.5, but at larger values of θ.

By equating the denominator of formula (5.23) to zero, we may obtain the equation of the locus of the foci of the stream in the form $x_F = f(\omega t_s)$

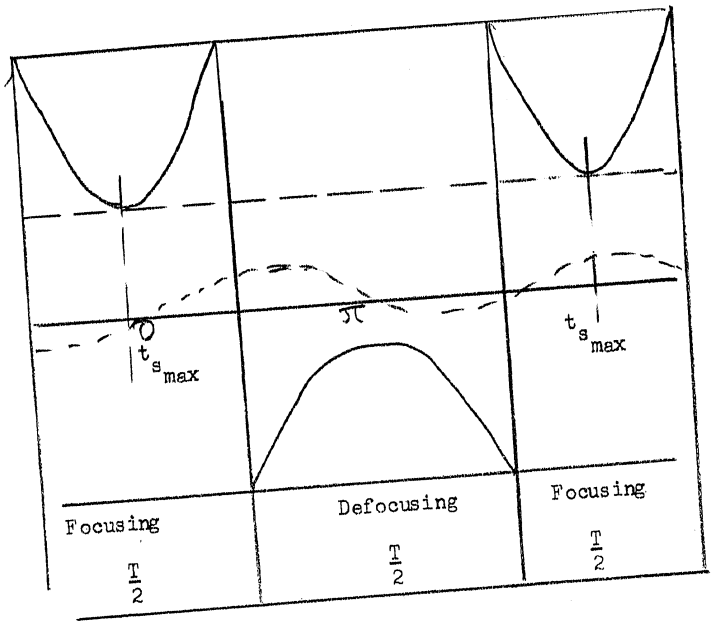

Figure 5.10

$$x_F = \frac{v_s^2}{\dot{v}_s} = \frac{2V_0(1+\xi \sin \omega t_s)^{1/2}}{\omega \xi \cos \omega t_s} \qquad (5.27)$$

and the corresponding mean angle of transit to the focus

$$\theta = \frac{x_F \omega}{V_0} = \frac{2(1+\xi \sin \omega t_s)^{3/2}}{\xi \cos \omega t_s} \qquad (5.27')$$

The curve representing the course of x_f according to equations (5.27) is presented in Figure 5.10. The curve θ has obviously an analogous course. A focus is physically possible only for positive values of x_F. Negative values of x_F are obtained in the intervals of defocusing. The packets with minimum or maximum exit velocities are focused at infinity, while for all the other packets the interval of focusing forms a focus at finite distance. The packets for which the exit phase is given by equation (5.26),

which is the condition of a minimum for the curve $x_F = f(\omega t_s)$, should be focused the nearest of all. The minimum focal length and the transit angle corresponding to it may be obtained from expressions (5.27) and (5.27') by substitution of the relation (5.26) in them:

$$x_{F\,min} = \frac{2V_0\left(2-\sqrt{1+3\xi^2}\right)^{3/2}}{\omega\sqrt{2+3\xi^2-2\sqrt{1+3\xi^2}}}, \quad (5.28)$$

$$\theta_{F\,min} = \frac{2\left(2-\sqrt{1+3\xi^2}\right)^{3/2}}{\sqrt{2+3\xi^2-2\sqrt{1+3\xi^2}}} \quad (5.28')$$

The latter formula indicates an interesting circumstance: the focusing in a stream modulated by a sinusoidal voltage begins when the stream passes a definite phase angle $\theta_{F\,min}$ which depends only on the modulation coefficient ξ. The relation between $\theta_{F\,min}$ and ξ illustrated by Figure 5.11 does not depend on any other parameters of the system. It will be seen that $\xi = 1$ the

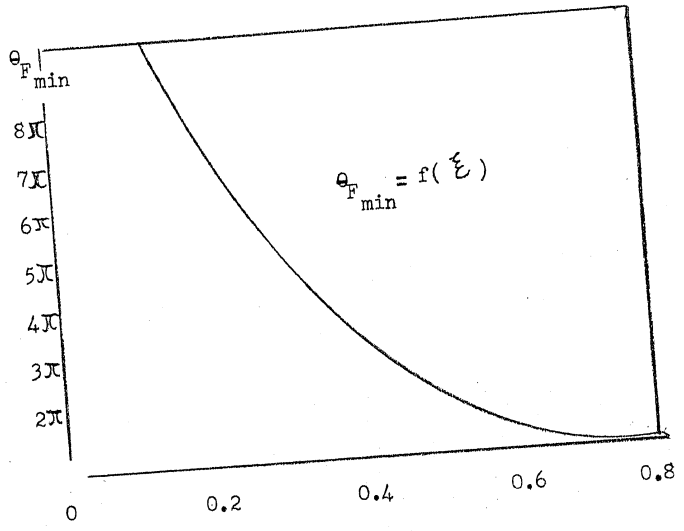

Figure 5.11

focus originates immediately at the very surface of the modulator. Physically, however, such a system is improbable. Usually we must deal with $\xi \leqslant 1$; in that case the magnitude of $\omega t_{s_{max}}$ may be taken as equal to zero in first approximation, which yields the following expressions for $x_{F_{min}}$ and $\theta_{F_{min}}$:

$$x_{F_{min}} = \frac{2V_o}{\omega \xi} \quad \text{and} \quad \theta_{F_{min}} = \frac{2}{\xi}. \tag{5.29}$$

The "focal curves" represented in Figure 5.10 are the curves of the locus of the values of x_F, i.e. the focal lengths of the electron packets having the respective exit angles of ωt_s. In solving certain problems connected with the study of velocity-modulated streams, time-distance diagrams of the movement of the foci may be useful. These may be obtained by developing the focal curves in time (Figure 5.12), i.e. by constructing the curves $x_F = f(\omega t)$, where t is the current time, defined as $t = t_s + \tau$, i.e. as the sum of exit time and transit time. The analogous relation also holds between the phases: $\omega t = \omega t_s + \omega \tau$. The current angle of transit before the focus $\omega \tau_F$, may likewise be expressed as a function of ωt_s.

$$\omega \tau_F = \frac{\omega x_F}{V_s} = \frac{2(1 + \xi \sin \omega t_s)}{\xi \cos \omega t_s} \tag{5.30}$$

From equations (5.27) and (5.30), the equation of the space-time graph of the motion of the focus may be set up, giving it, for example, by means of the parametric equations:

$$\omega t_F = \omega t_s + \frac{2(1 + \xi \sin \omega t_s)}{\xi \cos \omega t_s} \tag{5.31}$$

$$x_F = \frac{2V_o (1 + \xi \sin \omega t_s)}{\omega \xi \cos \omega t_s}$$

By using these equations, a graph of the motion of the focus may be constructed, which will be of the form shown in Figure 5.12. On considering it we note the following interesting circumstance: at each given moment t, for distances greater than $x_{F\,min}$ from the modulator, there exist, for each interval (half-period) of focusing, two foci, formed by the corresponding electron-packets in the stage of maximum condensation. At the following moment this state passes over to the next adjoining packet, and so on. A peculiar picture of the "motion" of the focus in space is thus obtained. In reality, too, this focus is displaced along the stream of maximum density in a manner analagous to that of any longitudinal wave. A very important property of this "motion of the focus" must be noted in this connection; the displacement velocity of the focal condensation equals the velocity of the electron packet being focused at the given moment:

$$V_F = \frac{x_F}{t_F} = V_0 \sqrt{1 + \xi \sin \omega t_s} = V_s \qquad (5.32)$$

We may also reach the same conclusion for any law of variation in the velocity, for instance, by using formula (5.7). On the graph of Figure 5.12 a number of singular points attract our

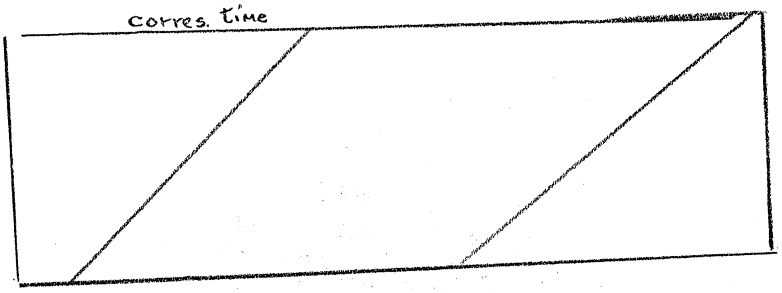

Figure 5.13a

attention. The point corresponding to a minimum focal length is the point of superposition of one branch of the curve on the other, both branches having a common tangent (as a result of the continuous variation of the electron velocities). Let us call this focal point one of the second order. As the branches of the curves related to the various focusing intervals reced from the modulator, they intersect each other, and at these points of intersection

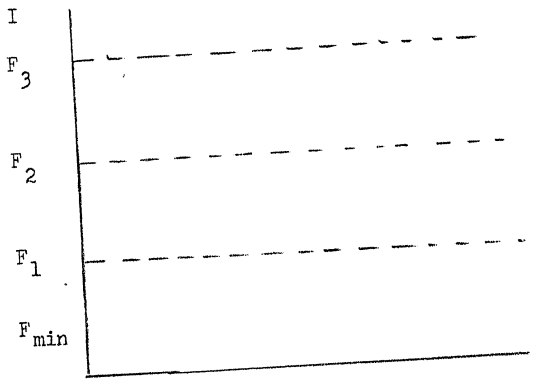

Figure 5.13b

"foci of higher order" likewise originate. Immobility is an important property of such foci.

In this manner a peculiar space-time interference pattern is obtained from the time-dsitance diagram of electron motion. In that pattern the charges undergoing displacement along the branches of the focal curves of condensation create immobile maxima, with even greater concentrations, at the points of intersection of these curves (Figure 5.13 a and 5.13b).

(B) The Accelerating Field in the Space of Transformation on Leaving the Modulator

If the electrons, on leaving the modulator, enter an electric field acting along the OX axis, then, depending on the orientation of this axis, they may undergo either acceleration or retardation changing their initial velocity. In the simplest case, this field is constant in time. The case of a retarding field is of special interest and will be considered in detail later; but for the present we assume that the electron stream on its exit from the modulator enters a uniform accelerating electric field of intensity E. Then the motion of the electrons is subject to the simple law of uniformly accelerated motion

$$v_x = v_s + a\tau_x; \qquad x = v_s\tau_x + \frac{a\tau_x^2}{2} \tag{5.33}$$

where $a = \frac{eE}{M}$ is the acceleration imparted to the electron by the field E. By using the general relations presented earlier, the following expression may be obtained for the dimensionless current density

$$i = \frac{2\left(1+\xi\sin\omega t_s + \frac{xE}{U_o}\right)\sqrt{1+\xi\sin\omega t_s}}{\left|2\left(1+\xi\sin\omega t_s + \frac{xE}{U_o}\right)\sqrt{1+\xi\sin\omega t_s} - \xi\omega\tau\cos\omega t_s\right|} \tag{5.34}$$

which, as is readily seen, becomes equation (5.23) for E = 0. The equation for the locus of the foci is obtained in the form

$$x_F = \frac{2\left(1+\xi\sin\omega t_s\right)^{3/2}}{\xi\frac{\omega}{V_o}\cos\omega t_s - 2\frac{E}{U_o}\sqrt{1+\xi\sin\omega t_s}} \tag{5.35}$$

The fundamental peculiarities of the curves $x_F = f(\omega t_s)$ are here almost the same as in the foregoing case. An accelerating field, however, "elongates" the stream, draws the focus away from the modulator, and compresses the focusing interval. In reality, x_F becomes infinite under the condition

$$\cos \omega t_s = 2 \frac{E}{U_0} \cdot \frac{V_0}{\omega \xi} \sqrt{1 + \xi \sin \omega t_s} \qquad (5.36)$$

At a sufficiently high acceleration, satisfying the condition

$$2 \frac{E}{U_0} \sqrt{1 - \xi} \geq \xi \frac{\omega}{v_0}, \qquad (5.37)$$

no focusing at all takes place, for the focusing interval is compressed to zero.

5.4 PECULIARITIES OF PHASE FOCUSING IN A CONSTANT RETARDING FIELD

Let us imagine a basic circuit (Figure 5.6) in which the electron stream leaving the modulator is subjected to the action of a uniform retarding field, constant in time. Its intensity vector E is parallel to OX. The motion of the electrons in this case is uniformly retarded, and the distance x_{max} by which they may be separated from the modulator is limited by the "height of ascent", which corresponds to the motion of a body thrown upwards in the earth's gravitational field. In consequence we must consider two electron streams, one going and one returning. If the field intensity at the modulator varies according to the law

$$U_M = U_o + U_1 \sin \omega t_s$$

with the negative acceleration a imparted to the electron by the field, then the transit time through the retarding field may be expressed as:

$$\tau_x = \frac{v_s}{a} \pm \sqrt{\frac{v_s^2}{a^2} - \frac{2x}{a}} \qquad (5.38)$$

The values of τ_x for the going stream give minus eight before the root, while the values corresponding to the return strean are obtained if the plus sign is taken instead.

For convenience in computation and compactness in the formulae, let us now introduce the "coefficient of retardation" $n = \frac{E}{U_o}$ with dimensionality 1/cm and equal to $a = \frac{1}{d}$ where d is the maximum distance from the modulator attained by an electron leaving it at velocity v_s. Let us, as before, designate the frequently encountered expression $\sqrt{1 + \xi \sin \omega t_s}$ by α_s. Then the formulae for acceleration, velocity and transit time assume the form

$$a = nv_o^2/2$$

$$v_x = \pm v_o(\alpha_s^2 - xn)^{\frac{1}{2}} \qquad (5.39)$$

(+ for going stream, - for returning stream)

in which the notation is the same as in formula (5.38).

By adopting these symbols and making use of the general formulae, the dimensionless current density may be expressed as

follows:

$$i = \frac{\alpha_s^2 (\alpha_s^2 - xn)}{\left| \sqrt{\alpha_s^2 (\alpha_s^2 - xn)} + \frac{i(\omega)}{nV_0} \cos \omega t_s \left(\sqrt{\alpha^2 - xn} \pm \alpha_s \right) \right|} \quad (5.40)$$

Current density must be separately computed for each stream when using this formula: the minus sign in the parentheses of the second term of the denominator is taken for the going stream, while for the return stream $i \equiv 0$ is obtained, which corresponds to the physical fact that there is no return stream at zero retardation. The character of the current curve $i = f(\omega t_s)$ is analagous to that for the cases discussed above: namely, i varies periodically and on reaching a certain value of x for which the denominator vanishes, it forms infinite maxima -- the foci. Foci may be formed in both the going and return streams. Thus, all the component packets of the electron stream may be focused:

(a) on the path from the modulator to the surface of return, located at distance x_{max}, the instantaneous value of which is determined as:

$$x_{max} = v_s^2/2a = \alpha_s^2/n = \alpha_s^2 d; \quad (5.41)$$

(b) at the surface of return itself, which may be judged by the expression for density of charge on this surface

$$\rho = \frac{2n}{|\omega \cos \omega t_s|} \quad (5.42)$$

Focusing at the surface of return, as is clear from the above, takes place independently of stream conditions at $\omega t_s = \frac{\pi}{2}, \frac{3\pi}{2}, \ldots$

(c) in the return stream between the surface of return and the modulator, and, finally,

(d) at the return to the modulator.

The peculiarities of focusing a stream in a retarding field may be investigated by the aid of "curves of the locus of foci" analogous to those discussed above. Their equation in the given case assumes the form

$$x_F = \frac{\alpha_s^2}{n}\left[1 - \frac{\frac{\varepsilon^2\omega^2}{v_0^2 n^2}\cos^2\omega t_s}{\left(\alpha_s + \frac{\varepsilon\omega}{nV_0}\cos\omega t_s\right)^2}\right]. \qquad (5.43)$$

The important parameters n, , and v_0 of the stream system are very frequently met in various expressions in the combination $\frac{nv_0}{\omega} = p$, which may be adopted as a new and more general parameter, the "factor of retardation in flight". Physically this represents a magnitude that is the reciprocal of the half-angle of flight of an undisturbed electron to the surface of return,

$$\frac{1}{p} = \frac{\omega}{nv_0} = \frac{d\omega}{v_0} \qquad (5.44)$$

while, according to formula (5.39) $\uparrow_{x_{MAX}} = \frac{2\alpha_s}{nV_0}$, or, for an undisturbed electron,

$$\uparrow_{0(x\,MAX)} = \frac{2}{nV_0};\ \omega t_0 = \frac{2\omega}{nV_0} = \frac{2d\omega}{V_0} = \frac{2}{p}$$

In the future we shall have occasion to make use of certain properties of this parameter p.

It will be seen from formula 5.43 that the curve of the locus of the foci lies with all of its points inside the space bounded by

the surface of return and makes contact with that surface only at the points for which $\cos \omega t_s = 0$ (cf. formula 5.42). With relatively weak retardation in the space between the modulator and the surface of return, the same electron packets in the going stream are focused as when there is no field at all, i.e. those packets for which $dv_s/dt_s > 0$. In the return stream, however, these packets that leave the modulator during the semiperiods of falling velocity also form foci. Thus, in contrast to what takes place in accelerating fields, the focusing interval is broadened in retarding fields. As the retardation coefficient n increases, the focusing interval expands, and at a certain definite value of n all of the packets leaving the modulator during the period of variation in the potential on it will form foci in the space oftransformation.

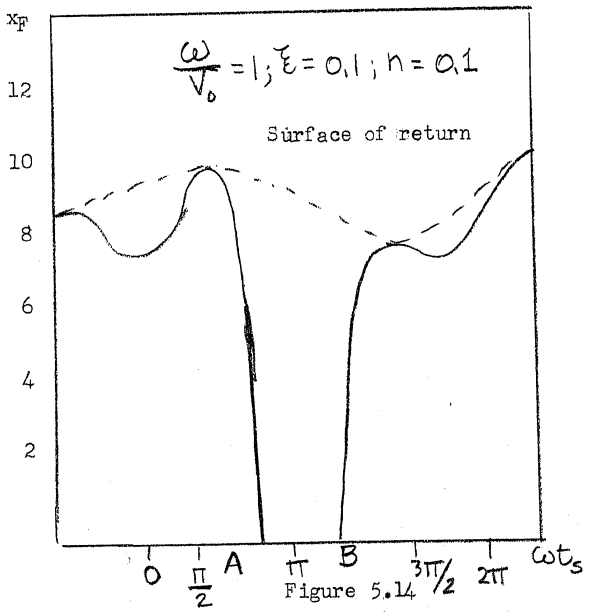

Figure 5.14

The form and general deformation of the curves obtained for the locus of the foci are shown in Figures 5.14 to 5.16, which

been plotted on the basis of $\xi = 0.1$ and $\omega/v_0 = 1$. Figure 5.14 gives the curves representing the surface of return (dash-dot line) and the locus of foci for n = 0.1. Those parts of the curve $x_F = f(\omega t_s)$ which are located between $-\pi/2$ and $+\pi/2$, between $3\pi/2$ and $5\pi/2$ etc, correspond to the foci of packets travelling in the going direction, while the segments DA and BC correspond to those in the returning direction.

The interval AB is the interval of defocusing which declines as n increases. At a certain value of n, equal to

$$n = \frac{2\xi\omega}{v_0} \qquad (5.45)$$

$$(\text{or } p = 2\xi)$$

the points A and B merge, and the very characteristic system depicted in Figure 5.15 is obtained. Here n = 0.2 for the same values of ξ and ω/v_0. The curve of the locus of the foci here meets the axis of abscissae at the place where points A and B merge ($\omega t_s = \pi$).

In this case we have to do with an interesting process: the concentration of charge that we call a focus undergoes a certain periodic movement between the surface of return and the modulator, which superficially reminds us very strongly of the mechanism of oscillation of a retarding field as pictured by some authors [9]. The process of "movement of foci" under consideration is, however, something different from the "swing" of the electron layer. It constitutes the displacement of a certain condition rather than of particles, and recalls rather the process of propagation of longitudinal waves.

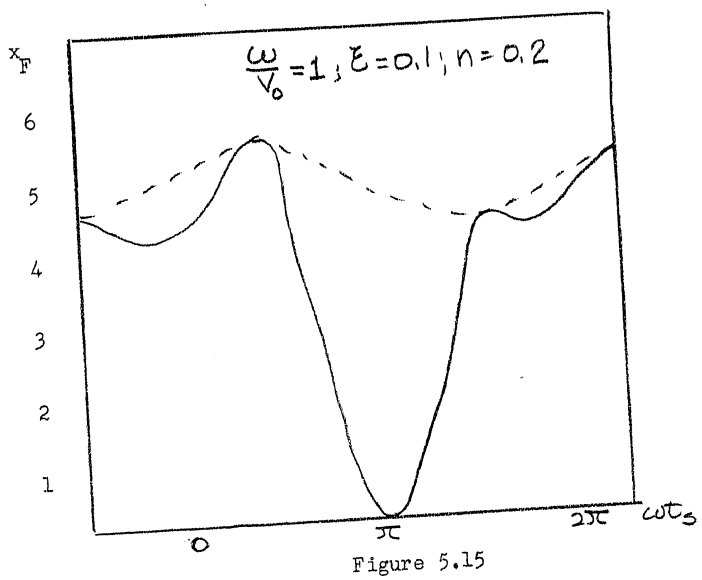

Figure 5.15

An analogous pattern is also obtained for greater retardation. (Figure 5.16). In this case the curve of the locus of the foci is situated entirely within the space of transformation, and approaches the surface of return as n increases. The oscillation of the focus approaches the sinusoidal, and the whole pattern of its behavior strongly recalls the idea of a "pulsating virtual cathode" which has been repeatedly applied to explaining the mechanism of oscillation both in the retarding-field circuit and in the magnetron.

The space-time graphs of the motion of the focus which are obtained by developing the curves in Figures 5.14 to 5.16 along the axis of current time t (or along that of the corresponding phase angle ωt), are also of considerable interest in this case. For this, the abscissa of each point of the curve must be increased by the corresponding value of ϑ_F or ωt_F, which may be determined from equations (5.39 and 5.43)

$$\omega\tau_F = \frac{\omega V_s}{\frac{V_0 \varepsilon \omega}{2\alpha_s}\cos\omega t_s + \frac{nV_0^2}{2}} \qquad (5.46)$$

Whence the current time of focusing is expressed as

$$\omega T_F = \omega t_s + \omega\tau_F = \omega t_s + \frac{\omega V_s}{\frac{V_0 \varepsilon \omega}{2\alpha_s}\cos\omega t_s + \frac{nV_0^2}{2}} \qquad (5.47)$$

The set of equations (5.43) and (5.47) may be regarded as the parametric equations of the space-time graphs of the movement of the focus. They are given in Figures 5.17 to 5.19 for the systems corresponding to Figures 5.14 to 5.16. When retardation is slight, these graphs, especially at the outset, near the points $x_{F_{min}}$, remined us of the corresponding curves for a stream traveling by inertia (Figure 5.12). However, the two branches of the curve formed here, which start at a certain minimum distance, do not proceed to infinity, but instead, each of them, on reaching its respective point (C or D) on the surface of return, again approaches the modulator and reaches it at points A and B, respectively. The descending branches of these curves correspond to the focusing in the return stream.

At increasing retardation the points A and B approach each other and at the value of n defined by equation (5.45), merge into one (Figure(5.18), corresponding to Figure (5.15)). In this manner both descending branches of the trajectory intersect at the instant they reach the modulator, and form at that point a periodically originating focus of the second order (the intersection of two focal curves having the same direction), which is equivalent to the rhythmic beat of electron concentrations against the modulator.

At the same time, we observe, at other regions of the graphs represented in Figures 5.17 and 5.18, the intersection of the trajectories of the foci of the going and returning streams (the ascending and descending branches of the curves). Two electron packets are consequently focused at each such intersection, one of which packets is traveling away from the modulator and the other towards it, by virtue

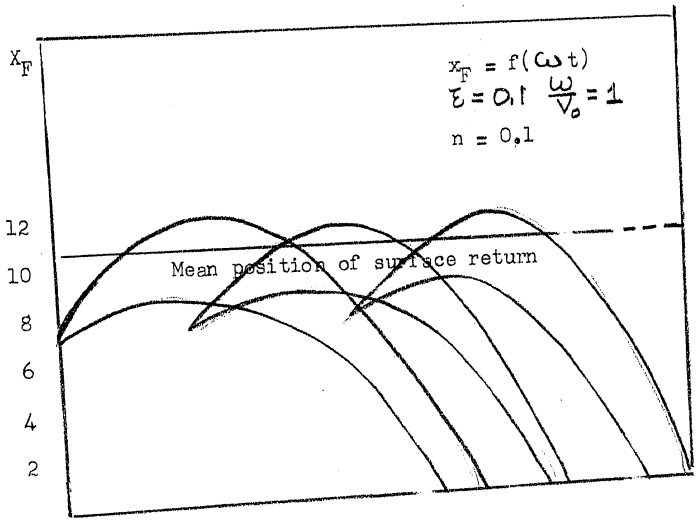

Figure 5.17

of which the energy effect of this superposition is either negligible or zero.

In the immediate vicinity of the modulator, under the system in which both branches of the focal curve return to a single point, or, as we shall put it during our future expositions, under the "system of focus return", conditions may be obtained that energetically favor the excitation or the maintenance of oscillations in the system connected with the modulator.

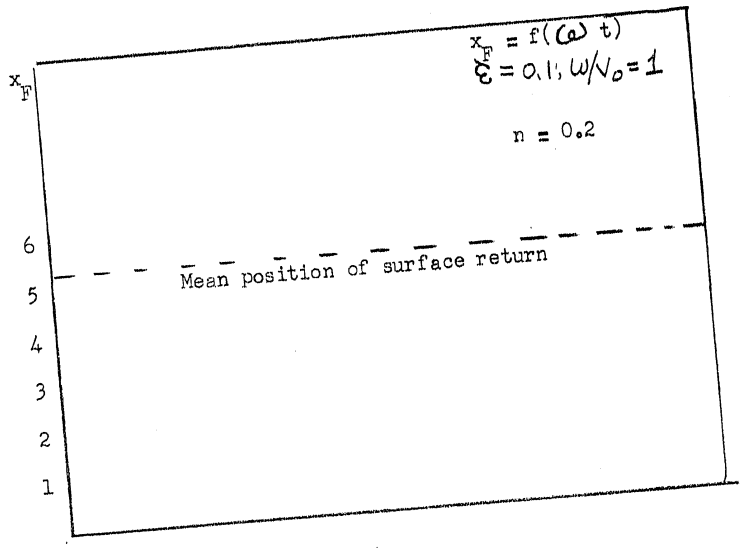

Figure 5.18

With further increase in retardation, the point of intersection of the corresponding [odnoimenniy] branches of the focal trajectories moves out from the modulator into the space of transformation and is gradually transformed from a singular point of the focal trajectory into an ordinary point thereof. All of the trajectories approach the surface of return, and, as has been shown in Figure 5.19, they fluctuate in its neighborhood, In this case the "pulsation of the virtual cathode", which here amounts to a "surface of foci", is manifested even more vividly.

We have now considered with the aid of the concept of phase focusing of the electron stream several electron mechanisms considerably more complicated than those discussed in Paragraph 2 of Chapter III. The fundamental difference of the mechanisms with phase focusing consists in the fact that they are described, not by the behavior of a single electron, but by that of a whole complex of electrons, organized by the action of the alternating elec-

tric field of the modulator and corresponding to selective flight conditions. The ordered nature of the motion and the energy interaction is obtained in this complex of electrons as the natural consequence of the dynamic conditions without the need for any special postulates whatsoever on the "selection" of any electron groups. Remembering that the displacement velocity of the focus is equal to the mean velocity of the electrons in the packet being focused, we are naturally able to reach the conclusion that the movement of the focus -- of this "collective electron" should be identical with that of the oscillating Barkhausen electron. As a matter of fact, if we set the condition of the system of "focus return", which for insignificant value of ξ may be formulated

$$n = 2\xi\omega/V_0$$

then, taking into consideration that $\omega = 2\pi c/\lambda$; $n = \frac{1}{d}$; $V_0 = \sqrt{2\frac{e}{m}U_0}$ a relation of the type of the Barkhausen equation may be obtained:

$$\lambda\sqrt{U_0} \approx 6\cdot10^3\xi d.$$

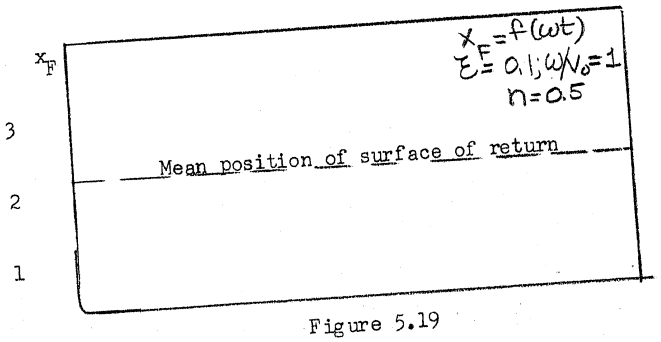

Figure 5.19

For $\xi \gtrsim 0.33$ this equation also well produces the so-called Barkhausen constant

$$\lambda\sqrt{U_o} = 2000\,d\,.$$

This preliminary and purely schematic discussion indicates the fruitfulness of the application of the idea of phase focusing to the study of UHF electronic generators.

5.5 THE ELECTRON STREAM IN AN ALTERNATING ELECTRIC FIELD

According to the foregoing assumption the electron stream is subjected to the action of an alternating field during a very short time interval in the zone of modulation. By virtue of this, all the processes of transformation of the stream take place in regions that are already beyond the boundaries of the modulation zone. In generators of the klystron type, and those similar to it, the situation occurs in practice. In a good number of cases, however, the modulation zone and the transformation zone are not spatially separated; for example, in a triode with retarding field, in magnetron, etc.

An elementary representation of the action of an alternating field on an electron stream impinging on it with a certain initial velocity may be set up in a fairly simple way. Assume that beyond the first grid of the modulator an alternating field of intensity $E = E_o \sin \omega t$ extends without limit along the x axis, with $\vec{E} \parallel OX$. The electrons enter this field as a unfirom stream with the velocity v_o acquired in the acceleration zone. The accelerating voltage has already ceased to act, and the electrons of the stream now undergo only the variable acceleration in this field

$$a = -\frac{eE}{m} = -\frac{e}{m} E_0 \sin \omega t = a_0 \sin \omega t \qquad (5.48)$$

The equation of motion for the electron

$$\ddot{x} = a_0 \sin \omega t$$

gives for its velocity

$$\dot{x} = v_0 \quad \frac{a_0}{\omega} (\cos \omega t - \cos \omega t_0) \qquad (5.49)$$

where t_0 is the instant of exit from the acceleration zone, at velocity v_0.

If x be measured from the first grid, successive integration gives

$$x = v_0(t - t_0) + \underline{\frac{a_0}{\omega} \left[\sin \omega t - \sin \omega t_0 - \omega (t - t_0) \cos \omega t_0\right]} \qquad (5.50)$$

The second, underlined term in this fromula appeared as the result of the action of the alternating field which is attributable to the alternating field ? Obviously, the general relation (5.10) may be employed here, if we only take account of the circumstance that the initial velocity v_0 of all the electrons is constant. In the given case we must seek the derivative dt/dt_0 (t_0 here plays the role of t_s in formula 5.10) by a somewhat roundabout path. Since we are interested in the current density j_x at some definite point x and at the corresponding instant t, we may interpret equation (5.50) as a certain function of the two variables t and t_0 and seek the quantity dt/dt_0 as the r ate of the partial derivative of this function

$$\frac{dt}{dt_o} = -\frac{\frac{\partial F(t,t_o)}{\partial t_o}}{\frac{\partial F(t,t_o)}{\partial t}}$$

From equation (5.50) we find:

$$\frac{\partial F}{\partial t_o} = -v_o - a_o(t - t_o)\sin \omega t_o,$$

$$\frac{\partial F}{\partial t} = v_o \frac{a_o}{\omega}(\cos \omega t - \cos \omega t_o).$$

Whence

$$\frac{dt}{dt_o} \quad \frac{v_o + a_o(t - t_o)\sin \omega t_o}{v_o + \frac{a_o}{\omega}(\cos \omega t - \cos \omega t_o)} \qquad (5.51)$$

and the current density

$$j(x, t) = j_o \frac{v_o + \frac{a_o}{\omega}(\cos \omega t - \cos \omega t_o)}{v_o + a_o(t - t_o)\sin \omega t_o} \qquad (5.52)$$

Formula (5.52) shows that the current density may be considered invariable either when the acceleration a_o is zero, that is, when the above postulated alternating field is absent, or when the time of flight $t - t_o$ through this field is incomparably smaller than the values we have been using in all our discussions.

In the case under consideration, the focusing of the stream may occur in the same alternating field, by virtue of the action of that field $E_o \sin \omega t$, so that velocity modulation and density modulation occur simultaneously. It is obvious that

$$\frac{\partial t}{\partial t_o} = \frac{\partial F}{\partial t_o} = 0$$

$$v_o + a_o(t - t_o)\sin \omega t_o = 0. \qquad (5.53)$$

will serve as the condition for the formation of a focus in this case.

Since $t - t_o = \tau$, the time of flight to the focus τ_F may be found from this:

$$\tau_F = \frac{-v_o}{a_o \sin \omega t_o} \qquad (5.54)$$

The role of the minus sign in this formula is evident from the circumstance that the focus is obviously real only when the action of the field of opposite direction produces a certain "compression" of the stress. The course of the curve τ_F is shown by Figure 5.20, in which at the same time the curve of variation

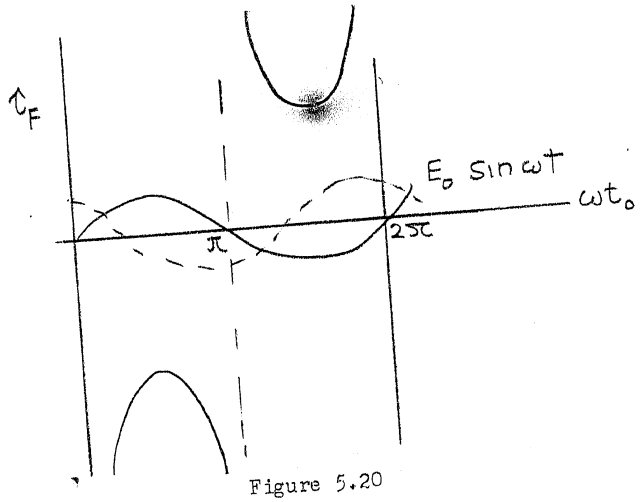

Figure 5.20

in field intensity and the curve of velocity (the broken line) have also been plotted. The focal length corresponding to the time of focusing may also be found by substituting in formula (5.50) the value of τ_F given by (5.54)

$$x_F = -\frac{V_0^2}{a_0 \sin \omega t_0} + \frac{a_0}{\omega^2}\left[\sin \omega\left(t_0 - \frac{V_0}{a_0 \sin \omega t_0}\right) - \sin \omega t_0 - \right.$$
$$\left. - \frac{\omega V_0}{a_0 \sin \omega t_0} \cdot \cos \omega t_0\right] \qquad (5.55)$$

It will be seen from this formula that for $a_0 = 0$, no focus at all will be formed ($x_F = \infty$), and the course of the focal curve is qualitatively analogous to that of the curve τ_F. In first approximation it may be supposed that the minimum focal length is obtained at $\omega t_0 \approx 3\pi/2$; in that case

$$x_{F_{min}} = \frac{V_0^2}{a_0} + \frac{a_0}{\omega^2}\left[1 - \cos \frac{\omega V_0}{a_0}\right] \qquad (5.56)$$

while

$$\tau_{F_{min}} = v_0/a_0$$

Thus, if an electron stream which is not velocity-modulated enters an alternating electric field, and proceeds far enough through it, velocity modulation and transformation of the stream will occur simultaneously in this field. The application of the considerations here developed to the zone of modulation makes it possible roughly to calculated the variation in the density of the current entering the modulator at the moment of its exit therefrom. Calculation by formula (5.52) shows that even if the transit angle of the modulator is taken as $\pi/2$, then, with $U_0 = 1000$ volts, $E_0 = 100$ volts/cm, and $\lambda = 50$ cm, the ratio of the maximum current to that entering it exceeds unity by only 3-4 percent. Inasmuch as actual modulators are constructed so as to assure a considerably lower transit angle, it is obvious that the disregard of transit time through the modulator by our assumptions is entirely legiti-

mate.

5.6 PECULIARITIES OF THE PHASE FOCUSING OF THE ELECTRON STREAM IN THE PRESENCE OF A MAGNETIC FIELD

Let an electron stream in the transformation space be subjected to the action of an electric and a magnetic field. A magnetic field, oriented in the same direction as the stream, assists the focusing thereof only geometrically and is not of fundamental interest in the investigation of electronic generators. The magnetic field usually applied, however, is perpendicular to the electric field and to the initial direction in which the electrons move, and introduces a number of substantial peculiarities into the focusing process. In fact, since the magnetic field bends the trajectory of the electrons and the radius of curvature is changed in dependence on the velocity of the electrons in accordance with the relation

$$r = \frac{mv}{e_H} = \frac{v}{\omega_H} \qquad (5.57)$$

the stream of electron packets formed at the exit from the modulator will describe paths of varying curvatures (Figure 5.21).

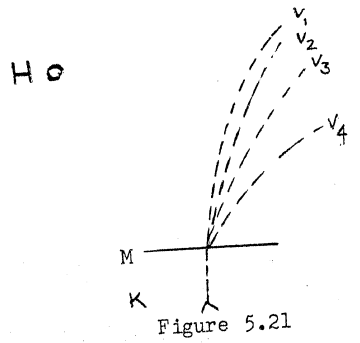

Figure 5.21

With such a behavior of the electron stream in the transformation zone, there cannot, of course, be any thought of phase focusing in the sense in which we have been using it.

Phase focusing in the presence of a magnetic field would have a meaning if a cross-section of the electron stream were far greater than the mean radius of curvature of an electron path, or if there were an axially symmetrical distribution of the electrodes. In both of these cases the collection of electrons corresponding to the above-mentioned packets is represented in the form of a certain layer, bounded by two fronts, sufficiently close together, of electrons traveling in phase. The former case will yield a packet in the form of a plane layer, while in the latter case the form of the layer will be symmetrical (Figure 5.22, a and b). If the acting electric field is directed only along the x axis, in the case of the plane distribution, or only along the radius, in the case of the cylindrical distribution, then the problem reduces down to a one-dimensional problem. By setting up equations for the motion of an electron in the plane case, for instance, and then integrating them, we may obtain the expression

$$X = \frac{1}{\omega_H} \cdot \frac{E}{H} \left[1 - \cos \omega_H t\right] + \frac{V_s}{\omega_H} \sin \omega_H t. \qquad (5.58)$$

Here E is the electric field vector, directed alont the OX axis, and v_s is the velocity of the electrons at their exit from the modulator in the direction of the same axis. By performing operations with these equations analogous to those indicated in the foregoing section, the equation of the locus of

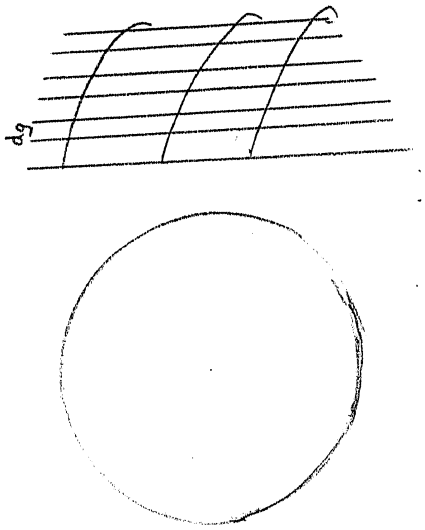

Figure 5.22

foci may be obtained in the form

$$X_F = \frac{1}{\omega_H} \cdot \frac{E}{H} (1 - \cos \omega_H \tau_F) + \frac{V_s}{\omega_H} \sin \omega_H \tau_F. \quad (5.59)$$

The focusing time may be determined from the equation

$$\omega_H \tau_F = \arctan \frac{V_s}{\frac{1}{\omega_H} \cdot \frac{dV_s}{dt} - \frac{E}{H}} \quad (5.60)$$

All of the fundamental quantities that characterize the phase focusing of a stream, for the case of its having a considerable corss-section, may be found from these fairly unwieldy equations. Assuming to be sufficiently small (low values for H and transit time), the case of the operation of a triode in a magnetic field which has been subject of repeated experimental investigations, may be considered with the aid of the simplifications of these

equations so obtained. In this way a fairly satisfactory correspondence may be shown between the theoretically expected behavior of the system and the data given by experiment /8/.

In the case of cylindrical electrodes -- which is of the most practical interest -- two variants must be distinguished. The first and simplest is the system of first-order oscillations, especially in the single-anode magnetron, in which the oscillatory system is included between the cathode and the anode. In this system it is possible, on considering the conditions for the focusing of a stream in a retarding electric field, to carry them over with a sufficient degree of accuracy to the "equivalent electric field" that corresponds to the course of the radial velocity (we have already become acquainted with a similar equivalent substitution in Chapter III, when we considered the simplest electron-kinematic mechanisms).

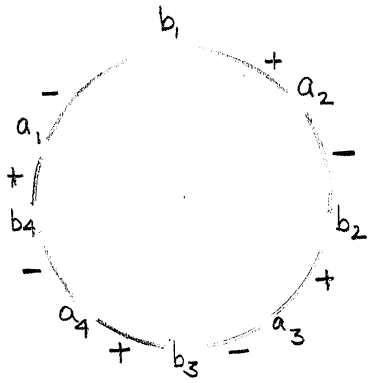

Figure 5.23

The behavior of an electron stream with electronic oscillations of high orders in the split-anode magnetron shows us

another and more complicated pattern In this case the principal role in the energy exchange with the alternating electric fields is played not by the radial components of the motion of the electron stream, but by its tangential components, which create a ring-current. It is in this ring-current that we must seek those processes of phase-focusing that control the oscillatory mechanisms of split-anode magnetrons, with their electronic oscillations of higher orders. Let us in fact imagine (Figure 5.23) the ring-current in a split-anode magnetron. This current represents a ring-shaped layer of electrons rotating in the neighborhood of the anode surface. In that layer, along the perimeter, there must necessarily arise places of maximum density. In the picture of a ring-current represented in Figure 5.23, the slots a_1, a_2, ..., in which the rotating stream traverses the intersegmental field of opposite direction that exerts a retarding action on it, should correspond to the maxima of current density, while the slots b_1, b_2, ..., with accelerating field, should correspond to the minima. During a semiperiod the entire distribution of current density is displaced along the perimeter by the width of a single segment, so as continuously to sustain the proper phase relation. In developing the ring current along the perimeter, it may be represented as a linear electron stream of finite length, in which, under the corresponding conditions of initial velocity (approximating the set ratio of E/H) and of transit time, the assigned spatial distribution of current density (Figure 5.24), should arise, with the initial and final boundary conditions of such density equivalent.

All that has been noted in this section is evidence that in the presence of a magnetic field that bends the trajectories of the electrons the pattern of the process corresponding to the phase focusing of the electron stream acquires very complicated and, under certain conditions, an entirely different meaning. In view of this the phase focusing method may be used only with the utmost caution to study the operation of the magnetron, and only for the very first approximation.

In the cases of the electron streams previously considered it could be assumed, without substantial deviation from the actual picture of phenomena, that the behavior of the entire stream was determined by its foci, places of maximum density sharply differentiated from the other portions of the stream, which are characterized by very low density. Thence, it follows that the effects of the space charge might be neglected -- a neglect that was amply justified.

But, in the presence of a magnetic field, the role of the space charge, especially in the field of the ring current in split-anode magnetrons, becomes exceptionally important. The fact that even though anode currents and emission currents in split-anode magnetrons are only of the order of a few milliamperes, ring currents of the order of an ampere and higher are observed, testifies to this importance.

For this reason the application of any "electrokinematic" or "electron-optical" methods of consideration can easily lead only to the crudest and most violently simplified representation of the processes that actually take place.

5.7 GENERAL ENERGY RELATIONS

The exchange of energy between the electron stream and the alternating electric fields is an extremely important process in the operation of any oscillator. Two energy stages may be distinguished in all cases: the control of the stream, connected with the consumption of energy in the input circuit, and the feed to the load, designed to take off the energy in the output circuit. The energy expended in controlling the stream should naturally be considerably less than the energy withdrawn on the output level. In other words, the alternating component of the current passing through the input circuit should be as low as possible, and the input resistance, consequently, should be higher. The static method of controlling an electron stream, which we have been discussing, would thus appear unsatisfactory in this respect. The output current from the cathode-grid space of a statically controlled tube has an alternating component, the formation of which is responsible for an active component of displacement current and a considerable input conductance. Dynamic control of the stream, effected in devices with velocity modulation, is less liable to these faults. This is manifested with particular distinctness in cases where the modulating device occupies only a very small segment of the path of the electron stream, which segment is traversed by that stream during a very short interval of time in comparison to the period of oscillation. In such a case, on the basis of the considerations developed in Paragraph 5.5, the current leaving the modulator should be considered practically direct current, while the energy consumed in controlling the stream proves to be negligibly small. It may thus, in first approximation, be simply disregarded.

Thus the fundamental energetic calculation of generators with dynamic control should be founded on consideration of the phenomena in the output zone, i.e. in the electric field of the generating circuit.

The energy output delivered by an electron beam to the circuit may be calculated, in the simplest case, by determining the work done by the charges in the alternating zone of the circuit /10/. If a certain current $I_x = Sj_x$ (where S is the cross-section of the electron stream) enters the ouput zone, then the elementary work of the charge carried by this current is obviously expressed as

$$dA = I_x U_k dt, \tag{5.61}$$

where U_k is the potential difference between the boundaries of the output zone. U_k is set by the circuit and varies according to the sinusoidal law: $U_k = U_{ok}\sin(\omega t + \varphi)$. For convenience we also take this opportunity to insert the exit time t_s of the corresponding packet from the modulator as an independent variable. The quantity φ records the actual phase of the alternating potential as the instant the packet arrives at the output zone. Let us assume in first approximation that the transit time of the electrons through the output zone is very small in comparison to the oscillation period. It must not, nevertheless, be forgotten that such a condition, in the present case, cannot involve all of the consequences noted above with respect to the modulator. On the contrary, the active interaction between electron stream and field is accompanied by velocity demodulation, and in the ideal case, when the stream gives up all of its oscillatory energy to the field, it would once more receive a direct current after passing the modulator.

Knowing the relationship of the current I_x and the voltage U_k to the time, the work performed by the electron stream during a period may be calculated as

$$A_1 = \int_0^T I_x U_k dt_s \qquad (5.62)$$

Passing now to the alternating t_s and bearing in mind the expression for the value of U_k, we may now express the power delivered by the stream to the alternating field:

$$P = \frac{1}{2\pi} \int_0^{2\pi} I_x U_{ok} \sin(\omega t_s + \varphi) d(\omega t_s), \qquad (5.63)$$

The electron stream is created by the cathode emission I_{em}, a part of which is absorbed by the grids and other electrodes, by virtue of which I_o may be represented as $I_o = \Psi I_{em}$. The coefficient $\Psi < 1$ here introduced takes into account this practical absorption of the electrons. Taking into consideration, as well, that according to the fundamental relation ,

the expression for the power may be put into the following sufficiently general form

$$P = \frac{I_{em} U_o}{2\pi} \xi_k \Psi \int_0^{2\pi} \frac{\sin(\omega t_s + \varphi)}{\left| \frac{dt_x}{dt_s} \right|} d(\omega t_s). \qquad (5.64)$$

Thence we obtain the "coefficient of voltage utilization"

$\xi_k = \frac{U_{ok}}{U_o}$ analogous to those in the ordinary generating tubes.

Since $I_{em} U_o$ represents the power drawn by the device from the DC source, that feeds it, its efficiency is obviously expressed by

$$\eta = \frac{P}{I_{em} U_0} = \frac{\varepsilon_k \psi}{2\pi} \int_0^{2\pi} \frac{\sin(\omega t_s + \varphi)}{\left|\frac{dt_x}{dt_s}\right|} d(\omega t_s) \qquad (5.65)$$

The integral that figures in equations (5.64) and (5.65) plays an important role in all energy relationships and may be termed the "power integral"

$$L = \int_0^{2\pi} \frac{\sin(\omega t_s + \varphi)}{\left|\frac{dt_x}{dt_s}\right|} d(\omega t_s) \qquad (5.66)$$

Thus the power delivered by the electron stream and the efficiency of the generator may be expressed as follows

$$P = \frac{I_{em} U_0}{2\pi} \varepsilon_k \psi \cdot L \quad \text{and} \quad \eta = \frac{\varepsilon_k \psi}{2\pi} L$$

Now that we have the expression for the power and efficiency, the conditions for sustained oscillation may be obtained from the general consideration that the energy delivered by an electron stream must cover its loss in the oscillatory circuit. The power loss in an oscillatory circuit with shunt impedance Z may be expressed as

$$P_{nom} = \frac{U_{ok}^2}{2Z} \qquad (5.67)$$

The conditions for sustained oscillation may consequently be represented in the form

$$L \geq \frac{\pi}{Z} \cdot \frac{\varepsilon_k}{\psi} \cdot \frac{U_0}{I_{em}} \qquad (5.68)$$

or also, since $U_o/I_{em} = R_o$, where R_o is the DC resistance of the apparatus, this reduces to

$$L \geqslant \frac{\pi}{z} \cdot \frac{\xi_k}{\psi} \cdot R_o \qquad (5.68')$$

in the presence of the known contour (z).

Thence we may obtain the condition that must be satisfied by an oscillatory system so that the oscillations in it of the given electron stream

$$z \geqslant \frac{\pi}{L} \cdot \frac{\xi_k}{\psi} \cdot R_o \qquad (5.69)$$

may be sustained.

These relationships are of an entirelygeneral character and may be applied to any case, all of which, of course, do not necessarily afford the same practical computational possibilities. They are obtained by considering the work performed by the charges formed by an electron stream in the electric field of the output circuit. But this is not the only method we have for calculating the energy.

Another method for energy calculation is based on the determination of the currents delivered by moving bharges to the electrodes that bound the output zone. The two methods are entirely equivalent and of identical value, as has been very clearly shown by one of the works of Katsman /11/. The method of currents delivered is particularly convenient in cases where, for example, the same interelectrode space discharges the functions of several zones, or

where the electron stream returns without reaching one of the electrodes that bound the output zone. The essential features of the method of currents delivered are as follows. The elementary charge dq traveling between the electrons delivers to the circuit connecting these electrodes the current di, which is equal to

$$di = \frac{v}{d}\, dq \qquad (5.70)$$

(cf. Chapter IV, Paragraph 1). The current delivered by all charges present in the interelectrode space is

$$i = \frac{V}{d} \int_{x}^{x+d} dq = \frac{Q}{\tau} \qquad (5.71)$$

where d is the distance between the electrodes.

It is clear from this that if we assume the same velocity v for all the charges present at a given instant in the interelectrode space, the current delivered may be expressed as the relation of all charges Q present in the interelectrode space to the transit time τ taken by the electrons to traverse this space.

The current delivered may be calculated by a more general method, using the following expression

$$di = \frac{i_0 dt_s}{d} v(t_s) \qquad (5.72)$$

where t_s is, as before, the instant when the electron packet $i_0 dt_s$ enters the zone in question. If $\tau(t)$ is the transit time,

then

$$i = \frac{i_0}{d} \int_{t_s}^{t_s + \tau(t)} V(t_s)\, dt_s \qquad (5.73)$$

In specific cases this integral may also occasion certain computational difficulties. The power may obviously be expressed as

$$P = \tfrac{1}{2} I U_{ok}, \qquad (5.74)$$

where I is the amplitude value for the current calculated by (5.73) (or more accurately) that of its component that coincides in phase with U_k.

A third method of calculation is also possible /12/. This is based on the computation of the alternating voltage impressed on the electrodes, using the law, well known for kinematic considerations, of the variation in electron current I(x, t) and the equation of the continuity of the current

$$I(t) = I(x,t) + \frac{1}{4\pi} \cdot \frac{\partial E_x}{\partial t} \qquad (5.75)$$

From this we find the intensity of the inductive field

$$E_x = 4\pi \int I(t)\, dt - 4\pi \int I(x,t)\, dt, \qquad (5.76)$$

and then also the potential difference

$$U = \int_x^{x+d} E_x\, dx = 4\pi \int_x^{x+d} \left\{ I(t)\, dt - \int I(x,t)\, dt \right\} dx \qquad (5.77)$$

In the absence of a charge the value of I(t) is zero, as is the first term on the right side of formula (5.77), while the second term gives the impressed "no-load voltage". If a circuit

that constitutes a load is now connected with the electrodes, then $I = I_L + I_0 + I_R$, from which the corresponding value of I may be found, and together with it the full voltage U, which may be used to compute the power.

These considerations represent only a scheme of possible methods of calculation. Before passing to their specific use on a number of interesting cases, it must be observed that the relationships obtained are, to say, of a summating nature (or recapitulatory). The point is that in the presence of phase focusing and of the density modulation that accompanies it the temporal and spatial relationships of current density are vastly different from the sinusoidal. In consequence of this we are compelled to have recourse to the expansion of the functions in question into a Fourier series and to the consideration of the harmonics that concern us, to which we must then apply the methods of calculation we have just set forth.

5.8 THE CASE OF "DRIFT" OF THE ELECTRON STREAM

Let us now consider the case in which a velocity-modulated electron stream, on traversing the conversion space, through which it moves by intertia ("drifts"), enters the alternating electric field of the second circuit, in the output zone. Let us apply to it the general relations of the preceding section.

For the case of the "drifting" of electrons we have obtained (cf. Paragraph 5.3) the following expression for the current:

$$I_x = I_0 \frac{1}{1 - \frac{\xi\theta \cos \omega t_s}{2(1+\xi \sin \omega t_s)^{3/2}}} \qquad (5.78)$$

The direct application of this expression to the calculations of the power integral would lead to very unwieldy operations that cannot always be analytically performed. In one of his works /13/ this author attempted such a calculation. It yielded results practically indistinguishable from those of the simplified calculations used in different variants by many authors, all of them giving almost exactly identical results. Let us retain all of the assumptions adopted in the preceding chapter: i.e. we shall continue to neglect the action of the space charge, and to assume that the transit time of any electron packet through the modulator and through the second circuit (contour) is small in comparison to the oscillation period, and that the modulation coefficient is considerably less than unity. The latter assumption greatly facilitates the calculation, and in essence does not conflict with the actual conditions of velocity modulation of a stream. By virtue of these assumptions, then, the expression for the current may be represented in the form

$$I_x = I_0 \frac{1}{1 - \frac{\xi\theta}{2}\cos\omega t_s} \qquad (5.79)$$

Let the alternating potential difference

$$U_k = U_{ok}\cos(\omega t + \varphi).$$

act between the plates of the condenser in the second circuit.

Then the elementary work of the charge dq passing through this condenser is expressed as

$$dA = dq \cdot U_{ok}\cos(\omega t + \varphi). \qquad (5.80)$$

But by the law of conservation of charge the value of dq is equal to

$$dq = I_x dt = I_0 dt_s.$$

Consequently,

$$dA = I_0 U_{0k} \cos(\omega t + \varphi) dt_s. \qquad (5.81)$$

Since $t = t_s + \tau = t_s + x/v_s$, then, by making use of the same simplifications (by virtue of the fact that $\xi \ll 1$), we may write (cf. equation 5.20)

$$\omega t = \omega t_s + \frac{\omega x}{V_0} - \frac{\omega x \xi}{2V_0} \sin \omega t_s \qquad (5.82)$$

which gives us the following expression for the power:

$$P = \frac{I_0 U_{0k}}{2\pi} \int_0^{2\pi} \cos\left(\omega t_s - \frac{x\omega\xi}{2V_0} \sin \omega t_s + \frac{\omega x}{V_0} + \varphi\right) d(\omega t_s) \qquad (5.83)$$

This expression may be represented as

$$P = I_0 U_{0k} J_1\left(\frac{x\omega\xi}{2V_0}\right) \cos\left(\frac{\omega x}{V_0} + \varphi\right) \qquad (5.84)$$

where $J_1\left(\frac{x\omega\xi}{2V_0}\right)$ is the Bessel function of order one with respect to the argument $\frac{x\omega\xi}{2V_0}$. Thus the power drawn off through the generator circuit depends on the values of the Bessel functions and of the cosines of the argument $\left(\frac{\omega x}{V_0} + \varphi\right)$. By selecting a value of φ determining a certain additional phase shift, the value of $\cos\left(\frac{\omega x}{V_0} + \varphi\right)$ may be made equal to 1 (i.e. $\frac{\omega x}{V_0} + \varphi = \pi$). In that case the stream will be "exactly in phase" with respect to the second circuit, and the power drawn off there (as is indicated by the minus sign), will prove to be equal to

$$P = \left| I_o U_{ok} J_1 \left(\frac{x \omega \tau}{2 V_o} \right) \right| \qquad (5.85)$$

Considering that $I_o = \psi I_{em}$, $U_{ok} = \xi_k U_o$

$$P = I_{em} U_o \psi \xi_k J_1 \left(\frac{x \omega \tau}{2 V_o} \right) \qquad (5.85')$$

The Bessel function $J_1(z)$ has maxima at the following values for the argument z:

$$z_{max} = 1.84;\ 8.54;\ 14.86 \text{ etc.}$$

The corresponding values of the function:

$$J_1(z_{max}) = 0.582;\ 0.273;\ 0.207, \ldots$$

In this way, for the maximum value $J_1(z) = 0.582$ and $\xi_k = \psi = 1$, we obtain

$$P = 0.582 I_o U_o \qquad (5.86)$$

which yields the maximum efficiency

$$\eta \approx 58\%.$$

It should be noted that under these optimum conditions the distance x of the output circuit from the modulator is $1.84\ x_{F\,min}$ by virtue of the fact that $\frac{x \omega \tau}{2 V_o} = 1.84$, while $\frac{2 V_o}{\omega \tau} = x_{F\,min}$. This may be explained by the circumstance that, as we have seen in the last chapter, the current curves in the "transfocal" region have a double maximum with a pocket between them, and, to a certain extent, reproduce the well-known pattern of increase in the efficiency of an ordinary generator, with feedback on the transition to oscillation at the cut-off.

Thus, the value of the power integral L in this case may be expressed as

$$L = 2\pi J_1\left(\frac{X\omega\varepsilon}{2V_0}\right) \qquad (5.87)$$

By virtue of this, the conditions for sustaining oscillation in the circuit can be represented as

$$J_1\left(\frac{X\omega\varepsilon}{2V_0}\right) \geqslant \frac{1}{2z}\cdot\frac{\varepsilon_k}{\psi}\cdot R_0 \qquad (5.88)$$

At the optimum conditions $J_1\left(\frac{X\omega\varepsilon}{2V_0}\right) = 0.582$, the selection of the circuit is determined by the relation

$$z \geqslant 0.86\, R_0\,\frac{\varepsilon_k}{\psi} \qquad (5.89)$$

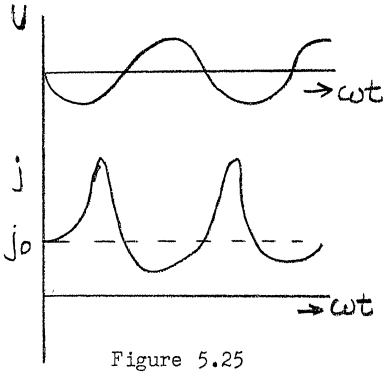

Figure 5.25

Under these conditions for obtaining optimum ouput it is necessary for the maximum density of the current traversing the electric field of the circuit to coincide in time with the maximum retarding voltage, as shown in Figure 5.25. This relation must hold for the "instantaneous" interaction between electrons and field, i.e. if the transit time through the circuit is incomparably shorter than the oscillation period.

This presupposition, however, is a simplification of the actual pattern of interaction between electron stream and field. Such in theory and practice a modulator may be traversed by the electrons in any conveniently short interval of time assigned, since its action reduces to certain relatively shallow variation of their velocity, given a constant current density through the modulator. In studying the phenomena in the output zone, we must reckon with that final velocity at which a "density wave" will be propagated in the stream, and with variation of this density not only in time but also along the x axis in the region of the output zone. Here a problem arises kinematically that is akin to that considered in Paragraph 5.5.

Some authors have reached the conclusion that maximum output corresponds to a transit time equal to an uneven number of semicycles

$$\tau = (2n+1)\frac{T}{2}, \tag{5.90}$$

which in the simplest and best case (in which the defocusing action of the space charges cannot express itself) reduces to

$$\tau = \frac{T}{2}. \tag{5.90'}$$

But the phase relations between current and voltage must be characterized somewhat differently if account is taken of the transit time through the output zone. The conditions depicted by Figure 5.25 will correspond to the center of the output zone. At an entrance into it defined by the instant t_e and the phase ωt_e, the curves of current and voltage will appear as shown in Figure 5.26, on which they are plotted in dependence on ωt_e. The further calculation of power made by these authors leads, however, to entirely identical

results, since if a small ξ is assumed, the same expression for the power integral is obtained /12/. This circumstance casts doubt on the above-described role of the transit time through the output zone. We shall analyze this question more in detail later on, and shall show that the final time of transit reduces the efficiency.

To conclude this section it is of interest to note that the concept of "focusing" is not a necessary element in the correct calculation of the energetics of an electron stream acting in a general generating circuit /14/. In fact, by assuming the velocity of an electron entering the generating apparatus to be dependent on the entrance angle δ the mean energy of an electron passing through the field during a period may be calculated as:

$$\frac{m}{2}\cdot\frac{1}{2\pi}\int_0^{2\pi}[v(\delta)]^2\,d\delta \qquad (5.91)$$

If the energy is less than $v_0^2/2$, the electron will give up its energy to the alternating field, and the efficiency of the oscillator may be found from the expression:

$$\eta = 1-\frac{1}{2\pi}\int_0^{2\pi}\left(\frac{v(\delta)}{V_0}\right)^2 d\delta \qquad (5.92)$$

If the value of (5.91) js greater than $mv_0^2/2$, then the electrons will take energy from the alternating field and will leave it at higher than their initial velocities. From this point of view the apparatus should operate as a generator of oscillations even in the case when there is only a single electron at a time in the alternating field. Assume that this electron on leaving the modulation zone has the energy

$$e(U_0 + U_1\sin\delta), \qquad (5.93)$$

and that it then travels the distance d to the output zone, which it enters at the phase

$$\delta + \frac{\theta}{(1+\varepsilon \sin\delta)^{1/2}} \quad \text{where } \theta = \frac{\omega d}{V_0} \qquad (5.94)$$

The energy acquired by the electron during its transit through the output zone, in which there is the potential difference U_k, is equal to

$$eU_k \sin\left[\delta + \frac{\theta}{(1+\varepsilon \sin\delta)^{1/2}}\right] \qquad (5.95)$$

Since the modulator in practice consumes no energy, the whole of the energy effect is obtained in the output zone; its calculation for the period likewise leads to a peculiar "power integral"

$$L_{\varepsilon\theta} = \frac{1}{2\pi}\int_0^{2\pi} \sin\left(\delta + \frac{\theta}{(1+\varepsilon\sin\delta)^{1/2}}\right) d\delta \qquad (5.96)$$

It will readily be seen that δ here plays a role that frequently figures in our exposition of ωt_s. On simplifying the expression under the integral by the assumption that $\varepsilon \ll 1$, we again obtain

$$L_{\varepsilon,\theta} = \frac{1}{2\pi}\int_0^{2\pi} \sin(\delta + \theta - \tfrac{1}{2}\varepsilon\theta\sin\delta)\, d\delta = \sin\theta \cdot J_1\left(\frac{\varepsilon\theta}{2}\right),$$

where $J_1\left(\frac{\varepsilon\theta}{2}\right)$ is a Bessel function of order one. Thus, the mean energy received by the electron in the output zone is equal to

$$eU_k \sin\theta \cdot J_1(\varepsilon\theta/2).$$

To sustain oscillation, this value must be negative, which may be realized either by means of U_k or $\sin\theta$. For $\theta = \pi/2,\ 3\pi/2,$

etc we have $|\sin\theta| = 1$, and the optimum efficiency is obviously expressed as

$$\eta = \frac{U_k}{U_0} \cdot J_1\left(\frac{\xi\theta}{2}\right)$$

or, in our former notation,

$$\eta = \xi_k J_1\left(\frac{x\omega\xi}{2U_0}\right)$$

which coincides with the formulae previously obtained.

5.9 THE CASE OF THE RETARDING FIELD

If the electron stream in the conversion zone is subjected to the action of a retarding electric field, then at small retardations a "compression" of the stream is obtained and its focusing facilitated, thus leading to an increase in the effective output zone /15/. If the retardation is so great that the stream returns to the modulator, then the modulator itself plays the role of an output zone with respect to the return stream. This superposition of modulation zone and output zone is characteristic for single-circuit devices, such as for instance the reflex klystron, the circuit diagram of which is given in Figure 5.27. Assuming a very small transit time through the modulator for both direct and return streams, and a very small amount of energy consumed in modulating the direct stream, let us consider the energetic interaction between the return stream and the modulator field. By reasoning in complete conformity with the foregoing, the work done by the return stream in the modulator field during a period may be represented as:

$$A = \frac{1}{\omega} \int_0^{2\pi} I U_1 \sin(\omega t_s + \varphi) d(\omega t_s) \qquad (5.98)$$

where I is the value of the current returning to the modulator, U_1 is the amplitude of the alternating voltage in it. The quantity φ characterizes, in essence, the time spent by an electron packet in the conversion zone, and depends on the exit angle ωt_s.

But since almost all the work during the period is performed by the focusing of the electron stream, φ may therefore be defined as the angle of transit until focusing of the corresponding electron packets, namely, those packets which must be focused at the instant of return to the modulator. Their exit phase, as we have seen in the preceding chapter (the system of "return focus") is equal to $\omega t_s = \pi$ for sinusoidal variation in the modulator voltage. Since a packet returning and being focused should encounter the maximum retardation, it is not difficult to see that $\varphi = \pi/2, 3\pi/2, \ldots$, etc, i.e. formula (5.98) may be represented in the form

$$A = \frac{1}{\omega} \int_0^{2\pi} I U_1 \cos \omega t_s d(\omega t_s) \qquad (5.99)$$

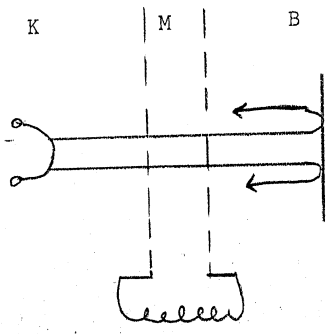

Figure 5.27

The current I returning to the modulator may be expressed by applying formula (5.40) under the condition that x = 0,

$$I = I_0 \frac{1}{1 + \frac{\frac{2\xi\omega}{nV_0}\cos\omega t_s}{\sqrt{1+\xi\sin\omega t_s}}} \qquad (5.100)$$

Under the condition of a return of focus $\left(n = \frac{2\xi\omega}{V_0}\right)$ the coefficient before $\cos\omega t_s$ in the denominator of this expression becomes unity. On writing $\frac{2\xi\omega}{nV_0} = \theta$, and noting that the regime of return of focus and those regimes adjoining it are energetically the most advantageous, we may simplify the calculation of the power integral by confining ourselves to the value $\theta = 1$. The power integral, which for the case under consideration is equal to

$$L = \int_0^{2\pi} \frac{(1+\xi\sin\omega t_s)^{1/2}\cos\omega t_s}{(1+\xi\sin\omega t_s)^{1/2} + \theta\cos\omega t_s} d(\omega t_s) \qquad (5.101)$$

is considerably simplified if we put $\theta = 1$ and $\xi \ll 1$,

$$L = \int_0^{2\pi} \frac{\cos\omega t_s d(\omega t_s)}{1+\xi/2\sin\omega t_s + \cos\omega t_s} + \frac{\xi}{2}\int_0^{2\pi} \frac{\sin\omega t_s \cos\omega t_s d(\omega t_s)}{1+\xi/2\sin\omega t_s + \cos\omega t_s}$$

Taking advantage of the well-known substitution

$$\sin x = \frac{2t}{1+t^2} \qquad \cos x = \frac{1-t^2}{1+t^2} \qquad \text{where } t = \tan x/2$$

and performing the necessary transformations, we obtain the following expression for the power integral under the regime of return of focus

$$L \approx \frac{16\pi + 4\xi(\pi-1)}{8+\xi} \qquad (5.102)$$

Since $\xi \ll 1$, it may be approximately assumed that

$$L \approx 2\pi;$$

whence, in first approximation, the very simple expressions for the power and efficiency under a system of "return of focus " may be obtained:

$$P \approx I_{em} U_o \xi \psi$$

$$\eta \approx \xi \psi \qquad (5.103)$$

In contrast to the two-circuit [or two resonator] apparatus, here represents at the same time the coefficient of velocity modulation and the coefficient of voltage utilization. The value $L \approx 2\pi$ leads us likewise to a very simple condition for the selection of the circuit:

$$z \geqslant \frac{R_o}{2} \frac{\xi}{\psi} \qquad (5.104)$$

where $R_o = U_o / I_{em}$. Taking into consideration the fact that the Barkhausen relation $\lambda^2 U_o$ = constant is rather well fulfilled in the regime s of electron streams under consideration, the following relation, which is not without interest, may be obtained:

$$z \geqslant \frac{2\pi^2 10^6 \xi^3}{e m \lambda^2 n \psi} \qquad (5.105)$$

Here n is the "coefficient of retardation" introduced in the preceding sections. A series of substantial consequences follows from a consideration of these relations:

(1) To obtain oscillations with the highest efficiency, the shunt-impedance of the circuit must, other things being equal, be increased.

(2) For an invariable circuit, increase in efficiency demands a regime of forcing, during which the emission current, other things being equal, should increase roughly as the cube of the efficiency.

(3) For varying length of the wave generated and constant circuit parameters, the accelerating constant voltage U_0 should vary proportionally to ξ^2 and inversely proportionally to λ^2; the emission current under these circumstances is proportional to ξ^3 and inversely proportional to λ^2; and, finally, the power consumed is proportional to ξ^5 and inversely proportional to λ^4.

These conclusions point to the very substantial difficulties that arise in principle when fairly high efficiencies and very short waves are produced by velocity-modulated electron streams. The conclusions are qualitatively applicable to all other electron generators with phase focusing of the electron stream, in addition to generating circuits using retarding fields.

5.10 THE INFLUENCE OF THE SPACE CHARGE

It has been assumed in all the foregoing discussions and conclusions that the effect of the interaction between the electrons in the stream is negligibly small. This is true, however, only for negligibly small current densities or for very short intervals of electronic interaction. In practice both these conditions are almost unrealizable, and account must therefore be taken, even though only qualitatively, of the effect of the interaction between the electrons in the stream on the energy relations. This effect should naturally make itself felt most of all in the conversion zone.

Let us analyze the simplest example of "drift" for which the velocities of the electrons in the conversion zone might be considered

as constant. This is true, however, only if we neglect the influence of the forces of electronic interaction. This influence manifests itself in a certain alignment or evening out of the density along the stream, and, with particular force, in the reduction of density at the places of focus-formation. A somewhat more detailed idea of the character of this interaction may be gained from the following considerations /15/. The instant t_x when the electrons leave the conversion zone is characterized, under the previous assumptions, by the expression

$$t_x = t_s + x/v_s.$$

Inasmuch as the uniformity of the motion of the electrons has been disturbed by reason of their interaction, this equation must be replaced by another one:

$$t_x = t_s + \int_0^x \frac{dx}{v_s} \qquad (5.106)$$

in which the velocity v_s is no longer independent of the electron's position, but varies from point to point.

From equation (5.106) we have

$$\frac{dt_x}{dt_s} = 1 - \int_0^x \frac{dx}{v_s^2} \cdot \frac{dv_s}{dt_x} \cdot \frac{dt_x}{dt_s}, \qquad (5.107)$$

where $\frac{dv_s}{dt_x}$ represents the acceleration of the electron in the field of the space charge E, with which it is connected by the relation

$$\frac{dv_s}{dt_x} = \frac{eE}{m} \qquad (5.108)$$

The latter in turn depends on the excess density of the space charge in the following manner:

$$\frac{dE}{dx} = -4\pi\rho = -\frac{4\pi}{v_s S}(i_x - i_0) \qquad (5.109)$$

$$E = -\frac{4\pi i_0}{S}\int_0^x \frac{i_x - i_0}{v_s i_0}\,dx,$$

where S is the cross-section of the electron stream, and i_0 and i_x are the values for the current intensity at the corresponding points, while $i_x/i_0 = dt_s/dt_x$ (by the law of conservation of charge).

By using this relation in equation (5.109), and then substituting equation (5.109) in the expressions (5.108) and (5.107) and performing the necessary transformations, we obtain:

$$\frac{dt_x}{dt_s} - 1 = -\frac{4\pi e i_0}{m S v_0^3}\int_0^x ds' \int_0^{x'}\left(\frac{dt_x}{dt_s} - 1\right)dx'' \qquad (5.110)$$

After two successive differentiations with respect to x, and introduction of the notation:

$$Y(x) = \frac{dt_x}{dt_s} - 1 = -\frac{i_x - i_0}{i_x}$$

$$\alpha^2 = \frac{4\pi e i_0}{m S v_0^3}$$

we obtain

$$\frac{d^2 Y(x)}{dx^2} + \alpha^2 Y(x) = 0 \qquad (5.111)$$

A solution of this equation is the function

$$Y(x) = A \sin \alpha x + B \cos \alpha x \qquad (5.112)$$

If $x = 0$, then it follows from equation (5.107) that

$$Y(x) = 0$$

$$\frac{dY}{dx} = -\frac{\omega V_s}{2V_0 U_0} \sin \omega t. \qquad (5.113)$$

The function satisfying equation (5.107) and the initial conditions of expression (5.113) may be represented in the following form:

$$Y(x) = \frac{dt_x}{dt_s} - 1 = \frac{i_0 - i_x}{i_x} = -\frac{\omega \varepsilon}{2V_0} \cdot \frac{\sin \alpha x}{\alpha} \sin \omega t$$

On integrating this equation, we have

$$t_x = t_s + \frac{x}{V_0} - \frac{\omega \varepsilon}{2V_0} \cdot \frac{\sin \alpha x}{\alpha} \sin \omega t_s. \qquad (5.114)$$

This expression for the time t_x should now be utilized by us in calculating the power, for which we now obtain the expression

$$P = I_0 U_0 \varepsilon_k J_1 \left(\frac{\omega \varepsilon x}{2V_0} \cdot \frac{\sin \alpha x}{\alpha} \right) \sin \left(\frac{\omega x}{V_0} + \varphi \right). \qquad (5.115)$$

Comparison of this formula with the expressions obtained earlier for generator power under electron drift reveals the presence of an additional factor $\sin \frac{\alpha x}{\alpha}$ in the argument of the Bessel function. For $\alpha x \ll 1$, a certain correction should be used to reduce the power and the efficiency of the generator.

Various authors have concerned themselves generally with the question of the defocusing effect of the forces of electron interaction, but it has not yet received a sufficiently rigorous and precise treatment physically. Quantiatively, too, the calculation of the influence of the space charge in the electron stream is very

important for the solution of a good many problems connected with the most advantageous practical utilization of electron-emitting apparatus. To this for example belongs the question of the limiting density in the beam, which has been touched upon in the literature from the point of view of electronic optics. The solution of this question is especially interesting with respect to the focal densities of the current, which are formally considered infinitely great on account of the condition $j_x = \infty$, but which are of course in fact limited by precisely the effect of the space charge.

Many fundamental calculations, however, are made with a very fair measure of success, and without greatly diverging from reality, without taking account of the space-charge effect. In essence the matter simply reduces to this: that the energy of electronic interaction will remain negligibly small as long as the dimensions of the electron concentrations in the direction of motion are less than the length of the corresponding zone. Let the total electronic charge q transferred by the stream during the oscillation period T

$$qN\frac{P}{U}T$$

where P is the power and U the voltage, be concentrated in the volume $v \cong l^3$ (l being the linear dimensions of volume). Then the electrostatic energy of this charge

$$\mathcal{E} = \frac{1}{l}\left(\frac{PT}{U}\right)^2$$

At the same time the total work done by the stream is equal to PT. And the relation

$$\frac{\mathcal{E}}{PT} \approx \frac{PT}{lU^2}$$

will thus characterize the role of the electrostatic interaction of the electrons.

Let us illustrate these considerations by an example of a very unfavorable regime: let $P = 10^9$ (100 watts), $U = 3.3$ (i.e. 1000 volts), $l = 1$ (which corresponds to an electrode area of the order of cm^2 and a distance between them of the order of mm), $T \approx 0.3 \cdot 10^{-9}$ ($\lambda \approx 10$ cm).

Then

$$\frac{PT}{IU^2} \approx \frac{10^9 \cdot 0.3 \cdot 10^{-9}}{3.3^2} \approx 0.03 \quad \text{etc}$$

i.e., even under such rigid conditions the influence of electronic interaction is very small. These and analogous considerations /1/ allow us to conduct our calculations with a satisfactory approximation to reality without taking the space charge into account, and drawing that charge into the picture only in cases where its action might produce considerably more appreciable changes in the results than in the examples we have just examined.

/1/ The considerations presented were expressed by Professor L. E. Gurevich in the discussion of the author's doctoral dissertation in the Academic Board of the Physical Faculty of the LGU on January 5, 1944.

BIBLIOGRAPHY FOR CHAPTER V

1. E. Bruche and A. Recknagel, ZS.f.Phys. , 108, 459, 1938.
2. V. I. Kalinin, IAN,s. fiz. X No 1, 1946.
3. F. Borgnis and E. Ledinegg, ZS f. techn. Phys. II, 256, 1940.
4. M. Tombs, Wireless Engineering, February 1940.
5. R. Koempfner, Wireless Engineering, 478, November 1940.
6. H. Hollmann, TFT 31, 281; 322 (1942); 32, 12; 37; 65 (1943).
7. D. Webster, Journ. Appl. Phys. 10, 189, 1939; 10, 864, 1939.
8. P. Y. Golubkov, ZhETF XIV, 289, 1944.
9. V. I. Kalinin, Detsimetrovnyye i santimetrovnyye volny (Decimeter and Centimeter Waves) Svyaz'izdat, 1939, Chapters III and IV.
10. V. I. Kalinin, Osnovy kinematicheskoy teorii generirovaniya elektronnikh kolebaniy (Principles of the Kinematic Theory of Generation of Electronic Oscillations), Doctoral Dissertation, LGU 1943.
11. Yu. A. Katsman, IAN, ser. fiz. IV, 506, 1940.
12. F. Ludi, Helv. Phys. Acta, XIII, 122, 1940.
13. V. I. Kalinin, IAN, ser. fiz. IV, 532, 1940.
14. V. Savel'yev, ZhTF, X, 1365, 1940.
15. E. Condon, Journ. Appl. Phys. 11, 502, 1940.

CHAPTER VI

MICROWAVE GENERATORS WITH DYNAMIC CONTROL

6.1 THE ELECTRON-STREAM DRIFT OSCILLATOR (KLYSTRON)

The klystron is an electron-radiating device that may be used in the UHF field as an oscillator, an oscillation amplifier, or a frequency multiplier. The electron streams in a klystron pass successively, in space and in time, through five principal

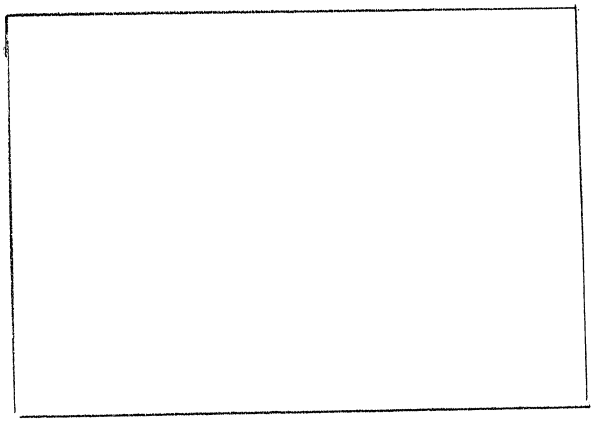

Figure 6.1

zones: (I) acceleration, (II) modulation (III) conversion, (IV) output, and (V) clearing (Figure 6.1), while the distinctive characteristic of the klystron is the drift of the "modulated stream", i.e. the absence of an electric field in the conversion zone. In its practical development, the two high-frequency zones II and IV may either belong to two different oscillating systems, constructed at corresponding frequency (the "ordinary" klystron of the Varian brothers) (Figure 2.35), or to the same system, as in the single-circuit klystrons of Ludi and Katsman (Figure 2.39) [1]. The tubes with dual modulators and output arrangements (the

Hahn and Metcalf type), which are described in Chapter II, likewise essentially belong to the class of klystron devices, since they all possess the characteristic klystron feature: the drift of the electron stream in the conversion zone.

(a) Kinematic Analysis of the Klystron

Let us consider the apparatus represented in Figure 6.1, consisting of the cathode K, emitting the electron stream, the grid condenser of the modulating circuit disposed along the path of that stream, the condenser of the second circuit CD and the collector-electrode E. The drift space (conversion zone) BC has the fixed length l. Both of the oscillatory circuits have the same positive potential U_0 with respect to the cathode. The interaction of the electron stream with the alternating field occurs within the condensers AB and CD. We retain the previous assumptions on the shortness of electron transit time through the modulator and through the second circuit. We determine the alternating voltage between the condenser plates as follows:

$$\text{Circuit I: } u_1 = U_1 \sin \omega t_s$$

$$\text{Circuit II: } u_2 = U_2 \sin(\omega t_s + \varphi).$$

When the klystron is operating as an oscillator, a certain part of the energy given up by the electrons in the second circuit is used up through the corresponding feedback connection to sustain the oscillations in the first circuit that control the stream. The phase difference φ between the alternating voltage in the first and second circuits is due to the feedback mechanism. We see a similar pattern in the ordinary regenerator triode, where

of the two possible methods of connecting the feedback coil only one can be employed, namely that which creates an alternating grid voltage of opposite phase from the anode. The klystron offers a greater degree of freedom in this respect: by providing a feedback connection in the shape of a line of definite length, any desired value of φ may be obtained, and it is this that constitutes the first substantial difference between the klystron and the ordinary triode generator with feedback. The second important difference is that the klystron can be operated as an oscillator at any value of φ, since it uses the "drift", i.e. electron transit time between the circuits, as an additional element of phase regulation. In fact, to have the stream give up energy to the alternating field in the condenser of circuit II it is only necessary for the maximum concentration of the stream to impinge on this condenser at the instant of maximum retardation. This condition may be met either by proper selection of φ by means of the feedback mechanism, or by adjusting the transit time. Experimental investigations [2] of the feedback action in the klystron have shown that the feedback line may have any length at all, but that it is preferable to avoid having it constitute a circuit tuned to the same frequency as the exciting oscillations. A tuned feedback line introduces a strong reactance into the main oscillatory circuit, while the load from an untuned line is almost imperceptible.

Let us now examine the kinematic conditions for klystron excitation at various values of φ, considering the drift space to be equivalent in first approximation to the minimum focal length $= x_{F_{min}}$. Let us analyze the case $\varphi = 0$, the case where the

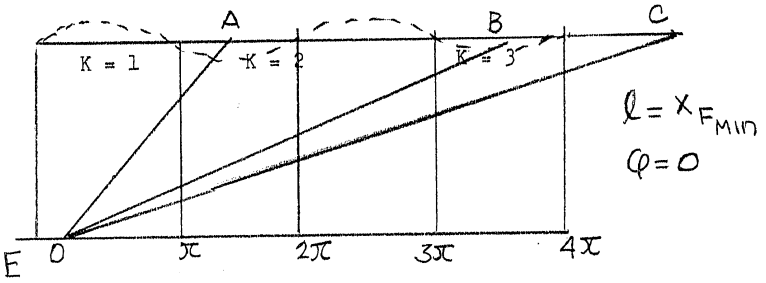

Figure 6.2

oscillations in both circuits are in phase. The curves of variation in the voltage in this case are plotted in Figure 6.2. The optimum condition for sustained oscillation is obviously the "arrival of the maximum current density at the condenser of circuit II at the instants marked A, B, C... The lines EA, EB, EC... represent the time-distance graphs of motion of the electron packets "that arrive at the maxima of the current density curve". The segment OE must represent $\omega t_{s_{max}}$ (cf. Chapter V, Paragraph 3). Thus, the transit angle of these packets to the points A, B, C... may be represented as

$$\omega \tau = (4k - 1)\frac{\pi}{2} + |\omega t_{s_{max}}| \qquad (6.1)$$

where the quantity k assumes the integral values k = 1, 2, 3,...

By virtue of the condition $\ell = x_{F_{min}}$, $\omega t = \theta_{F_{min}}$ should hold, and from formula (5.27') we may write

$$\frac{2(1 + \xi \sin \omega t_s)}{\xi \cos \omega t_s} = (4k - 1)\frac{\pi}{2} + |\omega t_{s_{max}}| \qquad (6.2)$$

To apply this formula to a specific case, the values of ωt_s, $\sin \omega t_s$ and $\cos \omega t_s$ that correspond to $\omega t_{s_{max}}$ must be substituted in it. But for small values of ξ we may assume $|\omega t_{s_{max}}| = \sin \omega t_{s_{max}}$. Then $\sin \omega t_{s_{max}} = -\xi$, and the foregoing formula takes the form

$$\omega \tau_F = \frac{2(1-\xi^2)}{\xi} = (4k-1)\pi/2 \qquad (6.3)$$

(We neglect the value of $|\omega t_{s_{max}}|$ by comparison with $(4k-1)\pi/2$).

Thence, the following equation may be set up for :

$$\xi^2 + (4k - 1)\pi/4\,\xi - 1 = 0,$$

from which we obtain an expression for ξ in terms of k:

$$\xi = -\frac{(4k - 1)}{8} \pm \sqrt{\frac{(4k - 1)^2}{64} + 1} \qquad (6.4)$$

which, on slight simplification, reduces to

$$\xi = \frac{4}{(4k - 1)\pi} \qquad (6.4')$$

We thus reach the very interesting result: the value of the modulation coefficient ξ would appear to assume various values as a function of the drift time, or to put it better, of the transit angle of the packet being focused. The latter, as is evident, assumes

discrete values determined by the instants of incidence of the focus at A, B, C,..., which values are found by formula (6.1). Consequently, to excite the klystron under the conditions described, the modulation coefficient $\mathcal{E}$ should have one of the discrete values defined by formula (6.4) or (6.4') and depending on the "order of excitation" k. The first excitation region k = 1 is characterized by the smallest transit angle and the highest value for $\mathcal{E}$. Let us calculate the value of for the first few excitation regions (Table 6.1).

Table 6.1

VALUES OF FOR SEVERAL EXCITATION REGIONS

k	1	2	3 ...
$\mathcal{E}$	0.4	0.18	0.12 ..

The selection of one excitation region or another may, obviously, be made on fixing the feedback, by means of varying the factors that determine the transit angle, i.e. the accelerating potential U_o and the generated wavelength λ. Let us introduce these quantities into our formula. On substituting $\sin \omega t_s = -\mathcal{E}$ in the formula, for $x_F = 1$, we obtain

$$\frac{l\,\omega}{2V_o} = \frac{1-\mathcal{E}^2}{\mathcal{E}} \qquad (6.5)$$

but since $$v_o = \sqrt{2\,\frac{e}{m}\,U_o} = 6\cdot 10^7 \sqrt{U_o},$$

but $$\omega = \frac{2\pi C}{\lambda} = \frac{6.28\cdot 3\cdot 10^{10}}{}$$

or since $\mathcal{E} \ll 1$

$$\lambda\sqrt{U_0} = 1570\ \frac{\mathcal{E}l}{1-\mathcal{E}^2} \qquad (6.6)$$

$$\lambda\sqrt{U_0} = 1570\ \mathcal{E}l$$

This formula is a relation of the type of the Barkhausen equation, first introduced for "electronic oscillations". This equation indicates the fundamental unity that subsists in the mechanism of all generators of electronic oscillations and makes it possible to compute the "working diagram", that is, the regimes or systems that correspond to the maxima of klystron excitation. Since $\mathcal{E}$ is determined by the number k of excitation region, the value of $\lambda\sqrt{U_0}$, at given dimensions of the device (l), is a function of the same quantity k. Its values for various excitation regions is as follows:

Table 6.2

VALUE OF U_0 FOR SEVERAL EXCITATION REGIONS

k = 1	k = 2	k = 3
$\lambda\sqrt{U_0} = 748\,l$	$\lambda\sqrt{U_0} = 328\,l$	$\lambda\sqrt{U_0} = 190\,l$

The physical meaning of these results is as follows. If the oscillating systems of a generator are tuned to a certain wavelength λ then, if their alternating voltages are in phase and the DC accelerating potential U_0 varies continuously, a whole series of discrete maxima of oscillation intensity should be produced. These maxima correspond to the values of U_0 expressed by the formula

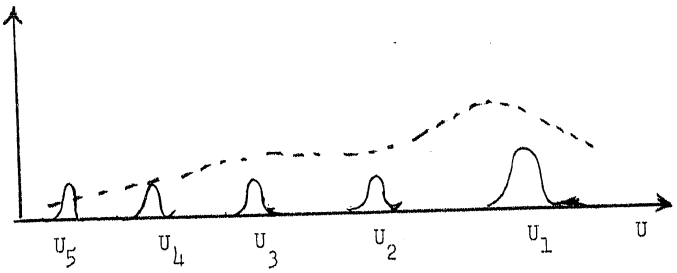

Figure 6.3

$$U_o = [1570 \frac{\varepsilon \ell}{1-\varepsilon^2} \cdot \frac{1}{\lambda}]^2 \qquad (6.7)$$

or, approximately,

$$U_o = [\frac{2000}{(4k-1)} \cdot \frac{1}{\lambda}]^2 \qquad (6.7')$$

Consequently, when we represent the oscillation intensity W_k as a function of U_o, we should obtain a series of maxima for the device in question similar to those shown in Figure 6.2. These maxima, however, cannot be very sharp, since in the corresponding phase condenser II will receive the current maxima in the "prefocal" regime ($\ell < x_{F_{min}}$) and "bicornute" or "two-pronged" maxima during the "transfocal" regime ($\ell > x_{F_{min}}$), and the oscillation will be sustained so long as the value of the energy given up by the stream is sufficient to cover the losses in the circuit, feedback and load line. Given this situation the separate regions of oscillation may merge in such a way that the generator is excited over a very wide interval of variation in U_o (the broken line in Figure 6.3). The discrete character of the excitation regions may be more readily noted, the larger the load is; and this has also been observed in practice.

Let us now examine the case where the circuits are operating

in opposite phases, i.e. where $\varphi = \pi$, other things being equal. This is illustrated graphically by Figure 6.4. Analogous treatment to the foregoing case yields the following results. The transit angle corresponding to the incidence of the focus at points A, B, C,... will be represented in this instance as

$$\omega\tau = (4k + 1)\,\pi/2 + |\,\omega t_{s_{max}}\,|. \qquad (6.8)$$

Here the k may assume the values k = 0, 1, 2, 3,... By computations analogous to the foregoing, we express ξ :

$$\xi = -\frac{(4k + 1)\pi}{8} \pm \sqrt{\frac{(4k + 1)^2\,\pi^2}{64} + 1} \qquad (6.9)$$

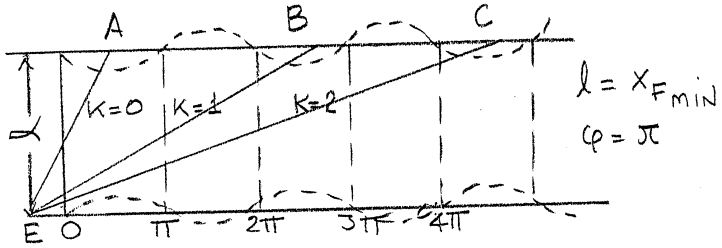

Figure 6.4

or, in somewhat simplified form:

$$\xi = \frac{4}{(4k + 1)\pi} \qquad (6.9')$$

This leads similarly to a series of discrete value for ξ, corresponding to the various excitation regions (Table 6.3).

Table 6.3

VALUE OF $\mathcal{E}$ FOR SEVERAL EXCITATION REGIONS

k	0	1	2	3	...
$\mathcal{E}$	0.68	0.24	0.16	0.10	...

For k = 0, the regime under examination allows us to obtain oscillations with a smaller transit angle ($\sim \pi/2$) and a higher modulation coefficient. From this a conclusion may be drawn as to the greater advantageousness of the second regime. Operation in the first excitation region, however, requires us to apply a very high accelerating voltage U_0, which may not always be possible in practice.

In this case the Barkhausen relation assumes the following form:

Table 6.4

VALUES OF $\lambda\sqrt{U_0}$ FOR SEVERAL EXCITATION REGIONS

k = 0	k = 1	k = 2	k = 3
$\lambda\sqrt{U_0} = 1975\,\ell$	$\lambda\sqrt{U_0} = 400\,\ell$	$\lambda\sqrt{U_0} = 258\,\ell$	$\lambda\sqrt{U_0} = 160\,\ell$

The voltages corresponding to the maxima of oscillation intensity may be calculated in this case by the formula

$$U_0 = \left[\frac{1570\,\mathcal{E}\,\ell}{1-\mathcal{E}^2}\cdot\frac{1}{\lambda}\right]^2 \qquad (6.10)$$

or, approximately,

$$U_0 = \left[\frac{2000}{(4k+1)} \cdot \frac{l}{\lambda}\right]^2 \qquad (6.10')$$

Let us illustrate these theoretically obtained excitation conditions by a few experimental data taken from the works of Devyatkov, Danil'tsev and Piskunov [2]. They studied a klystron with interchangeable feedback, by means of which φ could be adjusted, and operated it on a wavelength λ = 17.5 cm, at a drift length l = 5 cm. The values of U_0 for the maxima of the respective regions, computed and observed, are given in Table 6.5.

Table 6.5

VALUES FOR U_0 AT THE MAXIMA OF THE RESPECTIVE REGIONS

In-phase Operation $\varphi = 0$			Anti-phase Operation $\varphi = \pi$		
Region No	U_0 calculated	U_0 observed	Region No	U_0 calculated	U_0 observed
1	55,000	---	1	324,000	---
2	6,800	---	2	13,000	---
3	2,700	---	3	4,020	---
4	1,440	1320	4	1,920	---
5	905	820	5	1,130	1,060
6	620	615	6	740	745
7	448	453	7	520	535
			8	388	397

It will be seen from this table that the first and most advantageous excitation region requires the use of such high accelerating voltages as to be in practice impossible in this instance. In general the value of φ set by the feedback adjustment may be at any desired

level. Exactly the same thing may be done with $l \neq x_{F\,min}$. The latter is required by the energetic conditions for maximum output that we have considered above (Chapter V, Paragraph 8) under which $l = 1.84 \cdot x_{f\,min}$. Under any and all conditions we have to do with the relations between three quantities: the modulation coefficient ξ, the transit angle θ and the integer k of the excitation region. At a fixed natural frequency of the oscillatory system variation in U_o involves the creation of discrete excitation regions with differing values of ξ. However, for $l \neq x_{F\,min}$, the discreteness of the excitation regions tends more or less to disappear, and the value of ξ is no longer bound by such rigid and definite conditions as in the regimes where $l = x_{F\,min}$. All this diversity in the relations between the basic kinematic parameters of the regime leads to an exceedingly facile excitation of the klystron generator. Provided only that the energy borne by the electron stream to the generating circuit be sufficient to compensate for the losses of that circuit, the kinematic conditions determined by the formulae of the preceding section are, within a wide range, automatically established. This conclusion is in complete agreement with the sparse experimental data available in the literature, but the question of the excitation regions of the klystron generator still demands thorough going experimental investigation.

(b) The Question of the Power and Efficiency of the Klystron

The analysis given in Paragraph 8 of the preceding chapter of the energy relations for the electron stream during drift is, of course, entirely applicable to the klystron generator. Let us

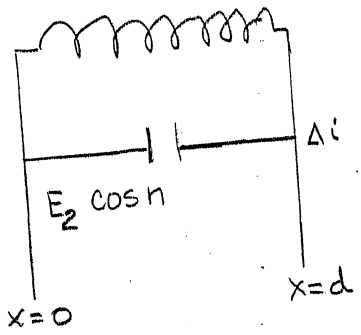

Figure 6.5

dwell here on certain factors that introduce a certain amount of detail into the examination of the general relationships. This detailed analysis involves the following circumstances: allowance for the finite transit time in the output zone, i.e. in the condenser of the second circuit, for the influence of this time of the value of efficiency, and for the non-sinusoidal currents passing through the output zone (manifestation of harmonics). Let us imagine an equivalent circuit for the output zone and the circuit connected with it (Figure 6.5). As a certain charge Δq passes from x = 0 to x = d, a current Δi, equal to

$$\Delta i = \frac{\Delta q v}{d} = \frac{(\rho v_0 \Delta t) v}{d} \qquad (6.11)$$

is induced in the circuit.

Since the velocity-modulation is small, we may assume the velocity of all electrons traversing the first grid to be equal to v_0. This approximation is equivalent, in the final result, to neglecting terms of the second order of smallness. The total current at any time t is obtained by integrating with respect to all the charges traveling in the intergrid space that have entered it dur-

ing the time-interval

$$i = \frac{v_0}{d} \int_{t-\tau}^{t} \rho_{t_0} v_t \, dt_0 \qquad (6.12)$$

Here t_0 is the moment that a certain elemental charge enters the space; v_t is its velocity at the instant t for which the current is to be determined; $\rho\, t_0$ is the density of the charge at x = 0 and t = 0. The space-interval τ represents the transit time of an electron leaving the output space through the second grid at precisely the instant t. The electrons here travel through an alternating field. For this reason, by analogy to Paragraph 5.5, we must write their equation of motion and integrate it to find the velocity v_t. Assuming the potential difference in the ouput zone to be

$$U_k \cos n(\omega t + \alpha)$$

where n is the number of the harmonic, an expression for v_t may be obtained.

$$v_t = -\left(\frac{v_0 \xi_k}{2\tau_0 n\omega}\right) [\sin n(\omega t + \alpha) - \sin n(\omega t_0 + \alpha)] + v_0 \qquad (6.13)$$

If, by virtue of its non-sinusoidal variation, the density of charge at any point be represented in the form of a Fourier series, then the following expression may be obtained, by kinematic analysis of the stream in the conversion zone, for the density of the charges entering the output zone under consideration:

$$\rho_{t_0} = \frac{i_0}{v_0}\left[1 + 2\sum_{n=1}^{\infty} J_n(nr)\cos n\omega t_0\right] \qquad (6.14)$$

where $J_n(nr)$ is a Bessel function of the first kind, of order n, and the quantity r is defined as $\frac{v\omega l}{2v_0}$; l being the length of the conversion zone and ω the frequency of the velocity modulation.

From the expression (6.12) we may now obtain the current:

$$i = \frac{V_0}{d} \int_{t-\tau}^{t} \frac{i_0}{V_0} \left[1 + 2 \sum_{n=1}^{\infty} J_n(nr) \cos n\omega t_0\right] \times$$

$$\times \left[V_0 - \frac{V_0 \mathcal{E}_k}{2\tau_0 n\omega} \left\{\sin n(\omega t + \alpha) - \sin n(\omega t_0 + \alpha)\right\}\right] dt_0. \qquad (6.15)$$

Calculation of this integral yields a direct current plus a series of alternating components, of which one has the frequency of the circuit and gives up energy to it. On calculation of the integral only the terms of this frequency, giving the current i', remain:

$$i' = i_0 \left\{\frac{\tau}{\tau_0} + \left(\frac{2 J_n(nr)}{\tau_0 n\omega}\right) \left[\sin \omega t - \sin n\omega(t - \tau)\right] - \right.$$

$$- \left(\frac{\mathcal{E}_k}{2(\tau_0 n\omega)^2}\right) \left[\cos n(\omega t + \alpha) - \cos n(\omega t - \omega\tau + \alpha) + \right.$$

$$\left. + \tau n\omega \sin n(\omega t + \alpha)\right\}. \qquad (6.16)$$

Here τ varies through time, while τ_0 represents the "undisturbed" transit time. Allowing for the course of the value of τ, the current intensity i' may be expressed in the form of a sum of terms of the following form:

$$i' = I_0 + I_1 \cos n(\omega t + \alpha) + I_2 \sin n(\omega t + \alpha). \qquad (6.17)$$

Here I_0, I_1, and I_2 are respectively the steady DC component and the amplitudes of the active and reactive alternating components of the current. Thence, we may obtain the mean power imparted to the circuit, allowing for the finite transit time:

$$P = U_0 i_0 \mathcal{E}_k \left\{J_n(n,r) \left[\cos\left(n\alpha + \frac{n\theta_0}{2}\right)\right] \left[\frac{\sin \frac{n\theta_0}{2}}{\frac{n\theta_0}{2}}\right] - \right.$$

$$\left. - \frac{\mathcal{E}_k}{4} \left[\frac{2(1 - \cos n\theta_0) - n\theta_0 \sin n\theta_0}{(n\theta_0)^2}\right]\right\} \qquad (6.18)$$

Thence, the efficiency is also obtained:

$$\eta = \xi_k \left\{ J_n(nr) \left[\cos\left(n\alpha + \frac{n\theta_0}{2}\right) \right] \left[\frac{\sin \frac{n\theta_0}{2}}{n\theta_0/2} \right] - \frac{\xi_k}{4} \left[\frac{2(1 - \cos n\theta_0 - n\theta_0 \sin n\theta_0}{(n\theta_0)^2} \right] \right\} \quad (6.19)$$

For $\theta_0 = \omega\tau_0 = 0$ (infinitely short transit time) these expressions reduce to those previously obtained without allowing for transit time (Paragraph 5.2). It is interesting to remark that the second term inside the main brackets of expressions (6.18) and (6.19), which is due to the additional modulation that results from the transit through the alternating field, reduces the amount of energy delivered to the circuit at values $n\theta_0 < 2\pi$, but at values $n\theta_0 > 2\pi$, in certain regions of variation of $n\theta_0$, it becomes negative, thus indicating the delivery of additional energy to the circuit by the stream. The curve of variation in the value of this term as a function of $n\theta_0$ is represented in Figure 6.6 . The phenomenon depicted by this graph is analogous to the negative resistance developed in a diode in the presence of a finite transit time.

Finally, a few words on the influence of the factor n. The optimum efficiency is obtained under the condition $\cos(n\alpha + n\theta_0/2) = 1$, which may be realized by the proper choice of a regime for the conversion zone. In that case expression (6.19) becomes

$$\eta = \xi_k \left\{ J_n(nr) \frac{\sin \frac{n\theta_0}{2}}{\frac{n\theta_0}{2}} - \frac{\xi_k}{4} \left[\frac{2(1 - \cos n\theta_0 - n\theta_0 \sin n\theta_0}{(n\theta_0)^2} \right] \right\} \quad (6.20)$$

The value for the efficiency expressed by this formula is at a maximum, other things being equal, at $\xi_k = 1$ and at maximum values for $J_n(nr)$. The maximum values for the Bessel functions are given in Table 6.6, while the maximum values for the efficiency are plotted in Figure 6.7 as a function of the transit angle θ_0. For $\theta = 0$ and $n = 1$, the value $\eta \approx 58$ percent is obtained, which value was also obtained previously.

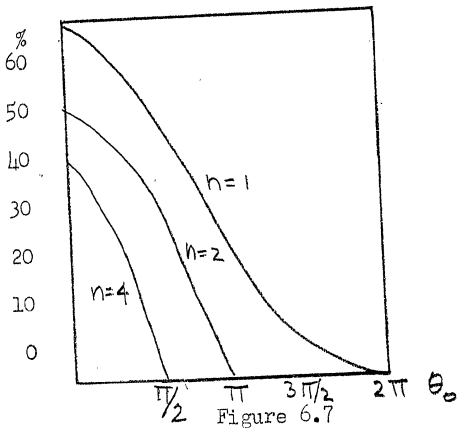

Figure 6.7

Thus, in spite of the assertion by some authors that maximum efficiency requires a transit time through the output zone equal to T/2, the influence of this transit time after all reduces down to the monotonous reduction of efficiency. This effect must under all circumstances be taken into consideration, since in practice θ_0 reaches $\pi/2$ and more. The case $\theta_0 = \pi/2$ corresponds, for $\lambda =$ = 10 cm, to the length d = 1.5 mm in a klystron operating at $U_0 =$ = 1000 volts. In this case we would obtain an efficiency 21% higher than the actual, if we did not allow for θ_0. Thus an output zone with "instantaneous" interaction, in which $\theta_0 \to 0$, proves to be the most efficient [3].

Table 6.6

TABLE OF MAXIMUM VALUES OF THE BESSEL FUNCTIONS

n	1	2	3	4	5	10
max $J_n(nr)$	0.58	0.49	0.43	0.40	0.37	0.30
r	1.84	1.52	1.40	1.33	1.28	1.20

6.2 VELOCITY-MODULATED DIODE-TYPE GENERATORS (ELECTRON RAY DIODES)

The difference between velocity-modulated diodes and ordinary statically-controlled diodes is that in the former the electron stream enters the alternating field with the considerable initial velocity v_o and passes through a potential difference that exceeds the saturation voltage, and is then subjected to dynamic control in a single space having an alternating electric field. This space functions simultaneously as modulation zone, conversion zone, and output zone. As a first simple example of such a dynamically controlled diode, let us consider the zone of modulation, allowing for transit time.

(a) Modulator, allowing for transit time. As is generally known a finite transit time through the modulation zone reduces the amplitude of the velocity modulation, causes a phase shift, and places a load on the feed line of the modulator. Assume that the modulating voltage is equal to $U_1 \sin \omega t_1$. Then the velocity of the electrons leaving the modulator will be

$$v_t = -\frac{v_0 \varepsilon}{2\omega \tau_0}\left[\cos \omega t_1 - \cos \omega (t_1 - \tau)\right] + v_0 \qquad (6.21)$$

or, if we set $\omega t_o = \theta_o$,

$$v_t = V_o \left[1 + \frac{\xi}{2} \frac{\sin \frac{\theta_o}{2}}{\frac{\theta_o}{2}} \sin \left(\omega t_1 - \frac{\theta_o}{2} \right) \right] \qquad (6.22)$$

For $\theta_o = 0$, this expression reduces to a somewhat more simplified expression for the velocity with which the electrons leave the modulator. The influence of the finite transit time is here characterized by the same factor

$$\frac{\sin \frac{n\theta_o}{2}}{\frac{n\theta_o}{2}}$$

as in the previous case.

The mean power consumption of the modulator may be obtained directly from the second term of formula (6.18) by setting $\xi_k = \xi$ and n= 1 in it, and changing the sign:

$$P_{Mod} = U_o i_o \xi \left\{ \frac{2(1-\cos\theta_o) - \theta_o \sin\theta_o}{4\theta_o^2} \right\} = \frac{U_1^2}{2} G \qquad (6.23)$$

Here U_1 is the amplitude value of the alternating voltage on the modulator, and G is the intergrid conductance of the modulator due to the electronic load. G may be expressed as:

$$G = \frac{i_o}{U_o} \left[\frac{2(1 - \cos\theta_o) - \theta_o \sin\theta_o}{2\theta_o^2} \right] \qquad (6.24)$$

The numerical value of G, expressed in mho for any transit angle, is obtained from the ordinates of the curve in Figure 6.6 by multiplying them by $2i_o/U_o$. For the angle of flight $\pi/2$, which corresponds to a distance of 1.5 mm between the grids, with λ = = 10 cm and U_o = 1000 volts, and a beam-current of 50 milliamperes, the value of G is $4.35 \cdot 10^{-6}$ mho, or $R_{mod} \approx 230{,}000$ ohms. This

value is of the order of the shunt-impedance employed in the klystron circuits. Under these conditions the alternating power consumed by the modulator is very insignificant, being equal to 0.0435 percent of $U_o i_o$, if $\xi = 0.1$.

The quantity G is equivalent to the input conductance of statically controlled tubes. It will be seen from the curves of Figure 6.6 that this quantity may be negative for certain transit angles. This leads to the excitation of the single-cavity resonator. The following relation between the positive shunt-impedance Z of the circuit and the parallel negative resistance $\overline{R}$ introduced by the electron stream:

$$\overline{R} \leqslant Z.$$

Thus, single-circuit systems corresponding to diodes may be excited on account of the negative resistance imparted by the electron stream. Oscillation intensity is low in such systems, as is also their efficiency, but they may be successfully used as detectors and regenerative receiving equipment [4]. The sensitivity and amplification coefficient of such devices depends on the transit angle. When the latter varies the former quantities pass through a series of maxima. In Figure 6.8 the following curves have been plotted as functions of the transit angle:

$1 + \frac{Z}{Z_e} = f(\theta_o)$ and the amplification factor $\mu = f(\theta_o)$; where Z is the shunt impedance of the circuit and Z_e the equivalent shunt-impedance of the stream; while Figure 6.9 shows the curve of sensitivity as a function of the transit angle.

In the region where the values of $1 + \frac{Z}{Z_e}$ become negative

the amplification factor μ and the sensitivity become infinitely great.

(b) The single-circuit generator of Muller and Rostas [5]. A self-exciting electron-radiating diode may be so designed as to allow the use of resonators with shapes of the highest quality. It was shown in Chapter I that it is precisely those shapes of hollow resonators whose connection with the electron stream under klystron conditions is difficult that possess the highest Q values. The principle of the electron-ray diode presuppose a single simple form of resonator, along the line of the electric field of which a stream of electrons is directed. Self-excitation takes place by means of the negative conductance which under certain regimes is produced by the interaction between the stream and the electric field of the resonator. Let us imagine the arrangement schematically represented

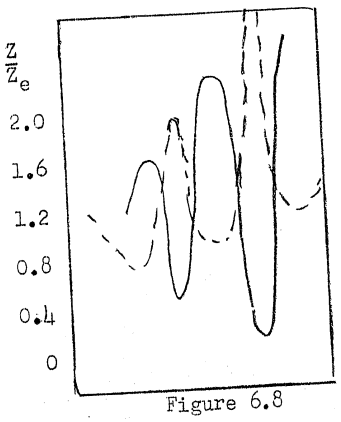

Figure 6.8

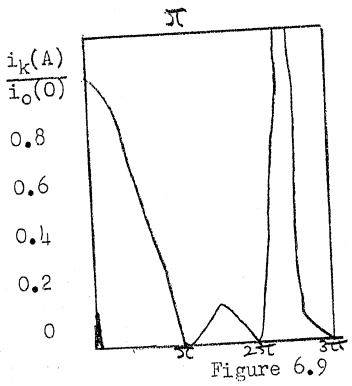

Figure 6.9

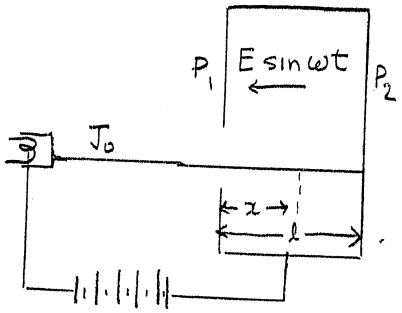

Figure 6.10

in Figure 6.10. The electron stream, accelerated by the DC potential U_0, enters the electric field P_1 P_2 of the resonator. Let us measure the coordinate x to the right, from the wall of P_1. The velocity with which the electrons enter the resonator is equal to $v_0 = \sqrt{2 \frac{e}{m} U_0}$; the voltage of the field within the resonator is $E \sin \omega t$, $U = El$, the amplitude of the alternating voltage; $\tau = U/U_0$; $\alpha = \omega t_0 / 2\pi$, where ωt_0 is the transit angle of an undisturbed electron; $\varphi_0 = \omega t_0$, the entrance phase, and $\varphi_1 = \omega t_1$, the exit phase, of the electron. The behavior of each electron inside the resonator is determined by its entrance phase and the variation in the field during the time of transit. During this time the electron receives positive or negative energy from the alternating field. We calculate this energy for each electron, and then sum all the values obtained for the length of a single period. If this total is negative, this means that the beam will sustain oscillation in the resonator.

From the equation of movement for the electron we obtain an expression for the "undisturbed" angle of flight

$$\omega t_0 = (\varphi_1 - \varphi_0)\left(1 + \frac{\tau}{2\omega t_0} \cos \varphi_0\right) + \frac{\tau}{2\omega t_0} (\sin \varphi_0 - \sin \varphi_1) \qquad (6.25)$$

The energy dW received by the electron from the field during the time dt is equal to $dW = e\frac{U}{l}\sin\omega t \cdot v\,dt$, which yields, on passing over to the energy received by the beam during a period, if there are n electrons acting:

$$W_1 = n\int_0^T dt_0 \int_{t_0}^{t_1} e\frac{U}{l}\sin\omega t \cdot v\,dt_1 \qquad (6.26)$$

Let us define the efficiency, or the coefficient of useful action, of the arrangement as the ratio of the value of W_1 to the energy received by the electrons during a period from the source of direct current

$$\eta = \frac{W_1}{nT\cdot\frac{1}{2}mv_0^2} \qquad (6.27)$$

By calculating the foregoing integral and taking relation (6.27) into consideration, we may calculate the "watt efficiency"

$$\eta = \frac{\xi}{2\pi\omega\tau_0}\int_0^{2\pi}(\cos\varphi_0 - \cos\varphi_1)\left[1 + \frac{\xi}{4\omega\tau_0}(\cos\varphi_0 - \cos\varphi_1)\right]d\varphi_0 \qquad (6.28)$$

The quantities φ_0 and φ_1 are here interconnected by equation (6.25). Our problem reduces to the solution of (6.25) and (6.28) for φ_1 and η. The quantity may be represented in the form of a series with parameter $\mu = \xi/2\omega\tau_0$

$$\eta = C_1\mu + C_2\mu^2 + \dots, \qquad (6.29)$$

where $C_1 = -2\sin\omega\tau_0 J_1(\xi/2)$

$$C_2 = 2 + \tfrac{1}{2}\cos 2\omega\tau_0 J_2(\xi) - \cos\omega\tau_0$$
$$\left[2J_0(\xi/2) + \frac{3\xi}{4}J_1(\xi/2) - \frac{\xi}{4}J_3(\xi/2)\right].$$

At infinitely small amplitudes, the efficiency η is expressed as

$$\eta = -\frac{\varepsilon^2}{4}\left[\frac{\sin\omega\tau_0}{\omega\tau_0} - \frac{\sin^2\frac{\omega\tau_0}{2}}{\frac{\omega\tau_0}{2}}\right] \qquad (6.30)$$

To sustain oscillation, η must be less than 0, which occurs at

$$2\pi < \omega\tau_0 < 3\pi;\ 4\pi < \omega\tau_0 < 5\pi, \ldots\ 2\pi k < \omega\tau_0 < 2\pi\left(k+\tfrac{1}{2}\right)$$

The oscillatory power may be represented

$$\frac{U^2}{2R_e} = \eta I_0 U_0,$$

or, setting $R_0 = U_0/I_0$, we obtain $R_e = R_0 \frac{\varepsilon^2}{2\eta}$, which leads to the following equation for equivalent conductance:

$$\frac{1}{R_e} = -\frac{1}{2R_0}\left[\frac{\sin\omega\tau_0}{\omega\tau_0} - \frac{\sin^2\frac{\omega\tau_0}{2}}{\frac{\omega\tau_0}{2}}\right]. \qquad (6.31)$$

R_e, the equivalent resistance of the stream, has its minima for the various oscillation regions, at which the conditions $\frac{U^2}{2R_e} > \frac{U^2}{2Z}$ must be fulfilled, where Z is the shunt-impedance of the resonator (i.e. $|R_e| < Z$). The value of these minima is as follows:

$R_{e1} = 19.6\ R_0$ for $\omega\tau_0 = 2.4$

$R_{e2} = 33\ R_0$ for $\omega\tau_0 = 4.48$

$R_{e3} = 44.5\ R_0$ for $\omega\tau_0 = 6.5$

The case of finite amplitudes. In this case too we use the series for η defined by expression (6.29), but limiting ourselves to its first term:

$$\eta = -\frac{\sin \omega t_0}{\omega t_0} \xi \cdot J_1\left(\xi/2\right) \qquad (6.32)$$

This expression is negative for $2\pi k < \omega t_0 < 2\pi(k+1/2)$ with $J_1\left(\xi/2\right) > 0$, or for $2\pi(k+\frac{1}{2}) < \omega t_0 < 2\pi(k+1)$ and for $J_1\left(\xi/2\right) < 0$. On the plane ξ, ωt_0 it defines a sequence of rectangles bounded by the vertical lines $\omega t_0 = 2\pi k; 2\pi(k+1)$ and by the horizontal lines corresp nding to the roots of the Bessel function J_1 i.e. by the values $\xi/2 = 3.83; 7.01; \ldots$ (Figure 6.11). Output reaches a maximum roughly at the midpoints of the hatched areas. The maximum output, equal to 14.5%, is obtained for first-order oscillations at $\alpha = 5/4$ and $\xi = 4$. It will be seen from this result that the amplitude of the alternating voltage considerably exceeds the DC accelerating potential, which cannot be accomplished in the ordinary diodes. Figure 6.12 gives the efficiency η at three different values of ωt_0, corresponding to the first three excitation regions. The following Figure 6.13 gives the optimum efficiency curve, and together with it also the curves of $|1/R_e|$ -- the equivalent conductance of the electron stream and of 1/Z where Z is the shunt-impedance of the circuit. For excitation it is necessary that $Z > |R_e|$; the condition for the establishment of oscillation is obviously the equality $Z = R_e$, which corresponds to point F of Figure 6.13.

To obtain very short waves from a generator of the type under consideration, the simplest resonator-shapes may be used -- spherical, for example, which is especially easy for oscillations of higher order. We present a few characteristic figures for the regime of single-circuit generators of the type described, operating at the maximum of the first oscillation region: U_0 = 1000 volts; I_0 = 100 milliamperes; k = 1; $\alpha = 5/4$; $\xi = 4$ (point F on Figure 6.13);

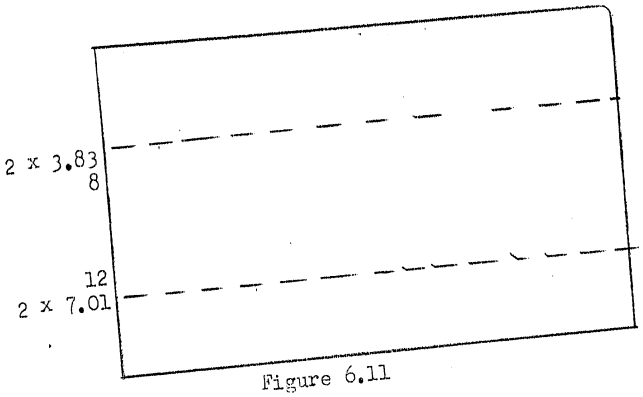

Figure 6.11

$Z = 2 \cdot 10^6$ ohms; $R = 4 \cdot 10^4$ ohms; $U = 4000$ volts.

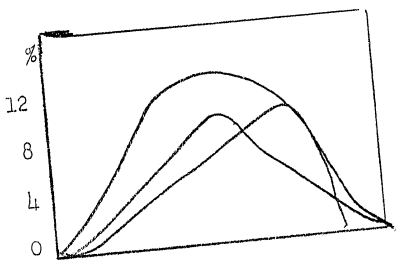

Figure 6.12

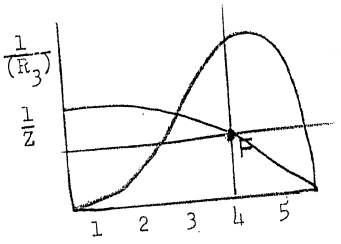

Figure 6.13

A generator of this type has a number of advantages: (a) in contrast to the ordinary diode, it allows use of the volume resonator in such a way that all of the DC accelerating fields remain outside it, which leads to good values for Q and Z; (b) the fact that there is only a single circuit eliminates the difficulties of mutual tuning of the circuits and also eliminates the limitation in the transit time through the alternating field, which is an advantage of this tube as compared to the klystron; (c) this generator makes it possible to base its design exclusively on the inductive connection of the electron beam with the circuit, following the general idea of the scheme depicted in Figure 6.14, which makes

provision for easy and convenient tube replacement.

6.3 RETARDING-FIELD GENERATORS

(a) Kinematic Analysis of Systems with DC Retarding Fields

The transition from the two-circuit klystron to the retarding-field system may be easily imagined by picturing the operation of "bending" the klystron scheme along the middle of the conversion zone and folding it in such a manner that the modulation and output zones are superposed. The typical scheme of the "reflex klystron", or of the retarding-field oscillator with bi-grid modulator, will thus be obtained. This system was first studied kinematically and energetically by the author in 1940-1941, as the analogue of the ordinary retarding-field system which developed historically out of the positive-grid triode.

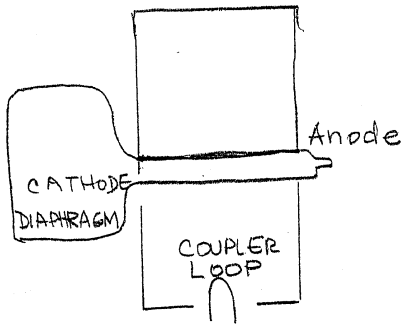

Figure 6.14

Let us investigate the kinematic conditions for sustaining oscillation, by applying the fundamental relations obtained in sections 5.4 and 5.9 to the circuit of Figure 6.15. We imagine the following simplified circuit (Figure 6.16): the electron stream

passes from the cathode K through the modulator AB, which consists of two grids and enters the direct electric field between the right grid of the modulator and the retarding electrode C (sometimes spoken of as a reflecting electrode). We assume that the potential of the modulator varies according to the law

$$U_M = U_o + U_1 \sin \omega t_s.$$

A certain direct potential U_B, which in most cases is negative, is imparted to the retarding electrode. Assuming the electrodes to be plane and the fields to be uniform, the retardation coefficient n may be expressed as follows:

$$n = \frac{E}{U_o} = \frac{U_o - U_B}{dU_o} \qquad (6.33)$$

For $U_B = 0$, this reduces to $n = 1/d$, as previously found.

In retarding field devices the following possibilities of combination with the oscillatory system and the excitation of oscillations may be imagined. Let us consider Figure 6.17a, which shows a variant of the arrangement with a two-grid modulator, across the grids of which the oscillatory circuit is connected. The excitation proceeds in the main by means of the return of the focus towards the modulator, as indicated by the arrow. The retarding electrode B does not participate in the oscillations and its potential is constant. However, the field between M and B may be considered constant, with a fair amount of accuracy, only when the oscillatory system connected with the modulator is endovibratory.

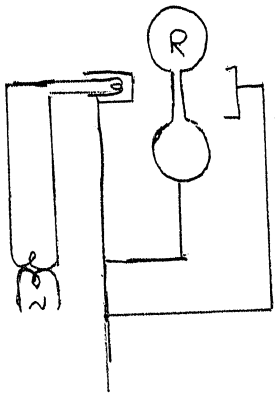

Figure 6.15

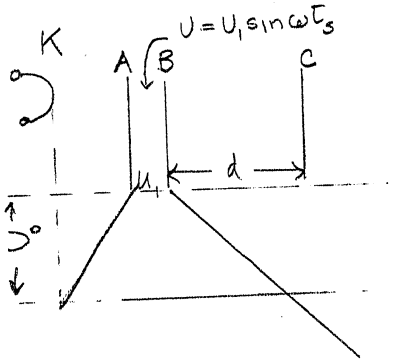

Figure 6.16

Figure 6.17 b gives another variant of the scheme. This is essentially the ordinary triode with a retarding field. The oscillatory system is connected between the "single-grid modulator" (the grid) and the retarding electrode (the plate of the triode). Consequently, a certain alternating component is superimposed on the direct field between them. We shall take this component into consideration later, but here we make an assumption that is characteristic for most theories of the retarding field circuit: we

assume that the alternating potentials on the electrodes and the alternating fields created by them to be so small in comparison with the direct potentials and fields that the motion of the electrons between M and B may be considered to depend only on the latter. Excitation here may occur either by the return of the focus towards the grid or by the arrival of the focus at the retarding electrode, or even by a combination of these two methods (see the arrow in Figure 6.17b). In our subsequent exposition we shall refer to these variants as variant A (the two-grid modulator) and variant B (the single-grid modulator), and shall discuss them in parallel sequence.

If we make use of the expression for the transit angle to the focusing, from equation (5.48), and take into account that the exit phase of the packets focused on their return to the modulator is π, 3π, 5π, etc (Under the condition of τ being small, to which for the time being we limit ourselves), and that the regime of return of focus is subject to the condition $n = \frac{2\ell\omega}{v_0}$, then the following expression may be obtained for the transit angle to the focus return

$$\omega\tau_F^* = \frac{4\omega}{nv_0} \qquad (6.34)$$

(quantities related to the focus return are marked by us with *)

To sustain the oscillation of the modulator (variant A) by means of focus return, this return must be timed to coincide with the instant of maximum retardation, i.e. with the instant of maximum potential U_m.

This condition is illustrated by Figure 6.18, on which, over the curve of variation of the alternating component of the voltage U_m, we have plotted the qualitative graphs of the motion of packets leaving the modulator $\omega t_s = \pi$ and returning under the most favorable conditions for excitation. It is not hard to see that for this the transit angle θ_0 must satisfy the following requirement:

$$\omega \tau_F^* = \frac{4\omega}{nv_0} = (2k - 0.5)\pi,$$

where k = 1, 2, 3,... This condition may be written in the somewhat more convenient form:

$$\frac{8\omega}{nv_0} = (4k - 1)\pi. \qquad (6.35)$$

Thus, to sustain oscillation in the modulator two conditions must be met: the phase condition just obtained, and the focus-return condition (5.45). It follows from the necessity of the simultaneous fulfillment of both these conditions that we require the definite discrete values of $\mathcal{E}$ at which the regime of sustained oscillation may take place by means of focus return:

$$\mathcal{E} = \frac{4}{(4k - 1)\pi} \qquad (6.36)$$

Whence we obtain the following series of values for $\mathcal{E}$ for several excitation regimes:

Table 6.7

VARIANT A

Values of for Several Excitation Regions

k	1	2	3	4	5	6
ξ	0.43	0.18	0.12	0.10	0.07	0.06

Under the reservations above made, analogous considerations may be applied as well to variant B (the single-grid modulator), which, as we have pointed out, approximately reproduces the classical retarding-field circuit. The properties of this case may be studied by introducing a different phase condition for the focus return, since output of energy in this case should occur in the plate-grid space, and the optimum transit angles to the focus return which, corresponding to excitation, are subject to the condition:

$$\omega t_F^* = \frac{4\omega}{nV_0} = 2k\pi \qquad (6.37)$$

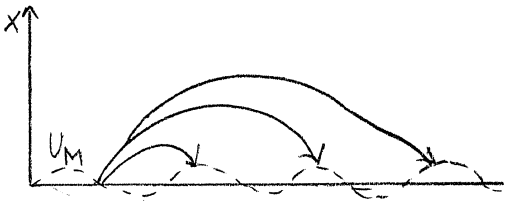

Figure 6.18

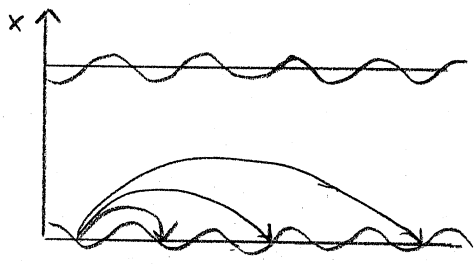

Figure 6.19

which is illustrated by Figure 6.19. This condition leads to the following expression for :

$$\varepsilon = \frac{1}{R\pi} \qquad (6.38)$$

which yields a somewhat different series of discrete values:

Table 6.8

VARIANT B

VALUES OF FOR SEVERAL EXCITATION REGIONS

k	1	2	3	4
ε	0.32	0.16	0.11	0.08

Variant B is interesting in that, under the ordinary assumptions of most theories (absence of influence of the alternating field on the motion of electrons between the electrods), we get a pattern fairly close to the actual operating conditions in a retarding-field oscillator without particularly complicated and unwieldy calculations.

(b) Oscillation Regions and Calculation of the Working Diagrams

In the retarding-field system, as with the klystron, the existence of discrete values of ε leads to the formation of discrete regions of oscillation. In this case, in consequence of the spatial superposition of modulation and output zones, a considerably greater sharpness in the "tuning of the phase conditions" may be expected than in the klystron. This circumstance should lead to the production of oscillation regions that are considerably narrower and more easily demarcated from each other. In fact, one of the classic questions in connection with the operation of the retarding-

field system was whether excitation in it was discrete or continuous. There were a good number of works published then on the subject, and their results were mutually contradictory. (Cf. Chapter III of this author's book Detsimetrovyye i santimetrovyye volny (Decimeter and Centimeter Waves), 1939. It must in the last analysis be considered established that besides the fulfillment of the Barkhausen relation $\lambda U_0^{1/2}$ = constant -- which, it appeared, should have been applied to the continuous variation of λ as a function of U_0 -- there are also certain other circumstances to which the invariably observed origination of discrete excitation regions is due. A continuous spectrum of electronic oscillations can be obtained only by using specially constructed tubes (aperiodic tubes) and simultaneous regulation of the frequency of the oscillating system [6]. However, all the circumstances connected with this question as to whether the excitation in a retarding-field system is discrete or continuous can be rather simply considered from the point of view herein set forth. If the values of τ obtained from formulae (6.36) and (6.38) are substituted in the focus-return condition $n = (2\tau\omega)/v_0$, and we pass from the quantities n, v_0, and ω to the quantities U_0, U_B, and d and λ, then for both variants of the system we may obtain equations that define the loci of the maximum points of the oscillation regions (the "crests" of the regions) on the plane $U_0 - U_B$, to which the experimentally found oscillation regions ($U_a - U_g$ -- the working diagrams) are usually referred. These equations are:

$$U_B = U_0 - \frac{8000\,d}{\lambda(4k-1)}\sqrt{U_0} \quad \text{(A)}$$
$$U_B = U_0 - \frac{2000\,d}{k}\sqrt{U_0} \quad \text{(B)} \qquad (6.39)$$

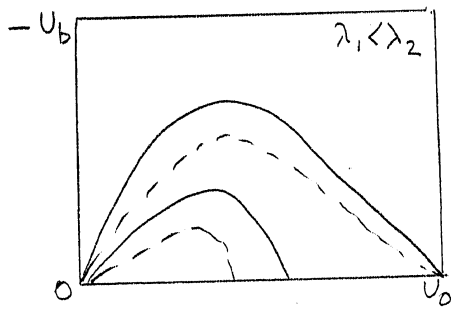

Figure 6.20

Figure 6.20 illustrates these equations. The negative values of U_B are plotted upwards along the U_B axis; it is these that are of the most interest to us. A series of discrete oscillation regions obtained at k = 1, 2, 3,..., corresponds to the excitation of each natural wave of the circuit. The maximum values of U_o and U_B for wavelength λ correspond to the first excitation region k = 1.

The "crest" curves of the oscillation regions cut the U_o axis at the points U_{o1}, U_{o2},..., etc. These points indicate that discrete oscillation regions are obtained at the given values of U_o and a zero potential on the retarding electrode. Setting $U_B = 0$ in the formulae of (6.39), we obtain the following expressions along the U_o axis for the centers of the oscillation regions:

$$U_{ok} = \left[\frac{8000\ d}{(4k-1)\lambda}\right]^2 \quad \text{(A)}$$

$$U_{ok} = \left[\frac{2000\ d}{\lambda\ k}\right]^2 \quad \text{(B)} \qquad (6.40)$$

which are similar to those we obtained for the klystron oscillator.

In the first approximation these results are in good agreement with the experimental facts. In this case we really have all of the most characteristic indicia of a retarding-field system: existence of discrete oscillation regions, entirely agreeing with the experimental data for the distribution pattern of these regions on the plane $U_o - U_B$; the character of the distribution of the intersection points of the "crests" of these regions with the U_o axis; and finally, the fulfillment of the Barkhausen condition $\lambda U_o^{1/2} =$ constant, within each of the excitation regions (along its maximum).

To values of $k > 1$, the conditions of excitation of "dwarf" waves apply, for which the Barkhausen constant is smaller. For the first "basic" region ($k = 1$), we have

$$\lambda\sqrt{U_o} \approx 2660\ d\ \frac{U_o}{U_o - U_B} \quad (A)$$

$$\lambda\sqrt{U_o} \approx 2000\ d\ \frac{U_o}{U_o - U_B} \quad (B) \qquad (6.41)$$

In this connection we note that equation (6.41 B) completely coincides with the expression obtained by Barkhausen and Kurz by using the idea of the "oscillation of electrons around the grid". For $U_B = 0$, the equations of (6.41) assume the form:

$$\lambda\sqrt{U_o} \approx 2660\ d \quad (A)$$

$$\lambda\sqrt{U_o} \approx 2000\ d \quad (B) \qquad (6.41')$$

To the next two excitation regions -- the regions of "dwarf" waves -- the following equations correspond:

$$\lambda\sqrt{U_o} \approx 1140 \text{ d} \quad \text{(A)}$$

$$k = 2; \qquad \lambda\sqrt{U_o} \approx 1000 \text{ d} \quad \text{(B)} \qquad (6.42)$$

$$\lambda\sqrt{U_o} \approx 730 \text{ d (A)}$$

$$k = 3; \qquad \lambda\sqrt{U_o} \approx 670 \text{ d (B)}$$

All the foregoing refers to the maxima of the oscillation regions. But if we take into consideration that both the focus-return condition and the phase condition may have certain "toler-ances" on either side, then each oscillation region should have a certain final width. The values for these "tolerances" , and con-sequently for the "width" of the oscillation region as well, de-pends on the energy conditions.

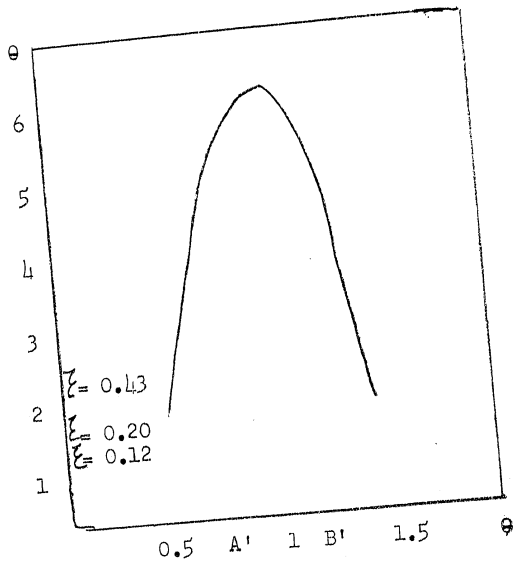

Figure 6.21

The latter (cf. Paragraph 5.9) leads to the following. Calculation of the power integral for the regime of focus-return brought us to the expression (5.102)

$$L = \frac{16\Pi + 4\mathcal{E}(\Pi - 1)}{8 + \mathcal{E}}$$

The oscillation-region maxima show by the curves of the working diagram of Figure 6.20 correspond to this quantity, L. Calculation of the power integral for the regimes adjoining the focus-return ($\theta \neq 1$) gives us the variation of L as a function of θ for three values of $\mathcal{E}$, as represented by the curves of Figure 6.21. It will be seen from this that, among other things, the factor exerts relatively little influence on the value and character of the variation in the power integral. We may take advantage of these curves to determine the boundaries of the oscillation regions and construct a complete working diagram of the retarding-field oscillator. The maxima of the curve $L = f(\theta)$ lie at $\theta = 1$, i.e. correspond to the focus-return condition. We draw the horizontal line AB so as to cut off on the axis of ordinates a segment defined by the condition for sustained oscillation in the given oscillatory circuit:

$$L = \frac{\Pi}{Z}\frac{\mathcal{E}}{\Psi} R_0.$$

Then, obviously all that part of the curve $L(\theta)$ which is situated above the straight line AB corresponds to that interval of the variation of θ (between the points A' and B') in which the excitation conditions are satisfied. Since $\theta = (2\mathcal{E}(\omega))/v_0$, the variations of θ during this interval may be converted to variations of another parameter, for instance, of U_0 or U_B, and thus the boundaries of the excitation regions may be found and the "crest" di-

agram turned into a full space diagram.

The power-integral curves may be utilized for calculating the efficiency of a retarding-field system:

$$\eta = \frac{\varepsilon\psi}{2\pi} L = \frac{\varepsilon\psi}{2\pi} \frac{16\pi + 4\varepsilon(\pi - 1)}{8 + \varepsilon} \qquad (6.43)$$

which gives the results shown in Table 6.9 for $\psi = 1$

Table 6.9

TABLE FOR THE VALUES OF EFFICIENCY

k	ε \ θ	0.5	0.8	1.0	1.2
1	0.43	0.14	0.39	0.42	0.33
2	0.18	0.06	0.15	0.18	0.13
3	0.12	0.04	0.10	0.12	0.08
4	0.10	0.03	0.09	0.10	0.07

As will be seen from this table, the maximum possible efficiency obtained is somewhat above 40%, without allowing for the absorption of electrons by the grids. The coefficient ψ which takes account of this, may have values ranging from 0.05 to 0.4, depending on grid design, as may be inferred from practical work with ordinary retarding-field oscillators. If we adopt, as one of the very probable values, $\psi \simeq 0.1$, then we obtain values for the efficiency from this table which are in good agreement with those that characterize the operation of a retarding-field circuit, namely $\eta \simeq$ = 2-4 percent.

6.4 CALCULATION OF THE ALTERNATING POTENTIALS IN THE RETARDING-FIELD CIRCUIT

(a) The Basic Elements of the Problem

Let us now consider a system (Figure 6.22) consisting of the cathode K, the plane modulator M, the role of which may be played by a single grid with potential U_m, and the flat retarding electrode B with the potential U_B, which in most cases is negative. Assume that on the electrodes M and B there are alternating components of the respective potentials, and that these components vary in directly opposite phases, since an oscillatory system is connected across these electrodes. We express the potential of the electrodes as follows:

Potential of modulator

$$U_m = U_{mo} + U_{m1} \sin \omega t; \tag{6.44}$$

Potential of retarding electrode:

$$U_B = U_{Bo} - U_{B1} \sin \omega t;$$

Then the field intensity in the space AB may be expressed as follows:

$$E = \frac{U_M - U_B}{d} = \frac{U_{Mo} - U_{Bo}}{d}\left(1 + \frac{U_{M1} + U_{B1}}{U_{Mo} - U_{Bo}} \sin \omega t\right) \tag{6.45}$$

To simplify the further calculations the following notation will be used

$$\frac{U_{M1}}{U_{Mo}} = \xi_M; \quad \frac{U_{B1}}{U_{Mo}} = \xi_B; \quad \frac{U_{Bo}}{U_{Mo}} = \beta \tag{6.46}$$

$$n = \frac{U_{Mo} - U_{Bo}}{d U_{Mo}}; \quad V_o = \sqrt{2 \frac{e}{M} U_{Mo}}; \quad \xi = \frac{\xi_M + \xi_B}{1 - \beta}$$

Here n plays the role of the "mean retardation coefficient", that of the "modulation coefficient of retardation". The acceleration of an electron is given by the expression

$$\ddot{x} = a = -\frac{nv_0^2}{2}(1 + \xi \sin \omega t). \qquad (6.47)$$

It will be seen in the general case that the variation in acceleration in the retarding space is determined, not by the modulation coefficient ξ_M, which is responsible for the variation in velocity as the stream traverses the modulator, but instead by the more complicated function ξ, which may be termed "modulation coefficient of retardation".

Let us now perform certain calculations without imposing any conditions on the values of ξ_M, ξ_B, and ξ. By integrating expression (6.47), we obtain the velocity of the electron

$$V = -\frac{nV_0^2}{2}(t - t_s) + V_0\sqrt{1 + \xi_M \sin \omega t_s} + \frac{\xi n v_0^2}{2\omega}(\cos \omega t - \cos \omega t_s) \qquad (6.48)$$

or

$$V = V_0\left[1 + \xi_M \sin \omega t_s - \frac{nV_0^2}{2}\right] + \frac{\xi n v_0^2}{2\omega}\left[\cos \omega t_s (\cos \omega t - 1) - \sin \omega t_s \sin \omega t\right] \qquad (6.48')$$

Here t_s, as before, is the instant of starting, i.e. of the electron's exit from the modulator into the conversion space, or in the given case the instant of flight through the grid M. By the following integration the path traversed by the electrons at any given instant t may be expressed

$$X = V_0\left[1 + \xi_M \sin \omega t_s (t - t_s) - \frac{nV_0^2}{4}(t - t_s)^2\right] + \frac{\xi n v_0^2}{2\omega^2}\left[\sin \omega t - \sin \omega t_s - \omega(t - t_s)\cos \omega t_s\right] \qquad (6.49)$$

or

$$x = V_0 \left[1 + \varepsilon_M \sin \omega t_s \cdot \tau - \frac{n V_0^2}{4} \tau^2 + \right.$$

$$\left. + \frac{\varepsilon n V_0^2}{2\omega^2} \left[\sin \omega t_s (\cos \omega \tau - 1) + \cos \omega t_s (\sin \omega \tau - \omega \tau)\right]\right] \qquad (6.49')$$

Formulae (6.48) and (6.49) are distinguished from the corresponding formulae for velocity and path in the constant retarding field exerted by the underlined terms. The condition $\frac{\partial F(t, t_s)}{\partial t_s} = 0$, by analogy to Paragraph 5.5, to solve the question of the focusing of the stream under the conditions being considered, if the behavior of the stream be considered at any given point x. By applying this condition to equation (6.49), we obtain the angle of transit to focus

$$\omega \tau_F = \frac{\omega V_0 \sqrt{1 + \varepsilon_M \sin \omega t_s}}{\frac{V_0 \omega \varepsilon \cos \omega t_s}{2\sqrt{1 + \varepsilon_M \sin \omega t_s}} + \frac{n V_0^2}{2}\left(1 + \varepsilon \sin \omega t_s\right)} \qquad (6.50) = \frac{\omega V_s}{\frac{dV_s}{dt_s} + a_s}$$

This formula differs from formula (5.46) only in the term $\frac{(\varepsilon\, n v_0)}{2} \sin \omega t_s$ in the denominator, which term takes account of the effect of the alternating field. Formula (6.50) determines the "curves of focusing time", which are not without interest, and may be represented in the form of the curves $\omega \tau_F = f(\omega t_s)$ or also $\omega t_F = f(\omega t_s)$ (bearing in mind that $t_F = t_s + \tau_F$). Figure 6.23 gives an idea of these curves, which may, like the curves $x_F = f(\omega t_s)$, be either continuous or discontinuous, depending on the value of the retardation. The broken lines show the curves $\omega \tau_F = f(\omega t_s)$ and $\omega t_F = f(\omega t_s)$ corresponding to weak retardation, while the solid lines show the curves that correspond to a stronger retardation. At weak retardation a certain interval of defocusing occurs, within which ωt_F may become infinitely

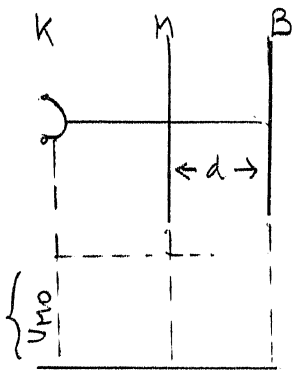

Figure 6.22

great. This occurs at

$$\left|\frac{dv_s}{dt_s} + a_s\right| = 0 \quad \text{or} \quad \frac{dv_s}{dt_s} = -a_s \qquad (6.51)$$

i.e. when the acceleration imparted to the electron at its exit from the modulator is equal and opposite to the speed with which its exit velocity varies. On substituting in equation (6.49) the expression obtained for $\Updownarrow_F$ an expression for x_F may be obtained, and the equation for the locus of foci may be given the following

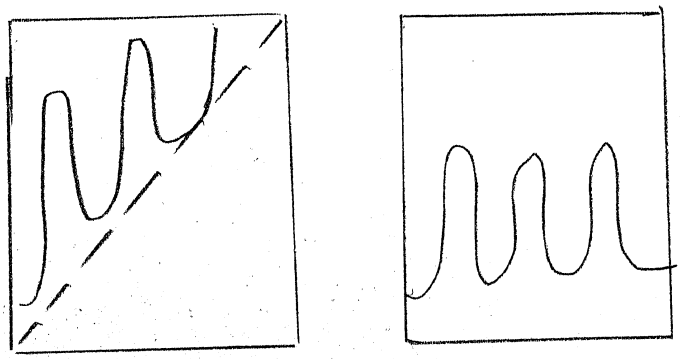

Figure 6.23

somewhat less cumbersome form for use in fairly accurate solution of the problem:

$$x_F = x_{F_0} + \frac{\varepsilon n V_0^2}{2\omega^2}\left[\sin \omega t_s(\cos \omega t_F - 1) + \cos \omega t_s(\sin \omega t_F - \omega t_F)\right] \qquad (6.51')$$

By x_{F_0} we must understand here the corresponding value of the locus of foci calculated by the formula for a direct retarding field (Formula 5.43). In this case the values of ωt_s, n, and v_0 should obviously remain the same, but in the expression of the value of α_s in formula (5.43), the coefficient ε_M must be used instead of ε. The latter enters only into the term that defines the effect of the alternating field.

(b) Graphic Methods

Expressions of the type of (6.51) cannot always be successfully used, on account of their unwieldiness. This compels us to have recourse to a combination of computational and graphic methods. The values of the errors introduced by various simplifications may be ascertained by the aid of such combinations, and we may then establish the admissibility of certain forms and methods of calculation borrowed from the simpler conditions of the direct field.

If a definite and specific case is set, a series of trajectories of individual electron packets may be constructed by formula (6.49), taken, for example, at every 0.1 π from the starting phase ωt_s for a whole period. We shall then obtain a series of curves $x = f(\omega t_s)$ similar to parabolas, but differing from them in the underlined terms of formula (6.49). From these curves, represented in Figure 6.24, another set of curves on the plane of

times (ωt, ωt_s) is constructed to represent the loci of the constant x's, i.e. the set of "horizontals".

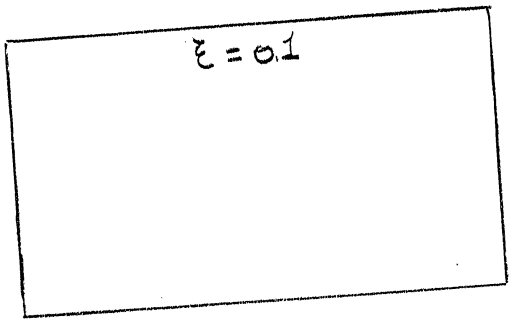

Figure 6.24

The surface $x = f(\omega t, \omega t_s)$ constructed in this manner makes it possible, with an accuracy determined by the accuracy of the drawing, to find the position and movement of any packet at any assigned instant of time. The "horizontals" x = const plotted in Figure 6.25 have still another useful property: their extreme points correspond to foci, for at such points the condition $dt/dt_s = 0$ is satisfied, i.e. the tangent is parallel to the axis of abscissae. These focal points may be found as points of intersection between the horizontals plotted and the curve $\omega t_F = f(\omega t_s)$ constructed by equation (6.50). This curve is indicated by the broken line in Figure 6.25 Having such a space curve $\omega t_F = f(\omega t_s)$ and plotting it on the corresponding planes of coordinates, we may obtain either the locus of foci $x_F = f(\omega t_s)$, or the trajectory of foci $x_F = f(\omega t)$. Such is the scheme of the most general graphic method, which may be very useful in studying the electron stream under the conditions of any assigned alternating field.

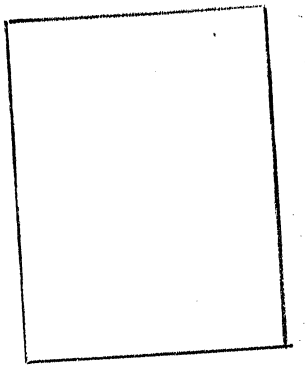

Figure 6.25

Another graphic method was applied with the aim of ascertaining the conditions of focus return to the modulator in the alternating field determined by the phase ωt $t_{\text{ж}}$ and the values of ξ corresponding to various excitation regions. Here the matter stands thus: starting out from the excitation scheme adopted, we assign such values to ωt_F^*, i.e. to the current time, as should probably, under the excitation conditions, correspond to focus-return. By employing the assigned ωt_F^* and the condition $x = 0$, we may obtain the relation between the modulation coefficient ξ and the angle of transit that corresponds to focus return: $F(\xi, \omega t) = 0$. As parameter to characterize the regime it is convenient to choose the quantity $p = nv_0/\omega$. With this we may make use of the expression for x written as follows

$$x = \omega t \cdot \frac{v_0}{\omega} \left[1 + \xi_M \sin(\omega t - \omega t) - \frac{nv_0^2}{4\omega^2}(\omega t)^2 + \right.$$

$$\left. + \frac{\xi nv_0^2}{2\omega^2}\left[\sin \omega t (1 - \cos \omega t - \omega t \sin \omega t) + \cos \omega t (\sin \omega t - \omega t \cos \omega t)\right]\right] \quad (6.52)$$

Whence, for $x = 0$ and $nv_0/\omega = p$, we have

$$p/4 (\omega t)^2 - \omega t \sqrt{1 + \xi_M \sin(\omega t - \omega t)} = \quad (6.53)$$

$$= \frac{\xi p}{2}\left[\sin \omega t (1 - \cos \omega t - \omega t \cos \omega t) + \cos \omega t (\sin \omega t - \omega t \cos \omega t)\right]$$

The family of curves $\omega\tau_F = f(\xi)$ with parameter p is thus constructed on the plane $\xi, \omega\tau$. In Figure 6.26 these are

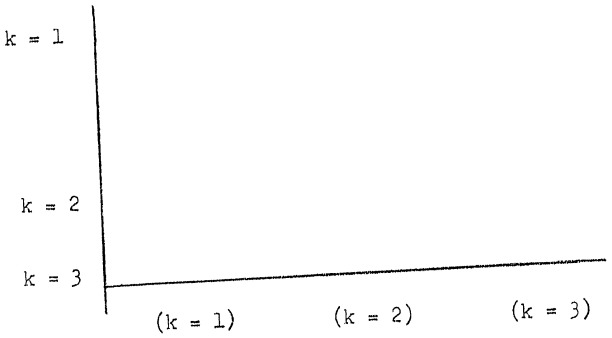

Figure 6.26

the curves a which constitute the locus of $\omega\tau$ and ξ corresponding to any (!) assigned focus. In just the same way, and for the same values of p, we construct the family of curves b, obtained under the condition x = 0, and the coordinates of which correspond to the return of the electron packets to the modulator. The points of intersection of those curves of the families a and b which correspond to the same values of the parameter p, from the curve c. The latter constitutes the curve $\omega\tau_F^* = f(\xi)$ that corresponds to the return of the focus to the modulator. The ordinates of those points on curve c whose abscissae are the values $\omega\tau_F^*$, found for the same values of p from equation (6.53), give us the values of

sought, for the various excitation regions.

By using such somewhat unwieldy methods it is possible to establish, without placing any limitation whatever on the value of the following important circumstances that characterize the operation of a retarding-field system in the presence of an alternating field in the interelectrode space. Study of the curves for the locus of foci shows that their character is qualitatively maintained. However, the phase of focus-return ωt_s, which in the case of a direct field we assumed to be equal, within fairly precise limits of accuracy, to π, varies here and increases with ξ. The corresponding values of the retardation factor n likewise increase. In brief, if ωt^*_s, n^* and ξ^* represent the quantities that characterize the regime of focus return to the modulator under the conditions of a direct field, then the values of these quantities that correspond to focus return ih an alternating field may be expressed as

$$\begin{aligned} \tilde{\omega} t^*_s &= \bar{\omega} t^*_s + \Delta \omega t^*_s \\ \tilde{n}^* &= \bar{n}^* + \Delta n^* \\ \tilde{\xi}^* &= \bar{\xi}^* + \Delta \xi^* \end{aligned} \qquad (6.54)$$

For the first excitation regions the following values are obtained:

Table 6.10

DATA FOR SEVERAL EXCITATION REGIONS

k	1	2	3	4
ωt^*_s	1.2	1.14	1.10	1.07
ξ	0.31	0.17	0.11	0.08

Comparison of these values with those that characterized the analogous regime in the case of a direct field (variant B) shows that the modifications introduced by the alternating field are very insignificant.

(c) Summary of the Results of the Investigation of the Various Regimes

Let us classify as follows the principle regimes of the system under examination:

(1) Regimes characterized by the equality of $\mathcal{E}$ and $\mathcal{E}_M$ occur either when $U_B = 0$, $U_{B1} = 0$; or when $U_{Bo} = -U_{Mo}$ and $U_{B1} = -U_{M_1}$; or under the condition that $\mathcal{E}_M U_{Bo} = -\mathcal{E}_B U_{Mo}$. All of these regimes may occur in a system with a single-grid modulator.

(2) The retarding electrode, possessing a direct potential, does not participate in the oscillation; then

$$\mathcal{E} = \frac{\mathcal{E}_M}{1-\beta}.$$

This case is of interest for the consideration of systems with a two-grid modulator and a retarding electrode.

(3) The most interesting case is that of the symmetric connection of the circuit across the grid and the retarding electrode; obviously here $\mathcal{E}_M = \mathcal{E}_B$ and

$$\mathcal{E} = \frac{2\mathcal{E}_M}{1-\beta}$$

To sum up in brief the results of the study of these regimes:

(1) The regime $\mathcal{E} = \mathcal{E}_M$. The parameter p for the various oscillation regions may be expressed as

$$p = \frac{2k\pi}{k^2\pi^2 - 1} \qquad (6.55)$$

We observe that in the case of a direct field for the variant B and the same focus-return conditions, this parameter is expressed as $p = 2/k\pi$.

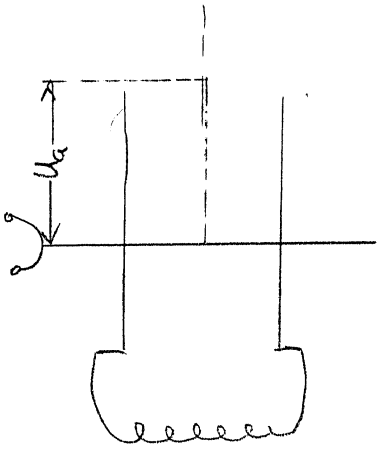

Figure 6.27

The equation of the working diagram on the plane $U_o - U_B$, which has the same qualitative appearance as that in Figure 6.20, assumes the form

$$U_{B_o} = U_{M_o} - \frac{6280\, k\pi\, d}{\lambda(k^2\pi^2 - 1)} \sqrt{U_{M_o}}$$

and, for $U_{B_o} = 0$, (6.56)

$$U_{M_o} = \left[\frac{6280\, k\, d}{\lambda(k^2\pi^2 - 1)}\right]$$

(2) The excitation of a two-grid modulator, allowing for the alternating field outside it: this is a regime for which

$$\tau = \frac{\tau_M}{1-\beta}.$$

Let us imagine the system represented in Figure 6.27, in which the oscillatory circuit is connected across the grids of a two-grid modulator, while the retarding electrode does not participate in the oscillation. In spite of this, there will be an alternating field in the space MB provided the modulator is not an endovibrator with grids close together. Analogous systems, for instance, were constructed by the author and Yu. F. Miller in 1940-41. The scheme of one of these tubes is shown in Figure 6.28. The oscillatory system is formed either of a concentric line ending at the modulator grids or a Lecher system connected to those grids.

In this case the factor $\beta = U_{B_0} / U_{M_0}$, which rather strongly deforms the "crest" curves of the oscillation regions, plays an important role in the calculation of the working diagram; this influence is illustrated by Figure 6.29 in which curves B and B' are calculated for the first two regions of the tube (d = 0.5 cm),

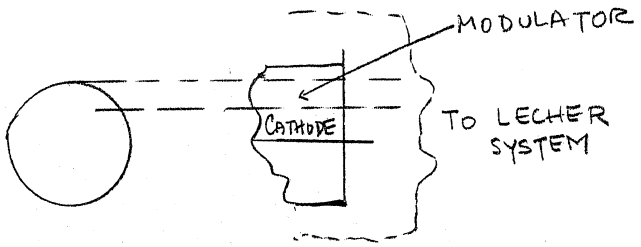

Figure 6.28

working on a wavelength 40 cm, without allowing for the factor. Curves A and A' are the same, but allowing for .

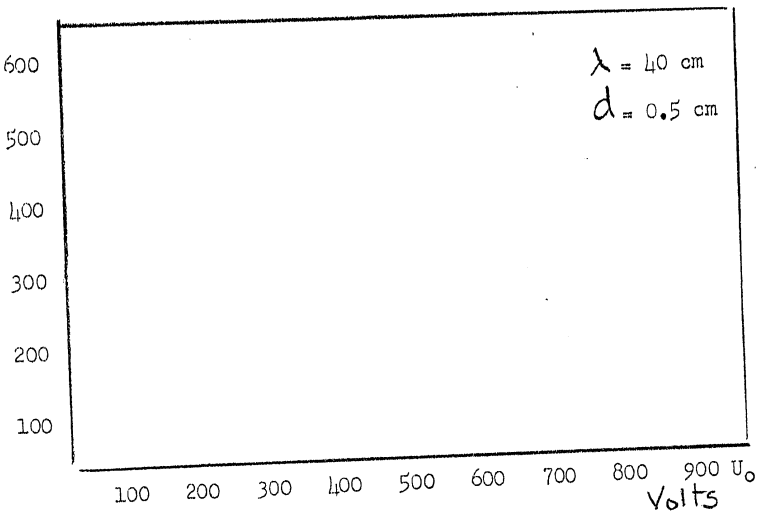

Figure 6.29

The "crest" equations become more complicated in this case:

$$U_{B_o} = \frac{(2k - 0.5)^3 \pi^3 - 4[1 + (2k - 0.5)\pi]}{(2k - 0.5)^3 \pi^3} U_{M_o} - \frac{12560\, d}{\pi\lambda(2k-0.5)^3}\sqrt{U_{M_o}} \qquad (6.57)$$

and, for $U_{B_o} = 0$:

$$U_{M_o} = \left\{ \frac{12560\, d(2k - 0.5)^2}{[(2k - 0.5)^3\pi^3 - 4[1 + (2k - 0.5)\pi]\lambda} \right\}^2$$

In spite of their evident unwieldiness, these formulae take on a very simple form on substitution of the numerical values of k. Thus, for k = 1 (the first region), we obtain

$$U_{B_o} = 0.8\, U_{M_o} - \frac{2660\, d}{\lambda}\sqrt{U_{M_o}}$$

$$U_{M_o} = \left[\frac{3220\, d}{\lambda}\right]^2$$

(3) The regime of symmetrical operation of the electrodes: $\xi_M = \xi_B$. This regime is the most interesting one from the point of view of verifying the theory by experimental results, since it corresponds to the ordinary operation of the retarding-field with the oscillatory system connected across the grid and anode. Analysis of this case yields the following equations for a parameter analogous to p:

$$\frac{v_o}{\omega d} \quad \frac{2k\pi}{k^2\pi^2(1 - \beta) - 2} \qquad (6.58)$$

and for the diagram of the excitation regions

$$U_{B_o} = \frac{k^2\pi^2 - 2}{k^2\pi^2}\, U_{M_o} - \frac{6280\, d}{\lambda k \pi}\sqrt{U_{M_o}} \qquad (6.59)$$

and, for $U_{B_o} = 0$,

$$U_{M_o} = \left[\frac{6280\, dk}{\lambda(k^2\pi^2 - 2)}\right]^2$$

Under a symmetrical regime, bilateral excitation of the system is possible, and study of this can give us not only the course of the "crests" of the oscillation regions on the diagram, but also the distribution of the maxima of intensity in these regions. In fact, by expanding the concept of the "beat of the focus" on both electrodes bounding the conversion zone, it may be shown that the optimum excitation conditions should occur in the case of the simultaneous "rolling under" [podkachka] of energy toward both electrodes,

which takes place only at certain discrete values of β defined by the equation

$$\beta=\frac{4\xi_M}{(\omega\tau_F)^2}(\sin\omega t_F-\sin\omega t_s^*-\omega\tau_F\cos\omega t_s^*)-\xi_M\sin\omega t_s\cong\frac{4\xi_M}{R\pi}), \quad (6.60)$$

For the first excitation zone, the following values of are obtained:

Table 6.11

VALUES OF FOR SEVERAL EXCITATION REGIONS

k	1	2	3	4	.....
β	-0.33	-0.12	-0.08	-0.05	.....

This circumstance actually leads in practice to the formation of oscillation regions located along the "crests", and of distinctly expressed maxima corresponding to the points of intersection between the "crests" and the straight lines β = const, plotted by equation (6.60). For values of β higher than -0.5 ÷ -0.6, any oscillations at all prove impossible, which is entirely confirmed by the experimental data.

The working diagram of the Muller tube [7] (Figure 6.30) may serve as an illustration of all these calculations. In this diagram the theoretically calculated "crests" of the maxima of the oscillation regions are plotted in juxtaposition to the experimental data. Here the curves A_1 and A_1' correspond to the first and second regions of excitation at wavelength 16.5 cm, while curves A_2 and A_2' are for the same regions at wavelength 21 cm. The inclined straight lines correspond to the values of β = -0.33 and β = -0.12

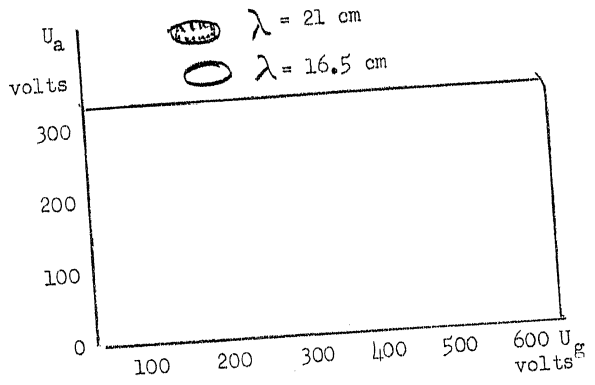

Figure 6.30

and intersect these curves precisely at the points of the experimentally determined maxima.

All our formulae were deduced for plane electrodes. On transition to the cylindrical electrodes, which are often used in practice, the quantity d, being the distance from modulator to retarding electrode, may be replaced by the condition

$$d = r_M \ln \frac{r_B}{r_M}, \qquad (6.61)$$

where r_M is the radius of the modulator or of the grid in the case of an ordinary triode, and r_B is the radius of the retarding electrode. It was precisely this change that was made in the formulae of (6.59) for the calculation of the "crests" of the working diagram for the Muller cylindrical tube, which is shown in Figure 6.30.

In this way, in the kinematic analysis of the retarding-field arrangement, allowance for the alternating field in the conversion space leads to the elucidation of a series of elaborative details

and to the establishment of computational formulae more in line with the actual phenomena.

(d) Energetic Analysis of the Retarding-Field System, Allowing for the Alternating Voltage

The excitation of the retarding-field system may be analyzed without imposing any limiting conditions whatever on the value ξ, if the calculation of induced current is made use of. This calculation is based on the formula we have repeatedly encountered:

$$i_{ind}(t) = -\frac{i_0}{d}\int_{t-\tau}^{t}\frac{dx}{dt}\,dt_s.$$

Here $\tau = t_r - t_s$: the time spent by the electron or electron packet in the interelectrode space. It may be found from equation (6.49), if x is equated to zero, and $t = t_r$, the instant of the electron's return to the modulator, bearing in mind the most interesting practical regime characterized by the condition $\xi_B = \xi_M$. Taking for dx/dt the expression for the velocity of the electron obtained by the first integration of the equation of motion, we obtain the following expression for i_{ind}:

$$i_{ind} = i_0\frac{\xi v_0^2(1-B)}{2d^2\omega^2}\left\{\begin{array}{l}\cos\omega t\left[2\cos\omega\tau - 2 + \omega\tau\sin\omega\tau\right] \\ +\sin\omega t\left[2\sin\omega\tau - \omega\tau(\cos\omega\tau + 1)\right]\end{array}\right\} \qquad (6.62)$$

The value of $\omega\tau$ is here a function of the time, and it must be expressed in terms of θ_0, the "undisturbed" transit angle, which characterizes the time spent by the electron in the retarding space, with $\xi = 0$, and which transit angle is equal to:

$$\theta_0 = \frac{4\omega}{nv_0} \tag{6.63}$$

On representing ωt in the form of an exponential series in the powers of ζ, the coefficients of which depend on θ_0 and t, and then substituting this series in expression (6.62), an expression for the induced current may be obtained in the form of a Fourier series. Omitting the fairly complicated mathematical transformations, we obtain, for the first harmonic of the current:

$$i_{ind} = i_0 \frac{\xi V_0^2 (1-B)}{2d^2\omega^2} \left\{ \sin\omega t (A_1 + A_3\xi^2) + \cos\omega t (B_1 + B_3\xi^2) \right\} \tag{6.64}$$

where the coefficients A_1, A_3, B_1 and B_3 are expressed in terms of θ_0 in the following manner:

$$A_1 = 2\sin\theta_0 - \theta_0 - \theta_0\cos\theta_0 \tag{6.65}$$

$$B_1 = \theta\sin\theta_0 - 2 + 2\cos\theta_0$$

$$A_3 = \frac{1}{\theta_0^3} \left\{ \left[(1 - \cos\theta_0)^2 + (\theta_0 - \sin\theta_0)^2 \right] \cdot \left[1 - \cos\theta_0 - \theta_0\sin\theta_0 + \frac{\theta_0^2}{2}\cos\theta_0 \right] + (\theta_0\sin\theta_0 - 1 + \cos\theta_0)\theta_0^2(1 - \cos\theta_0) \right\}$$

$$B_3 = -\frac{6}{\theta_0^3} \left\{ \left[(1 - \cos\theta_0)^2 + (\theta_0 - \sin\theta_0)^2 \right] \cdot \left[\theta_0\cos\theta_0 - \sin\theta_0 + \theta_0^2/2 \cdot \sin\theta_0 \right] - (\theta_0\cos\theta_0 - \sin\theta_0)\theta_0^2(1 - \cos\theta_0) \right\}$$

The term with $\cos\omega t$ forms the active component of the current, which component is either in phase with the voltage or lead is by π. The term with $\sin\omega t$ constitutes the corresponding reactive component. Designating by U the amplitude of the alternating voltage between the modulator and the retarding electrode, we establish the following relations:

$$-\frac{i_{1\,act}}{\tilde{U}} = \frac{1}{R_{osc}} = -\frac{I_0 V_0^2}{2d^2\omega^2 U_{M_0}}\left(B_1 + B_3\xi^2\right), \quad (6.66)$$

$$-\frac{i_{1\,react}}{\tilde{U}} = \frac{1}{\omega L_{osc}} = -\frac{I_0 V_0^2}{2d^2\omega^2 U_{M_0}}\left(A_1 + A_3\xi^2\right), \quad (6.67)$$

They represent the active and reactive conductances in the oscillator under consideration, which may be represented in the form of a parallel connection between the negative resistance R_{osc}

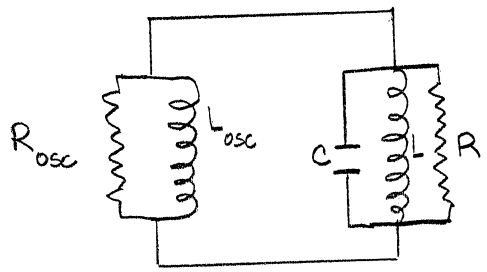

Figure 6.31

and the inductance L_{osc}, with the load of the oscillatory circuit LCR imposed on that connection (Figure 6.31). The oscillatory properties of the oscillator are thus determined by the magnitudes of θ_0, ξ, U_{M_0} and U_{B_0}. The variation of the coefficients B_1 and B_2, that determine the conductance, is shown in the curves of Figure 6.32 as a function of the transit angle θ_0.

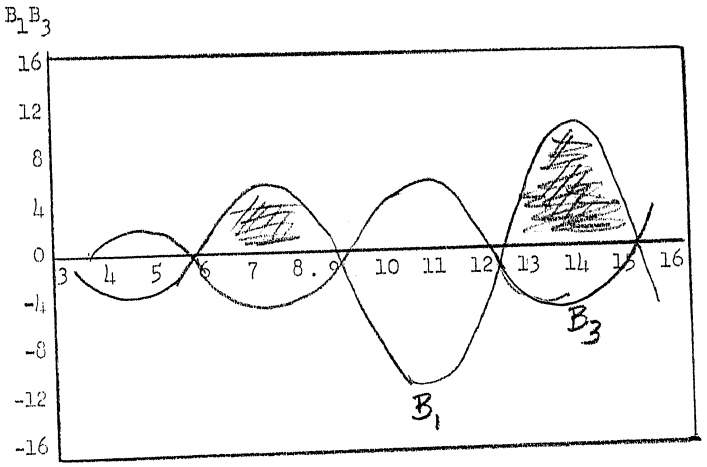

Figure 6.32

The condition for excitation of the circuit is obviously:

$$\frac{1}{R_{osc}} + \frac{1}{Z} < 0$$

(or $\frac{1}{R_{osc}} < 0$ for no-load operation).

Here Z is the shunt-impedance of the circuit. To satisfy the condition for self-excitation, it is necessary that $B_1 > 0$. It will be seen from Figure 6.32 that B_1 is positive in a whole series of successive regions of variation (which are hatched in the drawing). In each excitation region the negative conductance has a maximum, the size of which maximum increases with the number of the excitation region. This means that at high loads the regions of higher orders are more easily excited, and this is completely confirmed by experiment.

Remembering that θ_o is connected with the parameters of the regime by equation (6.63), the oscillation regions shown in Figure 6.32 may be converted to the ordinary working diagram of the oscillator, for the plane $U_{M_o} - U_{B_o}$. The result of such a conversion for a resonance tank [rezotank] with retarding field is shown in Figure 6.33. For each region three theoretical curves have here

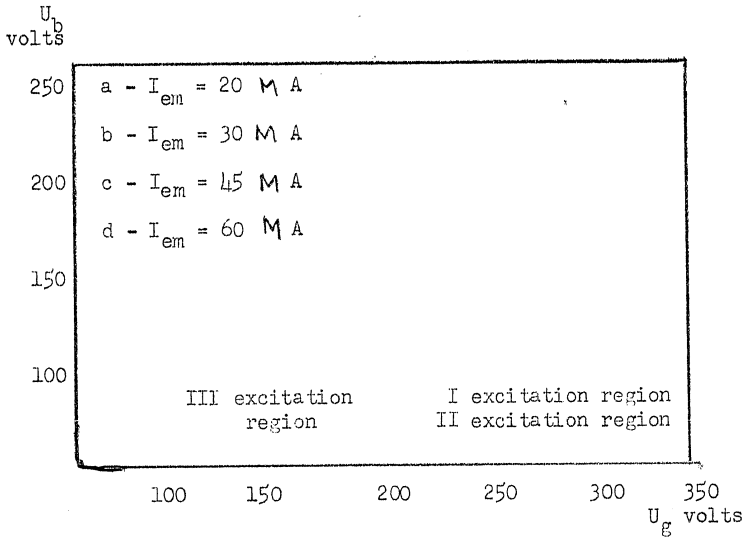

Figure 6.33

been assigned: the broken lines show the boundaries of the regions and have been calculated from the points of variation of B_1, where $B_1 = 0$; the dot-dash lines correspond to the maximum of B_1 and consequently to the "crest" of the oscillation region. The solid lines in Figure 6.33 show the boundaries experimentally determined, at various emission currents, for the oscillation regions. From the condition $1/R_{osc} + 1/Z < 0$ we may calculate that minimum strength of current i_o which will assure excitation of oscillations in the

system involved for a given transit angle θ_0. Thus, for instance, for the self-exciting resonance tank, the oscillatory system of which is characterized by the value $1/Z = 15.0 \cdot 10^{-6}$ mho, it is necessary to have

$$1/R_{osc} = -i_0 \cdot 3.4 \cdot 10^{-3} \text{ mho},$$

(by equation (6.66) with $\xi \to 0$), which gives, for the minimum current, $i_0 = 4.4$ milliamperes. The actual emission current, of course, must be $1/\Psi$ higher.

From the equations given above we may calculate the efficiency:

$$\eta = \frac{\frac{1}{2} i_{1\,act} \tilde{U}}{i_0 (U_{M0} - U_{B0})} = \frac{4}{\theta_0^2} [B_1 \xi^2 + B_3 \xi^4] \qquad (6.69)$$

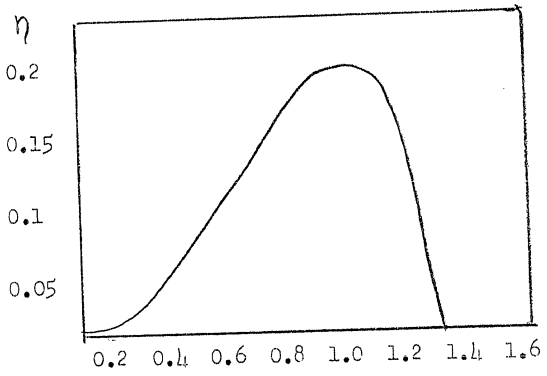

Figure 6.34

which for the maxima of the B_1 curve gives

$$\eta_{max}(\theta_0) = -\frac{B_1^2}{\theta_0^2 B_3} \qquad (6.70)$$

and, for the regions designated by higher numerals, approximately reduces to

$$\eta_{max} \approx 2/\theta_0 \qquad (6.71)$$

It will be seen that the efficiency falls in the regions with higher numbers, although their excitability increases with their numeral.

To illustrate the energy relations in this system we present two more graphs. Figure 6.24 shows the relationship of the system efficiency to $\mathcal{E}$ for the optimum transit angle $\theta_0 = 7.56$, in the first excitation region. As we note that the maximum efficiency,

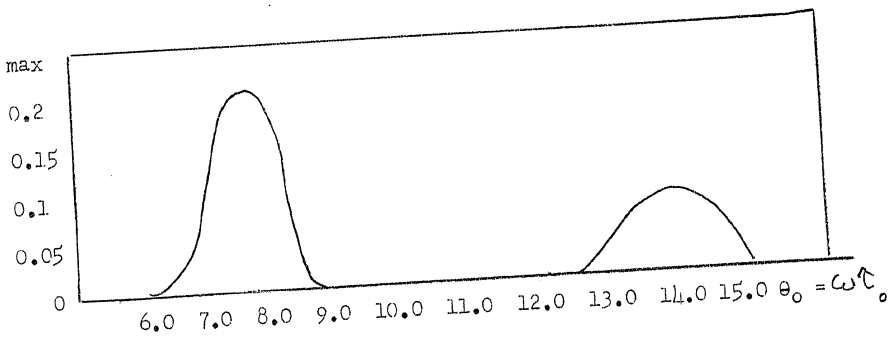

Figure 6.35

equal to about 22%, corresponds to $\mathcal{E} = 1$, we should not forget that this $\mathcal{E} = 2\mathcal{E}_M(1-\beta)$, i.e. is determined not alone by our customary coefficient of velocity modulation of the stream, but also by the ratio between the direct voltage om the modulator and that on the retarding electrode. For this reason, in order to obtain the maximum efficiency within each oscillation region, we must choose $\mathcal{E}$ so that it satisfies the condition

$$\mathcal{E}_{opt} = \sqrt{\frac{B_1}{-2B_3}}, \qquad (6.72)$$

whence, too, the maximum efficiency expressed by formula (6.70) will result.

Figure 6.35 represents the course of the curve of maximum efficiency for the first and second excitation regions, as a function of θ_o. The values obtained from the maxima of these curves, $\eta \cong 22\%$ for the first region, and $\eta \cong 13\%$ for the second, agree fairly well with those obtained by the above-described method of calculating the power integral for an oscillator with a two-grid modulator and a direct retarding field.

Turning now to the expression of the reactive conductance (6.67) and the graph of the coefficients A_1 and A_2 determining it, shown in Figure 6.36 as a function of the transit angle θ_o, we are now in a position to obtain an explanation of the variations in frequency observed on variation not only of U_o and U_B, but also, for instance, of the oscillation amplitude and load of the oscillator. The point is that the working frequency of the system is determined by all of the reactive elements that belong to the equivalent circuit, based on the condition

$$\frac{1}{\omega L_{osc}} + \frac{1}{\omega L} - \omega C = 0 \qquad (6.73)$$

i.e., at constant L and C, the frequency must vary if by virtue of any conditions whatever L_{osc} should vary. The condition (6.73)

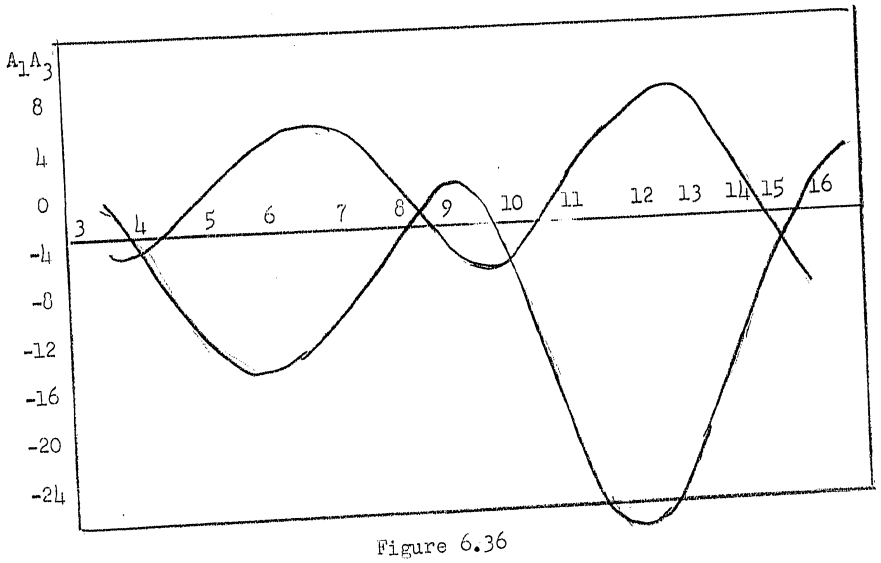

Figure 6.36

contains the explanation for most of the phenomena of the peculiar behavior of the frequency of oscillations on variation in the tuning of the external system connected to the electrodes, which have evoked a good number of theoretical explanations starting out from the postulate of interaction between the independent electronic oscillatory mechanism and an external tuning system (Cf. Kalinin, V. I. Detsimetrovyye i santimetrovyye volny, 1939, Chapter IV, Paragraph 4.3).

(e) Conclusion

In summing up all the material on the retarding-field system set forth in Chapters III, V, and VI, it may be definitely said that the dispute on the existence of "purely electronic" oscillations in the sense of the electronic oscillations of Barkhausen and Zilitinkevich has no longer any meaning at the present time. The most probable behavior of the electron stream in the retarding-field sys-

tem would appear to be as follows: between cathode and grid there is a direct current, which is determined by the total cathode emission current I_{em}. The current ψI_{em} passes through the modulator (whether it is single-grid or double-grid makes no difference in principle). All the events in the electron stream necessary to sustain oscillation occur on the path of that stream to the surface of return, and back to the modulator. If the modulator grids have the same "coefficient of absorption" ψ with respect to the returning electrons, then the return current entering the acceleration space is measured by the value of $\psi^2 I_{em}$ (on condition that the electrons do not reach the retarding electrode!). The coefficient of absorption must, however, in fact be larger for the returning electrons, since the vast majority of them give up energy, on the return path, to the alternating field, and arrive back at the grid with a lower velocity than they had on their outward flight through it. It is for this reason that the negligible part of the electron stream that penetrates back through the modulator into the acceleration space can play no part whatsoever in the excitation of oscillations. The factor that controls the electron stream with the aid of the alternating electric field and determines the frequency of that field, is exclusively the oscillatory system associated with the stream. On account of the reactive properties of the stream itself, only small variations may be made in the frequency of the circuit. Such frequency variations are more noticeable in the retarding-field system than in other electronic oscillators by virtue of its superposition of the functions of the modulator and generating circuit in a single oscillatory system. This circumstance leads to a much sharper differentiation of each individual oscillation region from others; and it is the discreteness of excitation in such regions that constitutes one of the fundamental characteristics that distinguish all electronic generators of ultra-high frequencies.

BIBLIOGRAPHY FOR CHAPTER VI

1. Yu A. Katsman, IAN, ser. fiz. X, 87, 1946.

2. Devyatkov, Danil'tsev and Piskunov, ZhTF, XI, 1348, 1941.

3. Yu. A. Katsman, IAN, ser. fiz. IV, 506, 1940.

4. V. Savel'yev, ZhTF, XI, 1340, 1941.

5. Muller and Rostas, Helv. Phys. Acta, XIII, 435, 1940.

6. V. I. Kalinin, ZhTF III, 332, 1933.

7. J. Muller. Ann. d. Phys., 21, 611, 1934/35.

CHAPTER VII

THE MAGNETRON

7.1 GENERAL CONDITIONS. THE MAGNETRON AS A THERMIONIC SYSTEM.

When we come to consider in greater detail the phenomena in the magnetron oscillator, we must analyze the fundamental properties that give the magnetron its somewhat special position among UHF oscillators. These properties are mainly due to that very peculiar character of the motion of electrons in the magnetron with which we have become acquainted, in its general outlines, in Chapter III.

Let us first take up the solid-anode (single-anode) magnetron. When the magnetic field is zero, this is a simple diode to which the Langmuir relations are applicable. This corresponds to the case of the distribution of potential and space charge, which has been thoroughly studied. If the anode voltage of the diode greatly exceeds the saturation voltage, then the space charge, in practice, disappears, and may be disregarded in the various considerations and calculations.

The existence of a magnetic field bends the trajectories, increases the time spent by the electron between the electrodes, and in consequence increases the density of the space charge. Its effect increases with the flux density of the magnetic field and becomes particularly important when the critical conditions are reached (cf. Chapter III, Paragraph 2). The work of Hull referred to in Chapter III was the first in a long series of researches that yielded very valuable results, but which over simplified the problem by ignoring the space-charge effect. To allow for this

effect in the case of the magnetron involves considerably greater difficulties than for the ordinary diode without a magnetic field, but at the same time it is more essential to the correct solution of the problem. As we have already seen, the critical conditions, and the magnetic flux density and anode potential associated with them, play a very important role. The critical relations between U_a and H obtained by Hull from a consideration of the motion of the electron, without allowing for the space charge, were excellently justified by experiment, together with a goodly number of consequences derived therefrom. According to Brillouin, this circumstance is the result of a curious coincidence due to the fact that the critical magnetic field depends only on the potential difference between cathode and anode and may be found without going into field distribution and shape of electron paths. The space charge powerfully affects these two factors, but has no influence on the potential difference assigned from without the system. The critical conditions, in fact, may be very simply found, even without knowing the shape of the electron paths. Using the notation and coordinate system of Paragraph 3.2 (Figure 3.8), and the expression for the angular velocity of the electron (formula 3.33), we have:

$$\dot{\theta} = \frac{\omega_H}{2}\left(1 - r_o^2/r^2\right) \tag{7.1}$$

where $\omega_H = eH/m$, and we may write the expression for the kinetic energy E_{kin} of an electron at point r at the given instant:

$$E_{kin} = \tfrac{1}{2} m(\dot{r}^2 + r^2\dot{\theta}^2) = \tfrac{1}{2}m\left[\dot{r}^2 + \frac{\omega_H^2}{4}\left(r - r_o^2/r\right)^2\right]. \tag{7.2}$$

By the principle of conservation of energy we may write:

$$E_{kin} + eU(r) = 0 \qquad (7.3)$$

if we assume the electrons to leave the cathode at zero velocity. The critical conditions are obtained from equation 7.3 by substituting (7.2) in it and bearing in mind that $\dot{r} = 0$ and $r = r_a$; whence

$$\frac{1}{8}m\omega_H^2(r_a - r_o^2/r_a) + eU_a = 0. \qquad (7.4)$$

The ordinary conditions for the critical regime are obtained from (7.4) with $r_o \ll r_a$:

$$H_k^2 = \frac{8m}{e} \cdot \frac{U_a}{r_a^2} \qquad (7.5)$$

or

$$H_k = \frac{6.72}{r_a} U_a^{\frac{1}{2}}$$

Thus, the true critical conditions are obtained from purely energetic considerations with no information whatsoever on the character of the distribution of the space charge and the form of the electron-paths.

Up to the present time, there is still no generally settled opinion on the distribution of the space charge in the magnetron and the shapes of the electron-paths due to it. We shall here discuss two very interesting view points represented in the works of Braude [2, 3] and Brillouin [1].

The initial assumptions of these works are identical. To the ordinary equations of motion of electrons in a cylindrical system of coordinates:

$$\ddot{r} - r\dot{\theta}^2 = \frac{e}{m}(E_r - H_r\dot{\theta})$$

$$\frac{1}{r}\frac{d}{dt}(r^2\dot{\theta}) = \frac{e}{m}H\dot{r} \qquad (7.6)$$

$$m\ddot{z} = 0$$

two supplementary equations are added, connecting the current I for unit electrode length ρ, the density of the space charge, and with field intensity $E_r = -\frac{dU_r}{dr}$;

$$\frac{1}{r}\cdot\frac{d}{dr}\left(r\frac{dU_r}{dr}\right) = 4\pi\rho \qquad (7.7)$$

$$I = 2\pi r\rho\dot{r}$$

It is also assumed that the electrons' exit velocity from the cathode is zero; and that at the instant of exit $t = 0$, $r = r_o$, $\dot{r} = \theta_o = 0$, and $E = E_o$ the field intensity at the cathode.

From equation (7.7) it follows that:

$$rE_r = 2I\tau \qquad (7.8)$$

where τ is the transit time of the electron from the filament, where $r = r_o$, to the point $r = r$. The same relation should obviously hold for ordinary tubes as well. Its application to magnetrons, however, encounters certain difficulties. The point, of course, is that for $H \geqslant H_k$, the current $I = 0$, but r is not zero. The question arises: what are E_r and τ ? A possible answer to

this question may be that since the electrons never reach the anode under this regime, $\tau = \infty$. This means that the product $I\tau$ yields an indeterminate quantity of the type $0 \cdot \infty$, thus making possible the existence of a finite value for E_r. Obviously we must be very cautious in the specific application of equations (7.7) and (7.8) to critical and postcritical current per unit electrode length instead of the anode current, as in precritical regimes. This substitution, however, appears somewhat formal and physically insufficiently grounded, although it helps us to perform a number of important calculations, with good results.

We shall employ the following notation: $\frac{eH}{2m} = \frac{1}{2}\omega_H = \omega_L$ (Larmor's cyclic frequency) and $\frac{e}{m} E_0 = \beta$; $2\frac{e}{m} I = \alpha$. Then from (7.6) and (7.7) the following basic equations may be obtained. Their solution enables us to find the distribution of potential, the density of the space charge, the magnitude of the rotational current, and the wavelength of the first-order electronic oscillations:

$$\dot{\theta} = \omega_L(1 - r_0^2/r^2) \qquad (7.9)$$

$$\ddot{r} + \omega_L^2 r(1 - r_0^4/r^4) = \frac{r_0\beta + \alpha t}{r} \qquad (7.10)$$

$$\frac{e}{m} U_r = \beta r_0 \ln\frac{r}{r_0} + \alpha \int_0^t t\frac{\dot{r}}{r}\, dt. \qquad (7.11)$$

The case of the absence of the space charge is obtained at $\alpha = 0$. Substitution of this condition in the basic equations quickly brings us to the well-known relations that we discussed thoroughly in Chapter III. Things are far more complicated where there is a full space charge, i.e. under the condition $E_0 = 0$ or

$\beta = 0$. Setting $\beta = 0$ in equation (7.10), the quantities r and $\dot{r}$ may be found, after mathematical transformations, in the form:

$$r = 2\sqrt{\frac{\alpha}{3\omega_L}}\,(\omega_L t)^{3/2}\left[1 - 10.5\left(\frac{\omega_L t}{10}\right)^2 + 44.5\left(\frac{\omega_L t}{10}\right)^4 - 88.5\left(\frac{\omega_L t}{10}\right)^6 + \ldots\right] \qquad (7.12)$$

$$\dot{r} = 3\sqrt{\frac{\alpha}{3\omega_L}}\,(\omega_L t)^{\frac{1}{2}}\left[1 - 24.6\left(\frac{\omega_L t}{10}\right)^2 + 165\left(\frac{\omega_L t}{10}\right)^4 - \ldots\right] \qquad (7.13)$$

By setting $\dot{r} = 0$, we determine the transit time τ for the critical regime, from the latter formula. In doing this it develops that we may consider $\omega_L \tau = \gamma\pi$, where γ is determined by the degree of proximity and is roughly equal to 0.9.

The value of field intensity for the precritical regime ($H < H_k$), is expressed as follows:

$$E = \frac{3}{2} k^2 \frac{U_a}{r_a} \frac{1}{R(\omega_L \tau)} \left(\frac{\omega_L t}{\omega_L \tau}\right)^{-\frac{1}{2}} \frac{1}{(\omega_L \tau)^2 R(\omega_L \tau)} \qquad (7.14)$$

Here $R(\omega_L \tau)$ denotes the series within the brackets of formula (7.12) with the transit time τ substituted in it, while $k = H/H_k$.

In the case $H \geq H_k$, according to Braude, the quantity I, in determining α, is taken as the rotational current instead of the anode current, which becomes equal to zero in that case. He calls the current passing from cathode to anode I_1 and the current passing from anode to cathode I_2, and then defines the rotary current as $I = I_1 - I_2 \approx 2I_1 \approx -2I_2$, and the anode current as $I_a = I_1 + I_2 \approx 0$.

For $H = H_k$, as already remarked, $\omega_L t = \gamma\pi$, and

$$E = \frac{3}{2}\frac{U_a}{r_a} \cdot \frac{1}{R(\gamma\pi)} \left(\frac{\omega_L t}{\gamma\pi}\right)^{-\frac{1}{2}} \cdot \frac{1}{(\gamma\pi)^2 R(\omega_L t)} \tag{7.15}$$

If the magnetic field is higher than the critical, then the space between the cathode and anode of the magnetron may be divided into two parts. The first extends from the cathode to the middle of the electron return space, and has radius r_m. A regime of full space charge may occur within it. The second part is included within the ring of internal radius r_m and external radius r_a, and contains no electrons. The position of the plane of demarcation is defined by the quantity $k = H/H_k$. Field intensity in it proves to be equal to

$$E_m = \frac{3}{2}\frac{U_m}{r_m} \cdot \frac{1}{(\gamma\pi)^2 R^2(\gamma\pi)} \tag{7.16}$$

where

$$U_m = U_a k^2 (r_m/r_a)^2,$$

and

$$\frac{r_m^2}{r_a^2}\left[1 + \frac{3}{2}\ln\frac{r_a}{r_m} \cdot \frac{1}{(\gamma\pi)^2 R^2(\gamma\pi)}\right] = \frac{1}{k^2} \tag{7.17}$$

The distribution of potential $U_r(r)$ in the case of the ordinary Langmuir diode ($H = 0$), is determined by the relation

$$\frac{U_r}{U_a} = \left(\frac{r}{r_a}\right)^{2/3}.$$

In the magnetron this also takes place at H H_k:

$$\frac{U_r}{U_a} = \frac{r^2}{r_a^2} \; k^2 \left[1 + \frac{9}{4}\left(\frac{Q(\omega_L t)}{\omega_L t}\right)^2\right] \qquad (7.18)$$

while for H $>$ H_k:

$$\frac{U_r}{U_m} = \frac{r}{r_m}\left[1 + \frac{9}{4}\left(\frac{Q(\omega_L t)}{\omega_L t}\right)^2\right] \qquad (7.19)$$

The quantity $Q(\omega_L t)$ in equations (7.18) and (7.19) represents the ratio $\frac{P(\omega_L t)}{R(\omega_L t)}$, while $P(\omega_L t)$ is the value of the series in formula (7.13).

The distribution of potential in the magnetron may be represented in simpler form as:

$$\frac{U_r}{U_a} = \left(\frac{r}{r_a}\right)^p \qquad (7.20)$$

The index p is here very close to unity. Figure 7.1 illustrates the various potential-distribution curves, calculated for tubes with $r_a/r_o = 0$. These curves are as follows:

1. $\frac{U_r}{U_a} = \frac{r}{r_a}$ (p = 1).

2. $\frac{U_r}{U_a} = \left(\frac{r}{r_a}\right)^{0.9}$ (p = 0.9).

3. $\frac{U_r}{U_a} = \left(\frac{r}{r_a}\right)^2 \left[1 + \frac{9}{4}\left(\frac{Q(\omega_L t)}{\omega_L t}\right)^2\right]$ for the critical regime

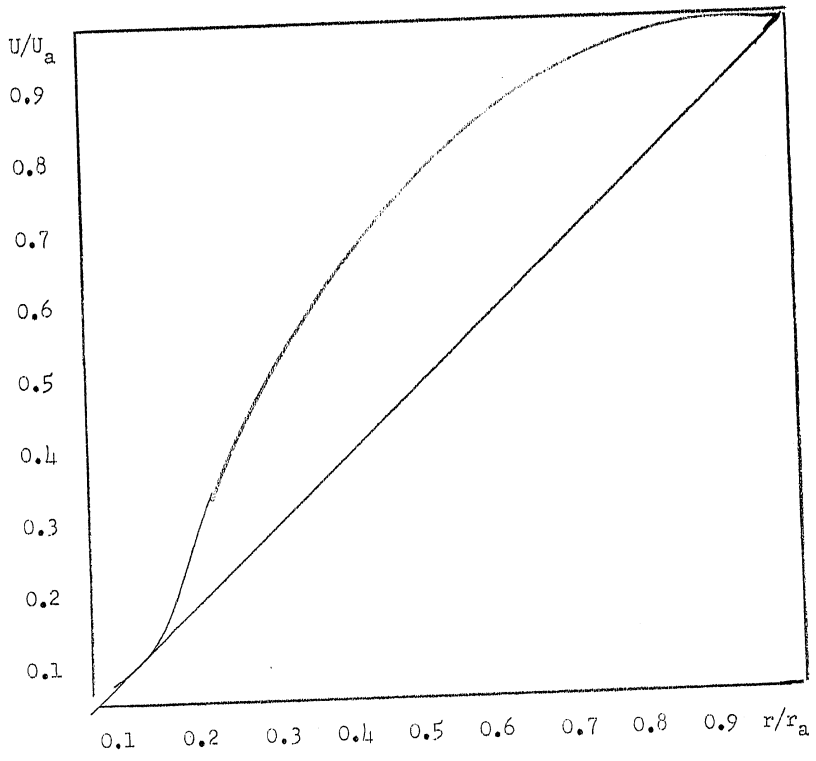

Figure 7.1

4. $\frac{U_r}{U_a} = \left(\frac{r}{r_a}\right)^{0.8}$

5. $\frac{U_r}{U_a} = \frac{\ln \frac{r}{r_o}}{\ln \frac{r_a}{r_o}}$ -- the distribution of potential without the space charge

6. $\frac{U_r}{U_a} = 1.$

7. $\frac{U_r}{U_a} = \left(\frac{r}{r_a}\right)^{2/3}$ -- the Langmuir distribution of potential.

It may apparently be considered with a sufficient degree of accuracy that the distribution of potential is almost linear with a full space charge in a cylindrical solid-anode magnetron. This inference of Braude differs, however, from the results of Brillouin, who gives the expression for distances far enough from the filament ($r_o \ll r$):

$$U(r) = \frac{m\omega_L^2}{2e} r^2, \text{ which leads to}$$

$$\frac{U_r}{U_a} = \left(\frac{r}{r_a}\right)^2. \qquad (7.21)$$

The origin of this divergence in the results of two very interesting works, both of which start out from the same premises, is in the respective treatment of the character of the electron-paths by each of these authors.

Braude starts out from the idea of the ordinary electron-paths of the type developed by Hull, which begin and end at the cathode and have the shape of a cardiod. These calculations have the result that if, in the absence of a space charge, the path of the moving electron covers an angle of 180°, this angle will increase to 270° if there is a Langmuir distribution of the space charge, and to 360° for a full space charge -- i.e. in that case it will cover the entire circumference. Figure 7.2 shows the electron-paths in these three different cases (a simple logarithmic distribution of the potential), the second to the Langmuir distribution (corresponding to curve 7 of Figure 7.1), and the third to the case of the full space charge, with p = 1 (curve 1 of Figure 7.1).

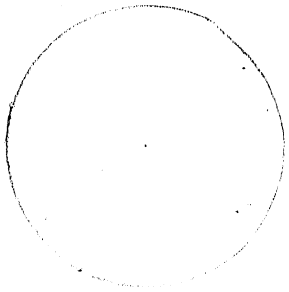

Figure 7.2

The pattern of electron motion is presented differently from the Brillouin point of view. The Hull type path, on which the electrons return to the cathode or describe a few loops on the plane perpendicular to the axis of the system, does not in his opinion correspond to the true situation, even if in their calculation the effect of the space charge is taken into account in the form we have just indicated. The fundamental principle of his position is that the problem of electron motion through the electrostatic and magnetic fields cannot be reduced to the ordinary problems of mechanics. The existence of the Lorentz force, which has no analogue in mechanics, is here responsible for specific difficulties. Brillouin brings in the Larmor theorem to overcome these difficulties. The fact that Hull-type paths are observed on experimental models (the works of Kilgore [4], Grechowa [5], cf. also infra, Paragraph 7.3) still cannot serve as a proof that they really exist. The point is that these experiments are performed with the aid of a narrow electron beam emitted by a slotted cathode of the model or a very small spot of oxide on a heated cathode. The electron path is rendered

visible either by filling the tube with gas (Kilgore) or by introducing some foreign substance into the interelectrode space (Grechowa uses fluorescent filaments). It is evident that in both these cases the electron beam encounters conditions fundamentally different from the real ones. The actual paths that appear probable on the basis of the theory developed by Brillouin, are shown in Figure 7.3, where the cases A, B, C, and D correspond to increasing values of the magnetic field intensity. Each path is determined

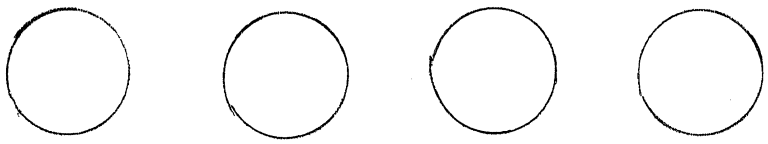

(A) (B) (C) (D)

Figure 7.3

by a "characteristic length" L_H, which according to Brillouin is determined by the expression:

$$L_H = \sqrt{-\frac{el}{m\omega_L^2}}$$

or, approximately (7.22)

$$L_H \approx 48\sqrt{\frac{I}{H^3}}$$

where I is the current in milliamperes per unit electrode length reaching the anode, and H is the magnetic field intensity in oersted. Geometrically L_H corresponds to the length of the radius-

vector of the electron path, which this path intersects at an angle of $\pi/4$. Case (A) corresponds to a very weak magnetic field intensity and a very great $L_H \gg r_a$. The electron paths are easily bent, however, Case (B) represents the path with a somewhat greater magnetic field intensity. Here $L_H \approx r_a$ and the electron impinges on the anode, describing a very considerable arc. Case (C) illustrates the situation when $L_H \ll r_a$ and the electron reaches the anode only after several convolutions of the spiral. The logical goal of this character of electron motion is the critical regime depicted in Figure 7.3d. Here L_H must be considered zero, for not a single electron impinges on the anode, the spirals are developed into a set of circles, and the entire space charge rotates around the cathode like the rotor of an electric motor.

Thus, for $H \geqslant H_k$ the electron paths have the character of circles, which may, perhaps, be to some extent analogous to the above remarked occupation of the whole 360° angle by the electron path under the condition of the full space charge. According to Brillouin, however, at $H \geqslant H_k$ the radial component of electron motion practically ceases to exist. The density distribution of the space charge is also directly connected with the shape of the electron path. Here, too, the two authors we have mentioned reach different solutions of this question. Without dwelling on the equations, we present only the graph of the distribution of the space charge. Figure 7.4 represents the relationships $\rho = f(r/r_a)$, according to Braude. Curve 1 gives the distribution of the density for the Langmuir diode ($H = 0$), i.e.

$$\rho = \frac{U_a}{9\pi r_a^2} \cdot \frac{1}{\left(\frac{r}{r_a}\right)^{4/3}} \qquad (7.23)$$

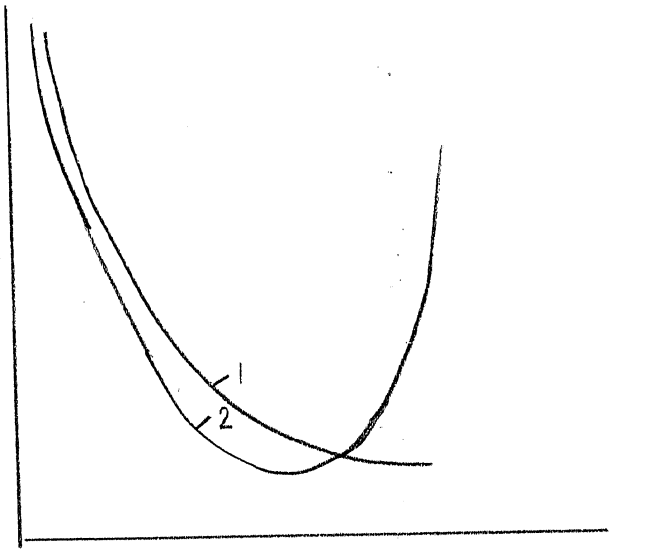

Figure 7.4

Curve 2 corresponds to the critical regime $H = H_k$. It will be seen that a virtual cathode occurs near the cathode in both cases, i.e. a considerable increase in the density of the space charge. At $H = H_k$, in the magnetron, there is also a second virtual cathode. This is around the anode, and with further increase in H it is displaced within the tube and moves closer to the actual cathode.

According to Brillouin, in correspondence with the distinctive character of the electron paths, the space charge proves to be

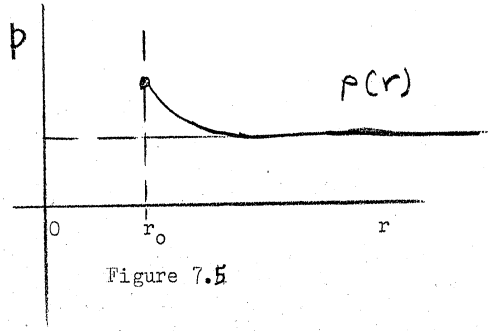

Figure 7.5

distributed according to the law

$$\rho(r) = \frac{m\omega_L^2}{2\pi e}\left(1 + \frac{r_0^4}{r^4}\right) \qquad (7.24)$$

which gives the distribution curve plotted in Figure 7.5. At great distances from the filament, constant density of the charge is obtained, increasing to double around the cathode. Under the critical regime there is thus a cloud of electrons rotating around the cathode and possessing uniform density and constant angular velocity. This cloud rotates inside the anode like some "solid body". This "solid electronic rotor", analogously to any other solid body, possesses a certain kinetic energy which according to the calculations of Brillouin proves to be equal to

$$E_{ergs} = 1.111 \cdot 10^{-5} \cdot U_{ab}^2 \,. \qquad (7.25)$$

By comparisom to other types of tubes this is a high energy. It is an interesting fact that it depends on the applied anode voltage (once assuming the critical conditions). If U_a = = 10,000 volts, the energy stored up in the rotating space charge amounts to 1111 ergs = $1111 \cdot 10^{-4}$ joules per cm of electrode length. A current of 10 milliamperes per 1 second against a resistance of 1111 ohms is sufficient to sustain it. On its conversion into high frequency energy, it can feed a 1-kilowatt transmitter for 10^{-7} second. These considerations, to some extent, reveal the reasons for the high efficiency of the magnetron oscillator under the pulse regime.

From where is this energy taken, and how is it subsequently diffused? Assume that we first turn on the magnetic field H and

the plate current U_a, and then heat the filament. The electrons it emits create the negative charge Q, which is located between the electrodes, at the same time that the positive charge Q appears on the plate. This positive charge charge passes through the anode battery, which imparts the energy QU_a accumulated in the magnetron. If the filament heater is now turned on, the rotating space charge that has been formed between cathode and plate continues to rotate around the filament as long as there is still a magnetic field. As soon as this field is turned off, all the electrons "fall" onto the plate, and the energy stored up in the rotating space charge is disseminated on the plate.

7.2 FIRST-ORDER ELECTRONIC OSCILLATIONS IN THE MAGNETRON

We now remind the reader that the term first-order electronic oscillations means oscillations with a period determined, in first approximation, by that of the electron "swing". By virtue of their axial symmetry, first-order electronic oscillations may be defined as "oscillations of radial type". Calculation of the rotation time of an electron, without allowing for the space charge, led [6], as is commonly known, (cf. Chapter 3) to the formula

$$\lambda_{(cm)}{}^{H}{}_{(ergs)} = 10,650 \qquad (7.26)$$

The examination in the same place (Chapter 3) of the radial processes in the magnetron, by analogy to the retarding-field system, leads, assuming $r_o \ll r$, to the relation

$$\lambda_{(cm)}{}^{H}{}_{(ergs)} = 13,400 \qquad (7.27)$$

On the basis of a full space charge, Braude obtained for the transit time

$$t = \frac{0.9\pi}{\omega_L} = \frac{1.8\pi}{\frac{e}{m}H}$$

which gives

$$\lambda_{(cm)}H_{(ergs)} = 19,200 \qquad (7.28)$$

for the wavelength of the first-order oscillations.

A somewhat more general expression which covers various distributions of potential and space charge is given there by this author:

$$\lambda H = \frac{10,650}{1 - \frac{p}{2}} \qquad (7.29)$$

where p characterizes the law of potential distribution in the magnetron (cf. formula 7.20). The foregoing expression $\lambda H = 19,200$ is obtained if series (7.12) and (7.13) are taken with ten members.

A still more general expression for the value of λH is obtained by introducing the factor k, which accounts for the influence of the field at the cathode:

$$k = \frac{E_o r_o}{E_a r_a} = \sqrt{\frac{r_o}{\beta r_o + \alpha t}} \qquad (7.30)$$

Obviously for $E_o = 0$ we have $k = 0$ (the case of full space charge) and for $\alpha = 0$ we have $k = 1$ (the case of absence of space charge). It follows from expression (7.30) that the transit time

depends on the factor k which must consequently also enter the expression for the wavelength of the traveling oscillations

$$\lambda H = 10,650 \ \frac{1 - k}{1 - \frac{p}{2}} \cdot \qquad (7.31)$$

For k = 0 this formula becomes formula (7.29), but is inapplicable to the case k = 1, since it gives λ H = 0 instead of λ H = 10,650. The point is that the distribution of potential adopted is true only for k $\ll$ 1, i.e. for regimes close to full space charge, which are practically the most important. In spite of its relatively narrow range of applicability, formula (7.31) permits us to allow through the parameter k for the influence of the emission current and plate voltage on the wavelength. Thus, with $E_o \neq 0$, an increase in emission current leads to a reduction of E_o and the parameter k, and consequently leads also to an increase in wavelength, as has been experimentally confirmed.

On the question of the origin of electronic oscillations in the magnetron Brillouin develops the following ideas. Radial cylindro-symmetric oscillations are determined by the natural frequencies of the rotating space charge. He considers these oscillations as the fundamental type, and calles them, in his terminology, zero-order oscillations n = 0 (in the usually adopted terms they would be first-order electronic oscillations). Any cylindrical layer between r and r + dr must have the natural frequency of oscillation ω (r) of zero (first) order

$$\omega^2(r) = 2\,\omega^2_L(1 + r_o^4/\,r^4). \qquad (7.32)$$

Whence the natural frequency of the layers contiguous to the filament is

$$\omega(r_o) = 2\omega_L, \qquad (7.32')$$

while for layers distant from the filament ($r \quad r_o$) it is

$$\omega = \omega_L\sqrt{2}. \qquad (7.32'')$$

It is evident that the oscillations of the space charge as a whole constitute a fairly complicated process that includes coupling phenomena between the successive layers by virtue of the necessary conditions of continuity. The principal part of course is played by the layers distant from the cathode. For this reason the natural frequency of the space-charge oscillations may be considered equal to $\omega_L\sqrt{2}$ for a magnetron with a sufficiently fine filament. This is likewise confirmed experimentally. Blewett and Ramo [7] studied a magnetron of the type shown in Figure 7.6, in which the outer conductor of the concentric line serves as plate and the inner conductor as cathode. They found that for the case of oscillations with cylindrical symmetry, the space charge behaves like a medium with the dielectric permeability

$$\varepsilon = \varepsilon_0 \left[1 - 2 \left(\frac{\omega_L^2}{\omega^2} \right) \right], \qquad (7.33)$$

i.e. $\omega = \omega_L\sqrt{2}$ is the natural wavelength of this medium.

This formula may be obtained theoretically under the assumption that $r_o \ll r$.

Under critical conditions, when plate current is zero and the magnetron is not using DC power, it represents a certain pure

reactance

$$Z = -\frac{i}{\omega C} = -\frac{i}{\varepsilon\omega} 2 \log \frac{r_a}{r_0} = \frac{i}{\varepsilon_0} \cdot \frac{2\omega}{2\omega_L^2 - \omega^2} \log \frac{r_a}{r_0} \qquad (7.34)$$

The situation becomes different when the magnetron is operating close to the critical conditions with the small plate current I_a and is using a certain DC power $I_a U_a$ from the plate battery, which replaces the energy being given up to the rotating charge to sustain the oscillation in the external circuit. In this

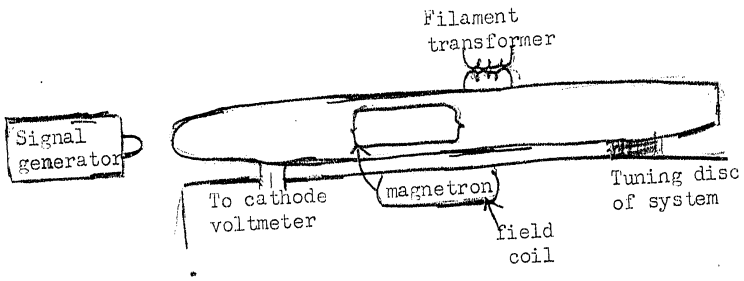

Figure 7.6

case the internal impedance of the magnetron has a real part R, which may be expressed as follows for the case most important in practice

$$R \approx \frac{\omega}{2\omega_L^2 - \omega^2} \frac{\cos\xi_0 (r_a/r_0)^2 - (r_0/r_a)^2}{2\xi_0 \left[1 + \frac{1}{\beta}\right]\left[r_a^2/r_0^2 - \sqrt{\beta}\right]} \qquad (7.35)$$

Here $\varepsilon_0 = \dfrac{\omega r_0^2}{2\omega_L^2 L_H^2}$ (L_H from formula 7.22), $\beta = \dfrac{-2\omega_L^2}{2\omega_L^2 - \omega^2 + is\omega}$

while s is a quantity characterizing the attenuation. The value of R becomes negative for $\cos\gamma_0\left|\left(\frac{r_a}{r_0}\right)^2 - \left(\frac{r_0}{r_a}\right)^2\right| < 0$ and its absolute value may reach high levels when the denominator of expression (7.35) is very small, i.e. when

$$\varepsilon_0 \frac{\omega^2}{\omega_L^2}(\omega^2 - 2\omega_L^2)^{1/2}\left[\sqrt{2}\omega_L - \left(\frac{r_a^2}{r_0^2}\right)(\omega^2 - 2\omega_L^2)^{\frac{1}{2}}\right] \to 0 \qquad (7.36)$$

(neglecting the attenuation term isω). The latter condition leads to $\omega = \omega_L\sqrt{2}$ or $\omega = \omega_L\left(2 + 2\frac{r_0^4}{r_a^4}\right)^{\frac{1}{2}}$, i.e. for $r_0 \ll r_a$, to the same result.

The variation in the value of R as a function of ω is plotted in Figure 7.7. It will be noted that the single-anode magnetron has a number of relatively narrow belts of negative resistance for frequencies in the immediate neighborhood of $\omega_L\sqrt{2}$. It should also be noted that the actual resistance R does not become infinite for $\omega = \omega_L\sqrt{2}$, if a more precise and unwieldy expression, which we shall not give here, is used instead of formula (7.35).

The physical meaning of the large number of regions of negative resistance is that the transit time in the magnetron may reach values very different from the oscillation period T. In fact, the maxima of negative active resistance occur:

for frequencies $\omega < \omega_L\sqrt{2}$, at $\omega t = (2n + 1)\pi + \frac{1}{2}\pi$

and for frequencies $\omega > \omega_L\sqrt{2}$, at $\omega t = 2n + \frac{1}{2}\pi$.

For the most sharply expressed frequency $\left[y = \frac{\omega}{\omega_L} \cong \sqrt{2}\right]$

$$y = \frac{\omega}{\omega_L} = \frac{2\pi c}{\lambda \omega_L} = \frac{21,310}{\lambda(\text{cm})\, H \text{ ergs}} = \sqrt{2}$$

or

$$\lambda H = \frac{21,310}{\sqrt{2}} \approx 15,000 \qquad (7.37)$$

may be obtained from the frequency relation:

$$y = \frac{\omega}{\omega_L} = \sqrt{2}$$

which agrees more or less well with the experimentally observed values of λH for the single-anode magnetron.

The behavior of the rotating space-charge cloud is determined with the first-order oscillations by the radial oscillations of this cloud as a whole. Each of the cylindrical layers composing it is simultaneously expanding and contracting throughout. This type of motion -- pulsation of the electronic cloud -- corresponds to the frequency $\omega_L \sqrt{2}$, which has nothing in common with the frequency of rotation.

These are the ideas that exist at the present time on the nature of the radial oscillations in the magnetron or of the first-order electronic oscillations. There is no essential contradiction between these two viewpoints. It is important to emphasize that these oscillations are due to the existence of some mechanism of axial symmetry. In this respect the case here may be reduced to the equivalent circuit of the retarding field not only formally but also when we allow for the most important physical peculiarities of the phenomenon. We have already set forth, in Chapter III, the fundamental idea of such an equivalent retarding-field circuit:

having the expression for v_r, the radial velocity of the electron, we may then introduce the "equivalent potential" U_{re} corresponding to this velocity:

$$v_r = \sqrt{2 \frac{e}{m} U_{re}} \qquad (7.38)$$

To conclude this section we shall now demonstrate the applicability of this equivalent substitution, as a first approximation, to two questions: (a) determination of the boundaries of the region of first-order oscillations, and (b) calculation of the efficiency.

Let us imagine the equivalent circuit to be excited within the regions of variation of the "undisturbed" transit angle θ_o which are plotted in Figure 6.32. Then by means of the expression

$$\theta_o = \frac{4\omega}{nv_o} = \frac{4\omega}{\sqrt{2 \frac{e}{m} v_o}} \cdot \frac{U_o d}{U_o - U_B} \qquad (7.39)$$

and the relations that characterize the transition from the parameters of the magnetron to those of the equivalent circuit (cf. Chapter III, Paragraph 2, equations (3.39) to (3.45), we may obtain the following expression:

$$\theta_o = \frac{8 \pi c r_a \left(1 - \frac{1}{k\sqrt{2}\, z}\right) C'}{(C' + k^2 - 1) \sqrt{2 \frac{e}{m} C' U_a}} \qquad (7.40)$$

We recall that here $k = H/H_k$, $z = \ln \frac{r_a}{r_o}$, $C' = C - \frac{\ln k}{z}$.

On introducing the value of H_k into expression (7.40) and slightly transforming it, we get

$$= \frac{84.4 \cdot 10^3 \left(1 - \frac{1}{k\sqrt{2}\, z}\right) C'}{\theta_o H_k (C' + k^2 - 1)}$$

and

$$H = C_o = \frac{84.4 \cdot 10^3 \left(1 - \frac{1}{k\sqrt{2z}}\right)\sqrt{C'}}{\theta_o (C' + k^2 - 1)} \qquad (7.41)$$

The expression for constant λ_H indicates its dependence not only on tube geometry but also on the transit angle θ_o.

Moreover, if the regime is changed by the aid of one of the parameters, for instance, H, it may be observed that oscillations arise in a certain interval of variation H around its critical value. Let us determine this interval, starting with the variation of the value of the region of oscillation. We take the first region in Figure 6.32. In it, θ_o varies from $\theta_o' = 6.28$ to $\theta_o'' = 9.0$, with the maximum at $\theta_o = 7.56$. Let us simplify formula (7.40) by assuming that $r_o \ll r_a$, which leads us to

$$\theta_o' \quad \frac{27.8005}{\lambda k^2 H_k} < \theta_o''$$

Let us take the value for H_k which is obtained by formula (7.41) for $r_o \ll r_a$ and $\theta_o = 7.56$, and which proves to be equal to H = 11,300.

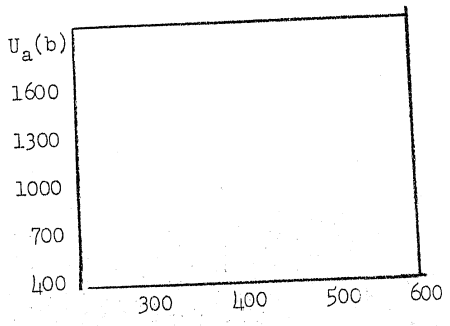

Figure 7.8

Then

$$\theta_o' \leqslant \frac{7.74}{k^2} \leqslant \theta_o''.$$

Thence, knowing the values of θ_o' and θ_o'', we find the boundary value of k

$$k' \cong 1.10 \quad \text{and} \quad k'' \cong 0.92 \qquad (7.43)$$

i.e. first-order oscillations originate in the region within which the intensity of the magnetic field varies from 0.92 H_k to 1.10 H_k. The experimentally observed oscillation region extends insignificantly, in fact, on both sides of the critical value H_k. Figure 7.8 shows the experimentally observed region (shaded), together with its boundaries (the broken lines) as computed theoretically by formula (7.43) [8].

The second question concerns the calculation of the power and efficiency of a magnetron under the regime of radial oscillations. In the laboratory of the author, I.I. Vasserman, using the idea of the equivalent retarding-field circuit, has calculated the power integral in a manner similar to that demonstrated in Paragraph 3, Chapter IV. Without adducing the calculations themselves, which are fairly involved, we shall merely indicate their results. The power developed under the regime of first-order oscillations proves to be equal to

$$P = \frac{3}{2} I_a U_a \frac{2}{(2\sqrt{n} + 1)} \left(1 - \frac{\ln k}{z} - \frac{\ln \sqrt{2z}}{z} - \frac{1}{2z}\right) \qquad (7.44)$$

which reduces for the first excitation region (n = 1), assuming that $r_o \ll r_a$ reduces to

$$P \approx 0.12\, I_a U_a, \text{ consequently, } \eta \approx 0.12. \qquad (7.45)$$

The value obtained here for the efficiency is satisfactory in agreement with the experimental data, according to which first order oscillations are characterized by efficiencies ranging from 5% to 10%. The curious fact may be noted that by virtue of the relation (7.44) the maximum oscillatory power for the given tube geometry and the given U_a should be obtained at the minimum value assumed for H, namely at k = 0.92. This inference agrees well with the ideas of Brillouin on the energetic balance of radial oscillations which have been set forth above.

We observe in conclusion that first-order electronic oscillations, (radial oscillations), while they are the typical and only mode of oscillation by a magnetron with solid cylindrical anode, may also be obtained in a multisegment magnetron with any number of segments, if under regimes near the critical, any "radial-nonstationary" processes should arise that might lead to the excitation and maintenance of oscillation in the tuned circuit connected to it.

7.3 MAGNETRONS WITH MULTISEGMENT ANODES OF ELECTROSTATIC REGIME

The most widespread magnetron design at the present time is the magnetron with a "split anode" or multisegment magnetron. An even number of segments is generally used, and their number is characterized by p, the number of pairs of slots. In practice, p = 1 and p = 2, i.e. the two-segment and four-segment magnetrons, are most often met. In recent years, the employment of multisegment magnetrons characterized by p = 4 - 10 has been gaining more and more ground in the field of centimeter waves.

The oscillatory circuit is connected to the multisegment magnetron either by dividing the segments into two groups, across which the circuit is connected (cf. Figure 7.49, infra), or connecting a circuit in the form of a small cavity or cell across each pair of adjacent segments (the multicell magnetrons, cf. Figure 7.51). The main distinction between the multisegment and the solid-anode magnetrons is in the character of the electrostatic field between the electrodes and the peculiarities of electron motion thereby conditioned. The fact of the matter is that upon the ordinary radial electrostatic field of the diode is superposed another field produced by the potential difference between the segments of the anode. If we imagine (Figure 7.9) the magnetron anode (p = 1) to be split in the direction of the x-axis and set the voltage $U_1 = U_o + \Delta U$ for the supper segment and the voltage $U = U_o - \Delta U$ for the lower, then the distribution of potential in the field between the segments will be described by the equation

$$U_{12} = \frac{2\Delta U}{\pi} \arctan \frac{2vr_a}{x^2 + y^2 - r_a^2} - 3\Delta U. \qquad (7.46)$$

The equipotential lines of this "transverse" field are the circles described by the equation

$$x^2 + (y - C)^2 = r_a^2 + C^2 \qquad (7.47)$$

where C is the parameter of the family of these circles equal to

$$C = \frac{r_a}{\tan\left(\frac{U_{12}}{2\Delta U}\pi\right)} \qquad (7.48)$$

At each point of the interelectrode space, besides the "transverse" electrostatic field, there also exists a radial one, which without allowing for the space charge, is of the usual log-

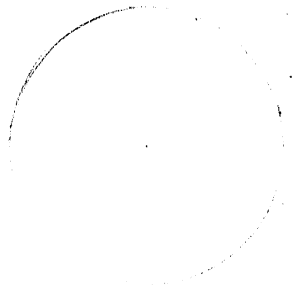

Figure 7.9

arithmic character, since the anode as a whole possesses the potential U_o with respect to the cathode. The electrostatic field that actually exists in the tube is the result of the addition of these two fields. The equipotential surfaces of the radial and transverse fields are shown in Figure 7.9. The total field attained in the split-anode magnetron has a fairly complex structure, and an idea of it may be obtained either graphically, by addition of the corresponding vectors of transverse and radial field at each point of the interelectrode space, or experimentally.

In the latter case the study of electrostatic field is conducted by means of one of the well-developed methods, which have been described in the literature in detail, involving the use of considerably enlarged models of magnetrons. The very widespread

"electrolytic bath method" [9, 10] and the "compensated sounding method" [11] are successfully employed. We shall not dwell here on the description of these very well-known methods which are widely employed in the solution of many problems of geometrical electron-optics.

We turn now to the examination of some of the results of the investigations of the electrostatic fields of multisegment magnetrons under different conditions of operation and with a varying number of segments. Let us commence with the two-segment magnetron. Figure 7.10 shows the equipotential lines of the electrostatic field in a two-segment magnetron, according to the measurements of Grozkowski and Kyiko [11] made by the "compensated sounding method". The figure represents the fields for four regimes characterized by

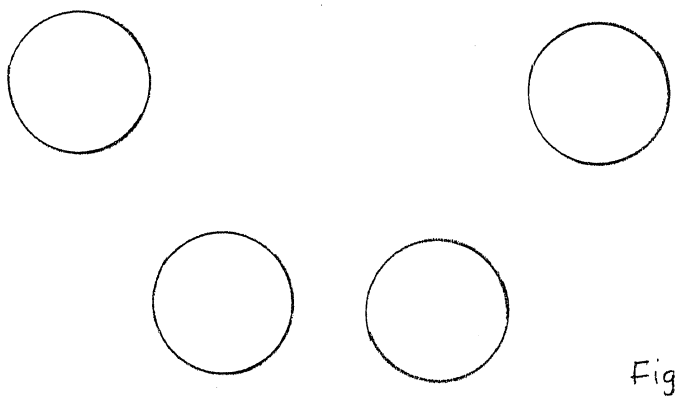

Figure 7.10

a varying degree of electrostatic asymmetry, i.e. with varying values of ΔU:

Field a	U_o = 500 volts	ΔU = 50 volts
Field b	U_o = 500 volts	ΔU = 100 volts
Field c	U_o = 500 volts	ΔU = 150 volts
Field d	U_o = 500 volts	ΔU = 200 volts

We direct attention to the following fact. One of the equipotential lines of the field, corresponding to the potential U_2 of the less positive segment, approaches the latter, according to this figure, at an acute angle (the line "450" in Figure 7.10a and the line "400" in Figure 7.10b), or even at an angle of almost zero (the line "350" in Figure 7.10c or the line "300" in Figure 7.10d). Lukoshkov and Il'inskiy, however, [12], noted that, in all cases where the potential of a field depends only on two coordinates, two equipotential lines of the same potential should intersect at a right angle. In the light of this remark, the course of the equipotential lines in the region of the less positive segment, as shown in Figure 7.10, appears doubtful, though some authors have used analogous field charts to study electron paths. This error was apparently the result of a not particularly careful study of

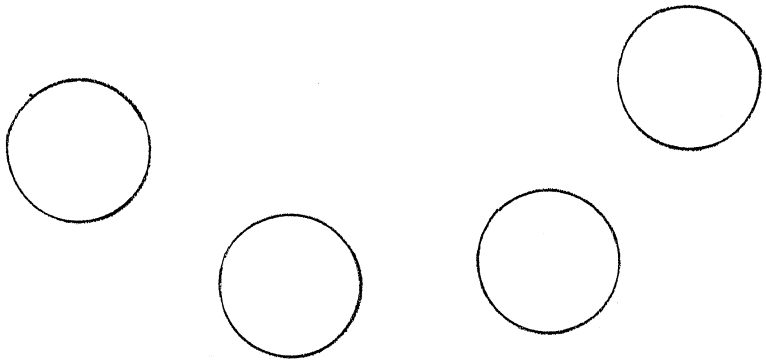

Figure 7.11

that region of the field in the neighborhood of the lowest-potential segment. The mutually perpendicular intersection of lines at the same potential may serve as a criterion of the degree of suitability of the field chart for further use, for instance in plotting the electron paths.

We present Figure 7.11 as an example of a field chart that is free from this error. This chart is taken from a work of Katsman and Rubina [13], and is clear without special commentaries. Attention should be paid to the behavior of the equipotential lines of the less positive segment, and they should be compared with the corresponding lines in Figure 7.10.

With increasing number of segments, the character of the electrostatic field in the magnetron naturally changes, since the geometrical relation of the zones of the transverse and radial fields also changes. A few examples of the fields in four-segment magnetrons are given in Figures 7.12, 7.13 and 7.14. Figure 7.12 is borrowed from the book of Gross [14], Figure 7.13 from the

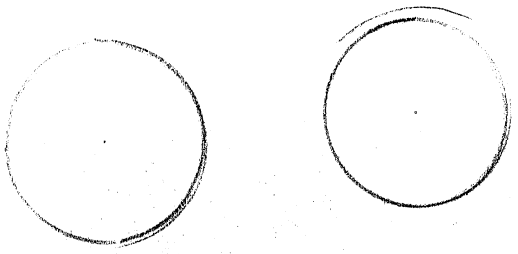

Figure 7.12

work of Groszkowski and Ryiko [11] and is also characterized by the incorrect course, already noted above, of the equipotential line corresponding to the potential of the less positive pair of segments. Finally, Figure 7.14 represents the results of measurements made on models of a four-segment magnetron by L. I. Vasserman [8, 28] in our laboratory.

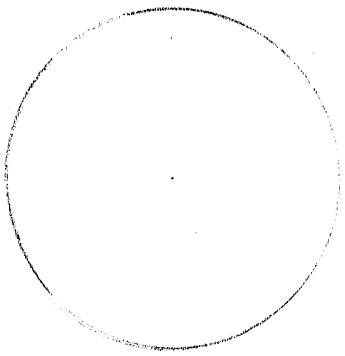

Figure 7.13

The character of the electrostatic field as the number of segments is further increased may be seen from the series of drawings represented in Figures 7.15 to 7.17, taken from the same works, and covering magnetrons with eight, twelve and sixteen segments respectively, at the same values for the degree of asymmetry $\alpha = \Delta U/U_0$, which characterizes the value of the intersegmental potential differences.

From this survey of the electrostatic fields of multisegment magnetrons it will be seen that the logarithmic distribution of potential, which is characteristic of the diode, experiences the maximum amount of distortion in the two-segment magnetron, since there is

a transverse field throughout the whole of the interelectrode space. Only around the cathode itself may equipotential lines of true circular shape be seen. As the number of segments increases, the zone of the undisturbed radial field near the cathode becomes more and

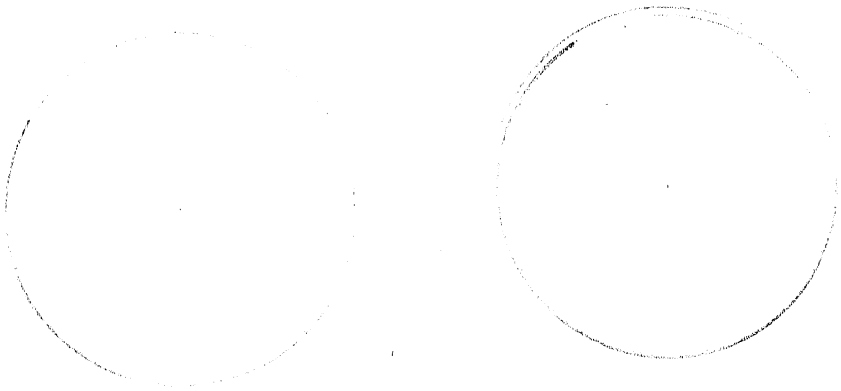

Figure 7.14

more noticeable, and the space in which the "transverse" intersegmental field operates is diminished, reducing to an external ring directly adjoining the anode. The depth of this external zone depends on the degree of asymmetry and the potential difference between the segments.

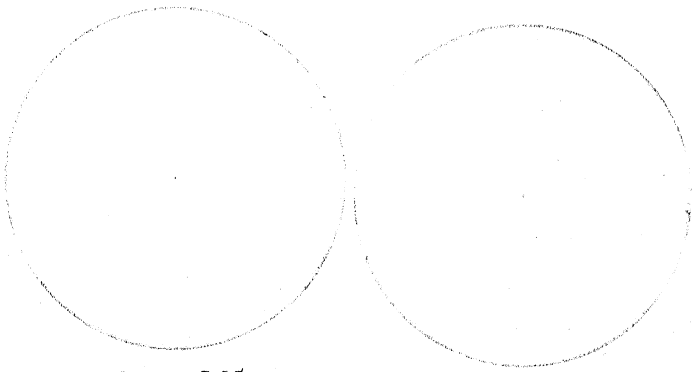

Figure 7.15

Thus for a considerable number of segments the distribution of the electrostatic field approaches that in the solid-anode magnetron, especially at small intersegmental potential differences. This circumstance is very essential in the investigation of the

Figure 7.16

peculiarities in the behavior of multisegment magnetrons under oscillatory regimes.

These peculiarities of field distribution in the slotted magnetron result in a considerably more complex electron motion than

Figure 7.17

obtains in the solid-anode magnetron. The critical conditions, and the course of the I_a - H characteristic corresponding thereto, which have already been considered, supra, acquire to some extent a conventional meaning, since in the presence of a certain intersegmental potential difference $2\Delta U$, there may be a situation in which $H < H_k$ for one group of segments (the more positive ones) at the same time that, for the other group, $H > H_k$. For this reason the convention must be adopted that the concept of critical intensity of the magnetic field relates to a certain fictitious solid-anode magnetron of the same radius and having a plate voltage equal to the mean of the actual segment voltages: $U_o = \frac{U_1 + U_2}{2}$. Experience has shown that when $U_1 \neq U_2$ and at corresponding values for magnetic field

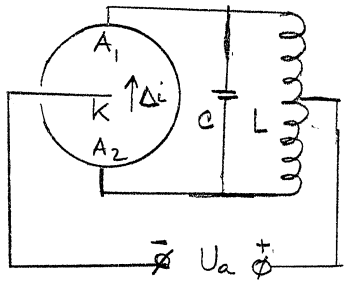

Figure 7.18

intensity, areas with a negative slope are observed in the static characteristic curve depending on the intersegmental voltage difference $U_2 - U_1 = 2\Delta U$. This phenomenon evidences the production of a negative resistance in the corresponding intervals of the regime, which resistance may be used to excite the circuit. If the magnetron has an even number of segments, interconnected in two

groups, to which the oscillatory circuit is connected, as is most often the case, then in the circuit diagram (Figure 7.18) we have to do with: (a) the currents i_{a1} and i_{a2} on the individual segments or segment-groups, (b) the total current $i_{a1} + i_{a2}$, which flows through the source of DC plate voltage, and (c) the current differences $\Delta i = i_{a1} - i_{a2}$. Sectors with negative mutual transconductance appear in the characteristics of the individual plate-currents i_{a1}, $i_{a2} = f(\Delta U)$ and in the difference-characteristic $\Delta i = f(\Delta U)$. For the ordinary circuit connections shown in Figure 7.18, the difference-characteristic plays the principal part. If the circuit, however, is connected between cathode and one of the segments, then the falling sector in the current flowing on the given segment may be the interesting one. Such a one-sided connection of the oscillatory circuit, however, is hardly ever used, and the behavior of the slotted magnetron is ordinarily represented by the difference characteristic $\Delta i = f(\Delta U)$. The typical course of this characteristic, with a well-defined sector of negative resistance, is shown in Figure 7.19, in which likewise the characteristic of total current $i_{a1} + i_{a2}$ has been plotted, and a skeleton diagram for taking these characteristics has also been included. Characteristics of this shape are very typical for two- and four-segment magnetrons, in which the sector of negative slope very distinctly appears, and as a rule is displaced with increasing H towards the region of high ΔU. It is of interest to note that with increasing number of segments, the falling sector of the difference-characteristic becomes less sharply expressed, and at $p \geqslant 6$ (a twelve-segment magnetron) disappears altogether. This property of multisegment magnetrons is illus-

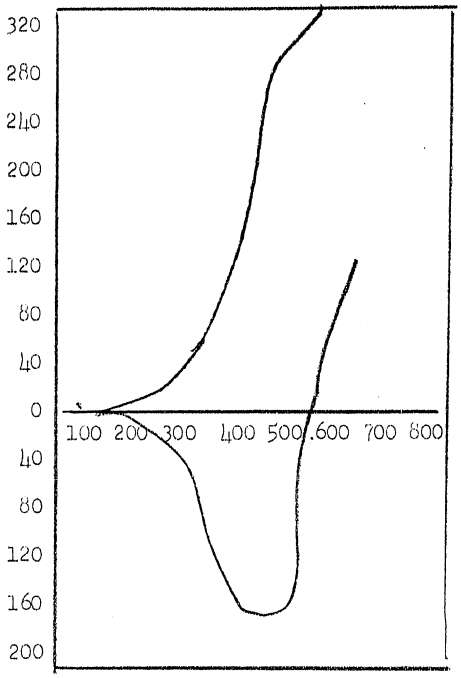

Figure 7.19

trated by the series of figures from 7.20 to 7.23, relating respectively to 8-, 12-, 16- and 20-segment magnetrons [8]. Together with the diminution and disappearance of the falling sector of the difference characteristic, a reduction in its slope is also observed with increasing intensity of the applied magnetic field.

The part played by the current difference in slotted magnetrons may be likened to that of the plate current in the ordinary oscillator tube: and in fact, a comparison of the slotted magnetron with the triode oscillator reveals the following:

(a) the phase relation between i_a and U_a required to sustain oscillation in the circuit of the triode oscillator (Figure 7.24 a

and b) is produced by the feedback mechanism that is responsible for the dynamic falling characteristic $i_a = f(U_a)$ (Figure 7.24c).

$p = 4$, $U_{ao} = 500$ volts, $d_a = 10$ mm

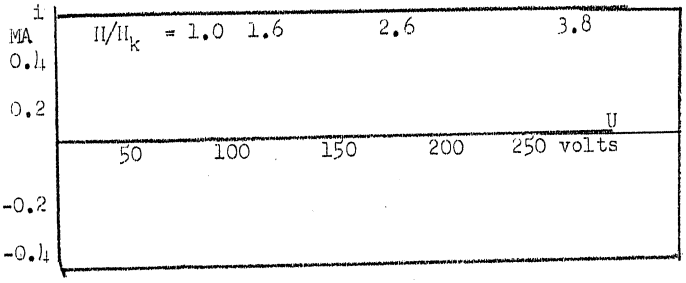

Figure 7.20

Thanks to this the triode may be treated as a certain negative resistance connected in parallel with the oscillatory circuit;

(b) passing now to the magnetron (Figure 7.25a), which has no special feedback mechanism, we note that the role of i_a and U_a in the triode oscillator is here played instead by the corresponding quantities Δi and $2\Delta U$, the connection between which results in a falling characteristic even under static conditions (Figure 7.25b). By virtue of this, the magnetron, in the circuit under consideration, may also be represented as a negative resistance connected in parallel with the oscillatory circuit.

p = 6, U_{ao} = 500 volts, d_a = 10 mm

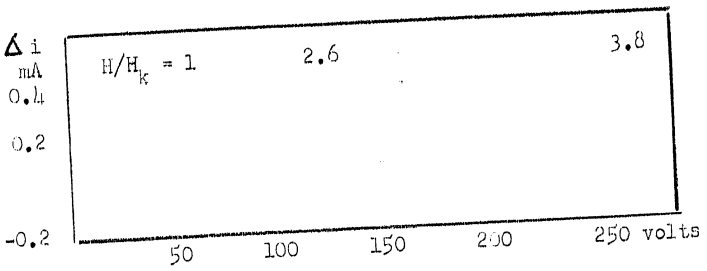

Figure 7.21

What, now, is the physical nature of the static negative resistance is found in slotted magnetrons?

p = 8, U_{ao} = 500 volts, d_a = 10 mm

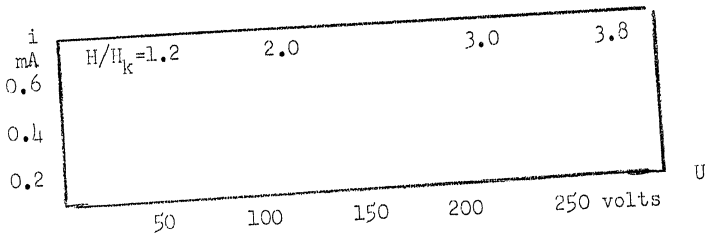

Figure 7.22

Since it originates as a result of a large number of electrons impinging on the less positive segment, it is natural that we should seek its cause in the peculiarities of electron motion in the slotted magnetron, and there have been a considerable number of both theoretical and experimental studies devoted to this question [4, 5, 12, 13, 15-17].

Let us consider, for instance, the electron path depicted in Figure 7.9. It may be noted that the electron, leaving the cathode

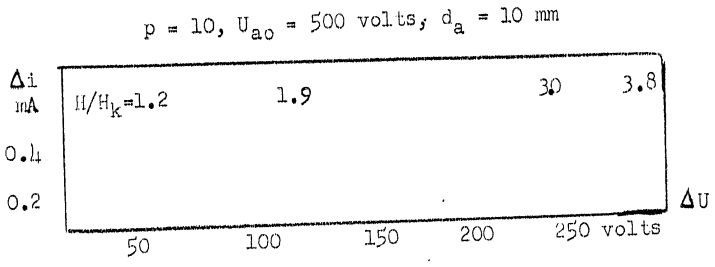

Figure 7.23

at point C, and traveling towards the side of the "more positive" segment, impinges under the influence of the electrostatic and magnetic fields in the tube, on the "less positive" segment of the anode (the dimensions and voltage, together with the value of the magnetic field intensity, are entered on the diagram). In passing from the field of the more positive anode segment into the region of the field of the less positive segment, the electron undergoes

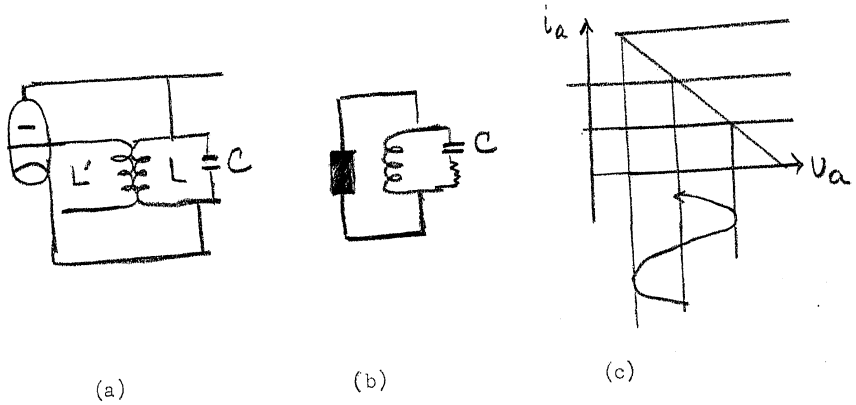

(a) (b) (c)

Figure 7.24

a certain retardation in the transverse field, which is most sharply expressed on the plane of the slots and especially in the vicinity of the slots. On account of this retardation and the

attendant loss of kinetic energy of tangential movement, the electron path bends outward more or less sharply and approaches the positive segment still more closely, ultimately impinging on it.

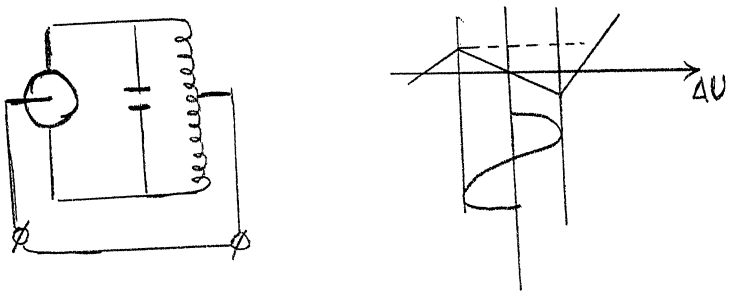

Figure 7.25

Study of electron motion in slotted magnetrons by the aid of graphic analytic methods [12, 13] is able to show that the electron paths are of fairly complicated form and possess a considerable number of loops, especially at high magnetic field intensities where $H > H_k$. If we plot the paths of electrons leaving the cathode at various angles to the plane of the slots, we find that most of the electrons in the regimes corresponding to the formation of negative resistance, describe a number of loops and then enter the zone of the less positive segment. (Figure 7.26). Loop formation is here observed to be even more frequently repeated and leads to a longer time being spent by the electrons in this zone and to the formation, as some authors put it [15] of a kind of "electronic sack". In the region of this "sack" the electrostatic field is weakened, and the electrons impinging on it will rotate almost on the same spot and slowly travel towards the less positive segment. Owing to the presence of forces of mutual repulsion, a certain equilibrium of motion

is established, under which some electrons leave the "sack" and are replaced by new ones entering it. The electrons expelled from the "sack" will mostly impinge on the nearer half of the anode with the lower potential. In cases where the electron path describes a relatively small number of loops, it may be plotted as far as the direct impingement of the electron on one segment or another. And in this case the trace of a series of paths for the electrons leaving the filament in different directions (e.g. Katsman and Rubina [13] took 8 exit directions of the electrons for each $\pi/4$), indicates that a large number of electrons will impinge on the less positive segment. In this way the mechanism

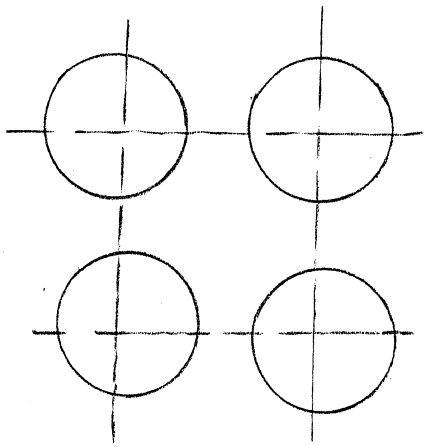

Figure 7.26

of static negative resistance may be explained as the result of the electrons' impinging primarily on the less positive segment.

Graphoanalytic study of the electron tracks undertaken without allowing for the space charge, leads to the following: at $H > H_k$, the tracks form loop-like curves, and the diameters of their loops

diminishes as H increases. The motion of the electron consists of two components: a rotary motion around the loop and a "translatory" motion along directrix of that loop, superimposed on the first component. The translatory motion is approximately along the equipotential lines. A number of characteristic examples are given in Figure 7.27 and 7.28 to illustrate these theses.

The effect of the space-charge may be accounted for, in first approximation, as follows: the electrostatic field of the slotted magnetron is represented as the aggregate of a radial field of potential proportional to the 2/3 power of the radius (Langmuir diode) and an intersegmental transverse field. The resultant field in this case should correspond better to reality. The electron tracks plotted in a field obtained in this manner under a regime corresponding to Figure 7.27 (where the space charge is not allowed for) are represented in Figure 7.29.

$\alpha = 40°$

Figure 7.27

On comparing these two diagrams we see that in the general character of the electron motion is qualitatively the smae, but that they do not impinge on the anode under this regime. Only when there is a certain reduction in magnetic field intensity do they again com-

mence to impinge on the less positive segment. Thus, other things being equal, the effect of the space charge manifests itself already in first approximation in a tendency to form a ring movement along the directrix, which probably shows up even more strongly under actual conditions.

All the data presented relate to a two-segment magnetron. The study of electron motion in magnetrons with a larger number

α = 50%

Figure 7.28

of segments is a very interesting and important problem, but unfortunately there is hardly any material about it in the literature. The application of the grapho-analytic method to the four-

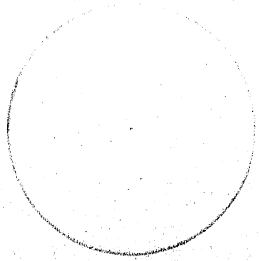

α = 40%

Figure 7.29

segment magnetron yields paths of the same character, as may be illustrated by Figure 7.30 [28].

As the number of segments is increased, the character of electron motion will be defined more and more by ring-shaped trajectories. The nature of the electrostatic field of multisegment magnetrons, as we have seen, becomes similar to that of the unslotted, solid magnetron, and at $H > H_k$, the electron path may be roughly represented in the form shown by Figure 7.31, on which the trajectory of an electron in an unslotted magnetron in the presence of a Langmuir distribution of potential, is represented. Brillouin's idea [1] of the character of electron motion in the magnetron, with which idea we have become previously acquainted, is apparently also applicable to the case of slotted magnetrons especially the multisegment ones.

Our knowledge of the distribution of electrons among the magnetron segments enables us theoretically to construct the static characteristic of that tube. This may be done by the simplest method as follows: having N trajectories plotted for each regime, we determine the number of trajectories n_1, ending with the most positive

$H = 1.1\ H_{kr}$
$U_a = 500$ volts
$\alpha = 20\%$

Figure 7.30

segment, and the number of trajectories n_2, ending with the least positive segment. Then $n_1 + n_2 = N$. We represent the quantities n_1 and n_2 as being proportional to the currents i_1 and i_2 on the corresponding segments, assuming that N corresponds to the total emission current. On the basis of the values for i_1 and i_2 obtained in this way, the static characteristic is plotted [13].

The static characteristics may also be calculated theoretically by a somewhat different method [16] from the motion and distribution of the electrons. To overcome the computational difficulties, the electrodes are "stretched out" and represented in the form of long parallel plates (Figure 7.32). The lower solid plate represents the cathode that emits the electrons, which in the given case describe a cycloidal path with maximum distance

$$a = \frac{1}{H}\sqrt{2\frac{m}{e}U}$$ and length $b = \pi a$.

Since the path of an electron in a cylindrical tube covers a 270° angle (cf. Paragraph 7.1), we must put the length of the equivalent plane of the system as equal to $l = \frac{4}{3}\pi a$. The equivalent systems replacing the two- and four-segment magnetrons, the electron paths in them, and the lines of force of the additional electrostatic field obtained as a result of the plate-segment potential differences, are represented in Figure 7.32 a and b. It is plainly noticeable here that the additional field produced by the potential difference between the segments and the corresponding "transverse" field of the ordinary cylindrical magnetron is perceptible throughout almost the entire interelectrode space in the two-segment magnetron, while in the four-segment magnetron it is only noticeable in the neighborhood of the anodes. We have already seen an analogous picture in the case of cylindrical designs (Fig-

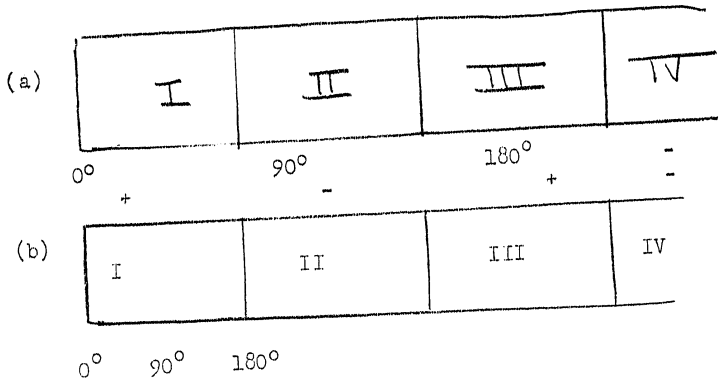

Figure 7.32

ure 7.11 - 7.17). This circumstance, confirmed by calculation, gives reason for considering that in practice the electron traverses the first part of its field (from 1/3 to 1/2, in the case of the four-segment magnetron) only under the influence of the stationary radial field.

Let us now examine the motion of the electrons in this "developed" model. Assuming that the critical magnetic field has been selected so that the electrons only touch the anodes, we obtain the trajectories plotted in Figure 7.32. The point of tangency of anode A' must obviously be 135° along the horizontal axis away from the point of departure, in the absence of a transverse field.

In the presence of a transverse field, however, the points of tangency are displaced in one direction or the other, according to the electron's point of departure. The trajectories beginning at 0° to 90° are displaced somewhat toward the right, and those beginning at 90° to 180° somewhat to the left (Figure 7.33).. The

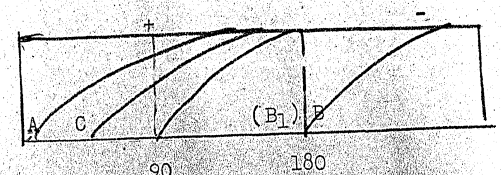

Figure 7.33

letters A, B, C, and D with the sign ' on this diagram designate the points of tangency in the absence of a transverse field, and with the sign ", in the presence of such field. Setting the dis-

$$U_x = U_o \frac{x}{a} + \Delta U \frac{x}{a} \sin \alpha y, \qquad (7.49)$$

tribution of potential according to formula (7.49), where $\alpha = \frac{3}{2a}$, with y measured along the cathode, the theoretical difference-characteristic for the two-segment magnetron may be obtained from a consideration of equations of motion of the electron. This characteristic is shown by the heavy line in Figure 7.34. In the real characteristic, the jump in the curve has a final slope transconductance (the fine line). In the four-segment magnetron a wider interval of negative resistance along the axis ΔU is obtained by this method, thanks to which a greater amplitude may be assumed for the oscillatory voltage. The motion of electrons in the four-segment magnetron and the characteristics obtained for it are represented in Figure 7.35, which may be followed without special commentary.

To illustrate the concept of the critical regime in its application to the slotted magnetron, we present in Figure 7.36 a family of current characteristic for i_1 from a pair of segments of a four-segment magnetron, taken at various values of H. Alongside of it the characteristic of the magnetron itself is given. The gradual transition from one curve to another is clearly shown in this diagram, as is the formation of the falling sectors. The widening pocket in the current curve as the magnetic field intensity increases is worthwhile noticing and is particularly plain at H = 800 oersteds. The nature of the pocket is clear: for

$H > H_k$, a high enough ΔU is necessary if the electrons are to be forced all the way to the anode. Corresponding to these regimes, falling sectors of the diversity characteristic are likewise obtained only at considerable values of ΔU.

Thus, the question of the origin of the static negative resistance in a magnetron may be solved with more or less accuracy by a purely theoretical method, and such resistance may even be quantitatively estimated to a certain extent. The direct experimental investigation of electron motion in a split magnetron is of no less interest. For this purpose specially designed magnetron models are usually employed. Such models have cathodes emitting a narrow electron beam in a definite direction. The trajectory of the electron beam may be demonstrated by filling the model with some inert gas, for instance argon, under pressure of a few microns. Owing to the ionization of the gas the entire path of the electron stream then becomes visible. The trajectories that Kilgor [4] observed by this method proved qualitatively identical with those considered above (Figure 7.26-7.31). A very substantial objection, however, may be raised against the adequacy of this method of observing electron paths: the model is filled with gas at a fairly high pressure; and the presence of the gas and of positive ions substantially modifies the conditions of electron motion, and so nothing more than a very remote qualitative agreement with the trajectories obtained without allowing for the space charge can be expected from this method.

The influence of the gas may be eliminated by investigating electron motion in a magnetron model at high vacuum. The work of

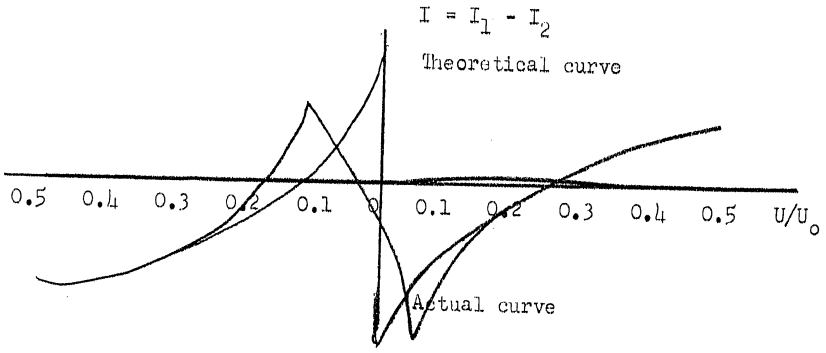

Figure 7.34

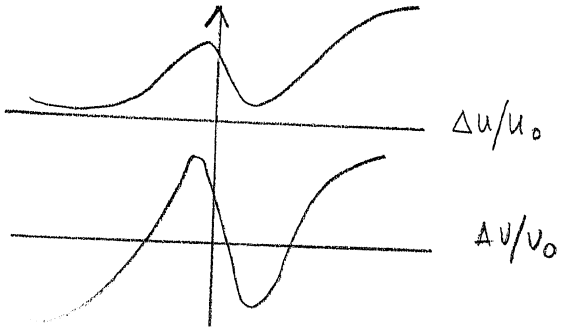

Figure 7.35

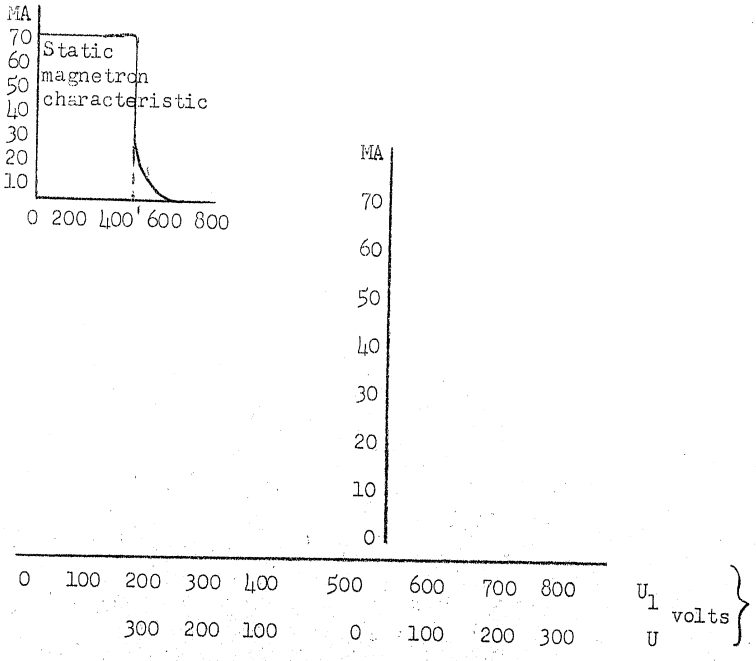

Figure 7.36

Grechowa [5] is an example of this method. The cathode of her model emitted a narrow beam of electrons. The inside surface of the anode was coated with a thin layer of fluorescent substance, thanks to which the electron beam emitted from the cathode formed a visible bright spot about 1 mm in diameter on the anode surface. In this way the initial point, initial direction and end point of the trajectory could be determined.. The course of the trajectory was approximately determined by these data. She used a more complicated model (Figure 7.37) to observe the intermediate points of the trajectory, which are of particular interest for $H > H_k$, when the electron may describe a number of loops. She kept the glass framework [ramochki] a_1, a_2, a_3 carrying thin glass threads coated with a fluorescent substance, between cathode and anode. By rotating the system of frames with the threads, by using a special slide, the behavior of the electron trajectory in the interelectrode space could be observed. For a certain "development" of the trajectory to assure its more convenient observation, the magnetic field could be applied at various angles and axes of the model. The trajectory then took the form of a helix, drawn out along the line of the cathode. The detailed study of these models also extended to the form of the trajectories, which were in good agreement with those discussed above (Figures 7.26 to 7.31). It developed in the course of this work that the trajectories of simplest form correspond to the four-segment magnetron, by virtue of which the incidence of the electrons on the less positive segment is facilitated and the interval of negative resistance lengthened. The eccentric location of the cathode between the segments of the anode also leads to the same results.

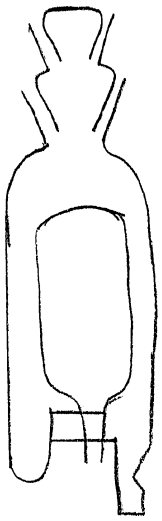

Figure 7.37

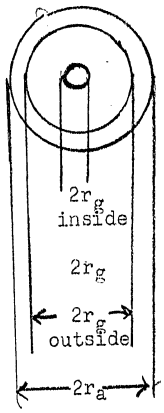

Figure 7.38

In concluding the present section, we shall dwell on the role of the secondary emission in the behavior of slotted magnetrons. Groszkowski [18] has constructed an electron tube with a solid cylindrical anode and a "grid" consisting of rectangular plates located along the tube at a certain angle to the radius (Figure 7.38). This tube, connected in the circuit of Figure 7.39, is placed in an axial magnetic field. Thanks to the original design of the grid, the current characteristics i_a and i_g, depending on i_m, assume a non-symmetrical character (Figure 7.40). When the direction of the magnetic field is changed, the electrons either pass between the elements of the grid or impinge on them, as is shown in the lower part of Figure 7.40. Electrons that impinge on the grid at small

angles provoke a secondary emission from it. The external magnetic field is so chosen as to establish certain critical relations between plate voltage and secondary grid current, with the electrons colliding almost tangentially with the grid plates (Figure 7.41) and producing a considerable secondary current. With increasing plate voltage the number of electrons passing through the grid without grazing it also increases, but the secondary emission current falls, which involves a general reduction in plate current. It is clear that this will occur only on condition that the secondary emission from the grid exceeds the current from the electrons impinging on it. By making the electrodes of the tube out of meckel, Groszkowski succeeded in obtaining a falling characteristic with a negative resistance of the order of 5000 ohms.

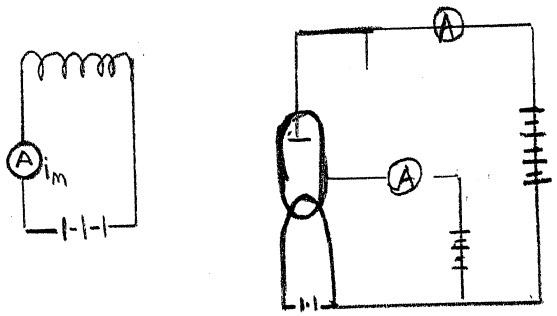

Figure 7.39

The Groszkowski triode just described represents a peculiar form of dynatron, in which, thanks to the application of a magnetic field, a falling sector of the plate characteristic is obtained. However the phenomenon of a secondary emission is also found in the operation of ordinary slotted magnetrons and determines a good many peculiarities of their behavior, which are by no means without interest.

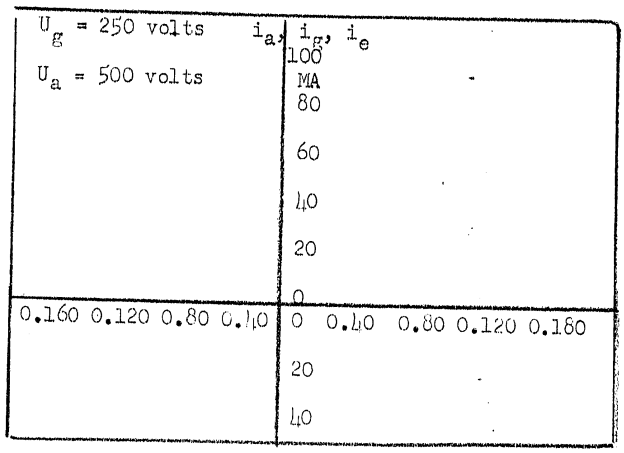

Figure 7.40

The researches performed in our laboratory by G. M. Gershteyn [19, 20] led to the discovery of a secondary emission effect in ordinary slotted magnetrons, especially in the multisegment types. It was noted that at certain values of the magnetic field and intersegment potential difference, the number of secondary electrons leaving the surface of the less positive segments exceeds the number of primary electrons, in consequence of which the plate current i_{a2} reverses its direction.

The relations obtained between the plate current and the value of the magnetic field are presented in Figure 7.42, a and b. The situation would appear to be much as follows: the electron stream, when it bombards the surface of the less positive segments, causes them to emit secondary electrons, which, if the potential difference between adjoining segments is great enough, impinge on the more positive segments. In the absence of a magnetic field the discharge of secondary electrons due to the normal incidence of primary electrons on the anode surfaces is extremely slight. With the appear-

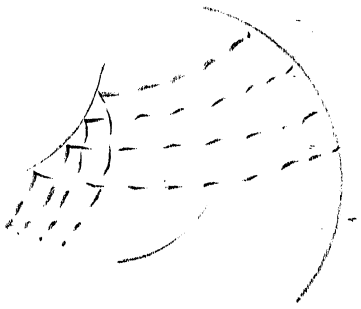

Figure 7.41

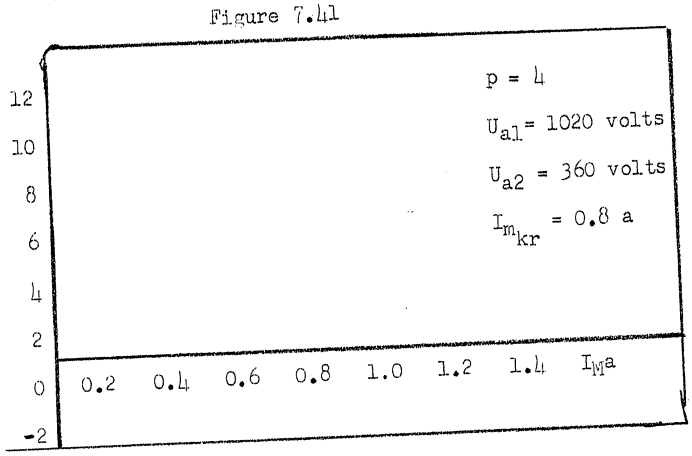

(a)

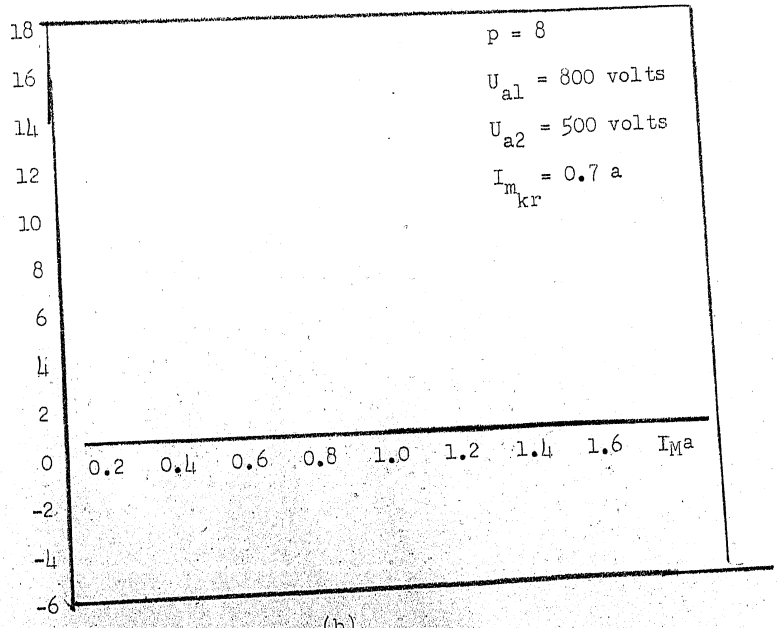

(b)

Figure 7.42

ance of the magnetic field, however, the angle of incidence increases, thus encouraging the growth of the coefficient of secondary emission. The most favorable conditions are created in the neighborhood of the critical regime, which produces a maximum of current in the opposite direction at magnetic field intensities close to the critical ones. The phenomenon of secondary emission was correlated with the above-mentioned variation in the course of the static characteristics of multisegment magnetrons with increasing number of segments. The appearance of secondary current proved to diminish the falling sector of the static characteristic. If it is taken into consideration that an "active" secondary effect can be obtained only from a certain part of the less positive segment which is subject to the direct action of the adjoining segment and is characterized by the coefficient ζ (its role is clear from Figure 7.43), while ζ increases with the increasing number of segments, it follows necessarily that the influence of the secondary effect must be greater in multisegment magnetrons. This circumstance may be explained, to a certain extent, by the above-described reduction in the falling sector in multisegment magnetrons. The attempts at quantitative computation made by G. M. Gershteyn for two- and four-segment magnetrons apparently justify this point of view.

7.4 ELECTRONIC OSCILLATIONS OF "HIGHER ORDERS" (TANGENTIAL OSCILLATORY PROCESSES) IN THE MAGNETRON

We have already made the acquaintance of the classification of magnetron oscillation types connected with flight conditions (Chapter III, Paragraph 2, and Chapter VII, Paragraph 2). It distinguishes radial oscillatory processes, or first-order oscillations,

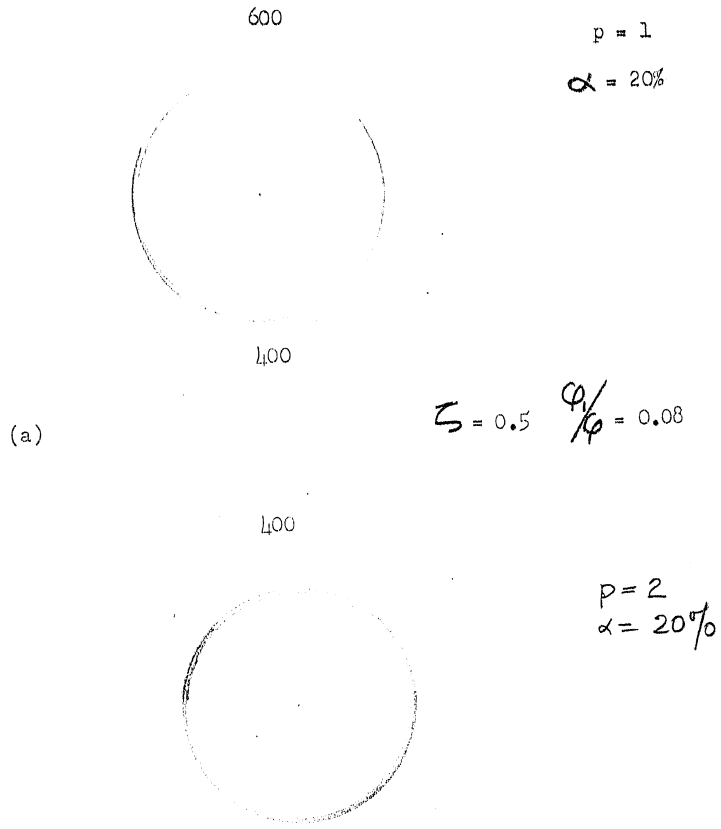

Figure 7.43

and tangential oscillatory processes, or higher order oscillations. These terms can hardly be called satisfactory, but we are using them since they are universally employed and there are still no particular objections against them. These two types of oscillation are connected with the manifestation of electron inertia and are externally characterized by the fact that they arise ihdependently of the presence of static negative resistance, which, as we have already shown, occurs under certain regimes in the slotted magnetron. We observe

that electronic oscillations of higher order likewise occur in the slotted magnetron.

Another type of oscillation, which is similarly observed only in slotted magnetrons, is obtained on excitation of a circuit connected to the magnetron taking place on account of the static falling characteristic. The character of the stationary movement of the electrons plays a large part in the creation of such characteristics, as we have seen; but transit time, or to put it better, the time taken by the electron to go around a single loop of its trajectory, has absolutely no significance in this connection, since it is very small in comparison with the oscillation period. This time of revolution should not, of course, be confused with the total time spent by the electron between cathode and anode, which may be very considerable, owing to the complicated nature of the trajectory. The conditions for excitation of oscillation of this type may thus be briefly formulated as follows (by analogy to section (4.1):

$$\text{Static negative resistance of magnetron} \leqslant L/RC,$$

where L, R and C are the parameters of the connected circuit; and

$$\frac{\text{travel time of electron around a loop}}{\text{oscillation period}} \approx 0.$$

This type of oscillation, to which the term "dynatronic" has very unfortunately been assigned, occurs relatively seldom in the generation of the shortest waves, but plays no small part in magnetron operation in the upper part of the decimeter bands ($\lambda >$ 25-30 cm). By virtue of the fact that the oscillatory properties of a system are determined, in the given case, by the static characteristic

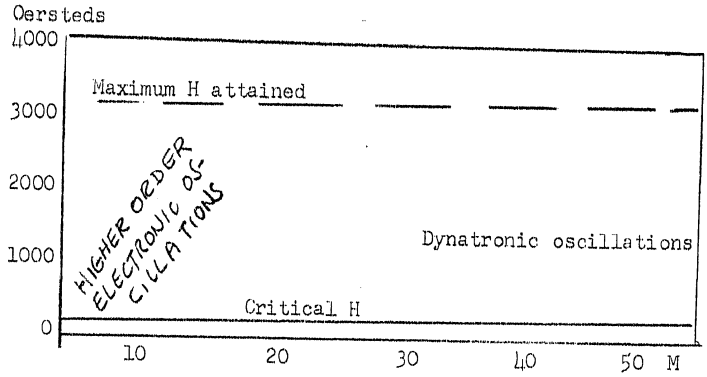

2-Segment Tube

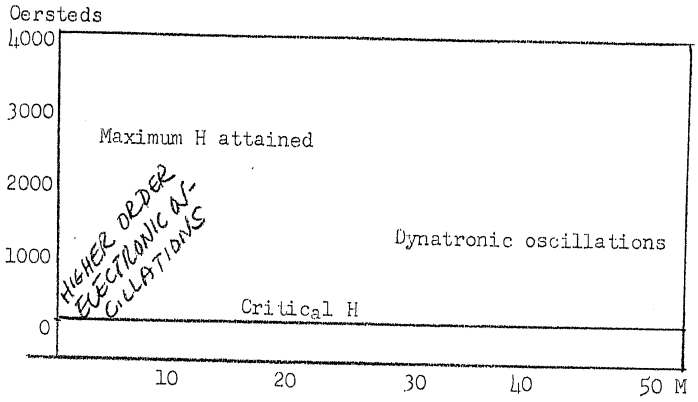

4-Segment Tube

Figure 7.44

it is possible to carry the theory of "dynatronic" oscillations to the stage of technical computation, similar to that for the ordinary oscillator tube.

The wavelength regions and regimes embraced by these oscillation types may be illustrated as follows. Figure 7.44 shows the regions of the several oscillation types for two- and four-segment magnetrons. It will be seen from these graphs that there is a

smooth transition between the region of higher-order electronic oscillations and that of dynatronic oscillations. The boundary between them is in fact essentially arbitrary, and it is of course impossible to indicate very confidently just where the oscillatory process begins to be determined by the properties of the falling static characteristic.

In light of these considerations on the regimes of higher-order electronic oscillations, it would be logical to designate such regimes as may be characterized by relatively low integers n, by their "order of oscillation"

$$n = \frac{\omega_H}{\omega} \qquad (7.50)$$

where ω_H is the frequency of first-order oscillations and ω is that observed in the given regime (unfortunately the term "higher order oscillation" which has gained currency in the literature is very inept, since it factually refers to oscillations of lower frequencies. Review and reorganization of microwave terminology would, it is thought, be most opportune).

The origin of these oscillations should apparently be intimately linked with the behavior of the same electronic "rotor", which rotates as a whole, and which we first met in section 7.1. The primitive description of the tangential oscillatory processes given in section 3.2 likewise refers to their actual mechanism, as Barkhausen's "electronic swing" does to the actual processes that occur in the electron stream in the retarding-field circuit.

While first-order oscillation is characterized by complete cylindrical symmetry, the process is observed in the case of higher-

order oscillation to be dependent on the coordinate angle θ of type sin θ (or cos θ), sin 2θ (or cos 2θ),.... sin $p\theta$ (or cos $p\theta$). This fact leads to the formation of p "waves" along the perimeter of the rotating electron cloud. What is the nature of these "waves"? Various answers may be given to this question, but all of them lead to the same quantitative characterization of the phenomenon. Brillouin [1], for instance, imagines these "waves" as the consequence of peculiar elastic deformations of the rotating electron cloud, as a result of which it represents a peculiar kind of rotor of an alternator with 2p poles when higher-order oscillations are involved. The variations in the space charge for the first four "orders" of oscillation are shown in Figure 7.45. Each type is represented by three curves, the broken line showing the position at equilibrium and the two solid lines showing the two extreme positions at a phase difference of π. The perimeter of the "electron rotor" that is changing in this manner may be symbolized by the ideas developed in Paragraph 3.2 about the motion of the electron along a cycloidal curve laid out along a circular directrix. We recall that at that time we had to satisfy the condition $E = \bar{H}\omega r$ (formula 3.47) to obtain constant angular velocity of rotation, and to assume, without any visible ground, that the distribution of the space charge is uniform throughout the interelectrode space of the magnetron. It was subsequently shown by us however (Paragraph 7.1) that the presence of this kind of uniform space charge is very characteristic for the magnetron and allows us to explain the mechanism of first-order oscillations. By confining ourselves to a uniform space-charge cloud, rotating along the perimeter of a curve that satisfies the conditions of Paragraph 3.2, and taking due account of the condition of synchronization (3.52),

the same formula given by Posthumous for the wavelength of the excited oscillations may obviously be obtained:

$$\lambda = \frac{94^2 r_a H}{p U_a} \qquad (7.51)$$

The operation of two- and four-segment magnetrons at $H > H_k$ is shown in Figure 7.46, together with a representation of a possible deformation of the space charge. To sustain oscillation, a "hillock" must be formed in the space charge opposite the negative segment, while a "pitlet" is similarly formed opposite the positive segment (according to the general conditions of the transfer of oscillatory energy to a circuit by the electron stream).

The oscillatory process in the multisegment magnetron, which is connected with the displacement of "pitlets" and "hillocks", may also be described somewhat differently if we consider the "waves" that we brought in above -- and which are formed along the perimeter of the rotating stream -- to be longitudinal waves that require no deformation, in a radial direction, of the cylindrical, rotating cloud. In this case the principle part im sustaining oscillation is played by the tangential component of the current formed by the rotating space charge in the zone of action of the intersegment alternating potentials. This tangential or ring component, as shown by experiment, has a considerable magnitude (over an ampere at total filament emission of the order of a few milliamperes). The process of energetic interaction between the ring current and the intersegment fields is localized, in the given case, in the ring zone that adjoins the anode surface. When we picture to ourselves the instantaneous pattern of the ring current in the multi-electrode mag-

netron, as shown in Figure 5.23, we see that the electron stream is retarded opposite the slots a_1, a_2,...., while it is accelerated opposite the slots b_1, b_2,..., in both cases by the inter-segment electrostatic fields acting there. It is therefore necessary, in order to sustain oscillation in a circuit connected to a group of segments, that the density of the ring current opposite the a slots shall exceed that opposite the b slots. This may occur in consequence of some process analogous to the phase focusing in a linear electron stream which was treated in section 5.6. Without making it our object here to consider the details of the behavior of the ring current and of the mechanism by which condensations are formed in it, let us imagine that mechanism to consist of density-maxima and minima disposed in a certain definite sequence along the perimeter, as indicated by the broken lines in Figure 5.23, while taking into consideration the above-mentioned conditions for sustained oscillation. Assuming in the simplest case a sinu-

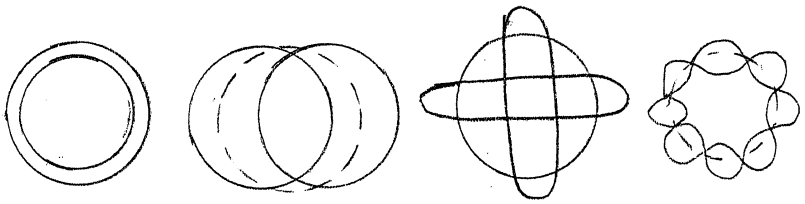

n = 0 n = 1 n = 2 n = 3

Figure 7.45

soidal distribution of the tangential-current density along the perimeter, its value may be represented in the form

$$j_t = j_o + j_1 \sin mx \qquad (7.52)$$

(it is not difficult to see that sin mx is equivalent to Brillouin's sin pθ), where x varies from some arbitrary origin to $2\pi r_a$, while $m = 2\pi / \lambda$. λ' here represents the "density-wavelength". The existence of these density waves, and allowance

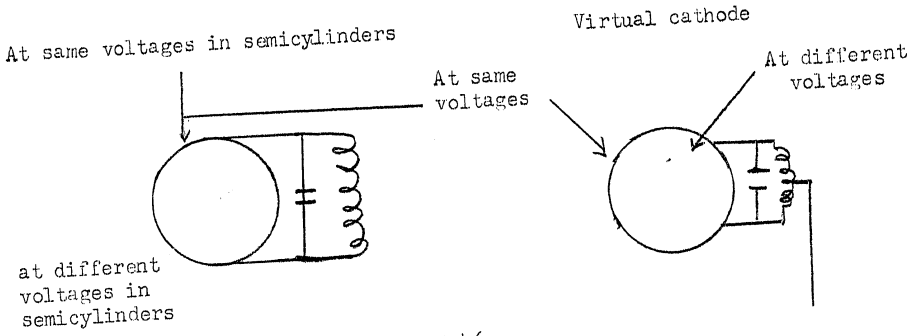

Figure 7.46

for them, is obviously equivalent to the introduction of the periodic functions of the coordinate angle (sin pθ or cos pθ, cf. supra). The condition of operation "in phase", or that of synchronization, will obviously be

$$\lambda' p = 2\pi r_a \quad \text{or} \quad \lambda' = \frac{2\pi r_a}{p}$$

which leads to the following expression for j_t:

$$j_t = j_o + j_1 \sin \frac{p}{r_a} x. \qquad (7.53)$$

On the ground that the velocity of displacement of a focal condensation in the electron stream is equal to the velocity with which focusing electron-packets move (cf. section 5.3), and deeming the mean tangential velocity determined by the well-known relation $v_t = E/H$ (assuming an inconsiderable amplitude for the vari-

ation of the current density j_1), we may conclude that

$$\lambda' = v_t T = \frac{2\pi v_t}{\omega} = \frac{2\pi E}{\omega H} \qquad (7.54)$$

where T and ω are the period and angular frequency of the oscillations generated. Taking account of the expression for λ', we obtain

$$\omega = \frac{E}{H} \cdot \frac{p}{r_a}$$

which leads to the expression

$$\lambda = \frac{2\pi c r_a H}{Ep}$$

for the wavelength of the oscillations generated.

By virtue of the uniform space charge we have adopted, we now take for E the well known expression $E = \frac{2U_a r}{r_a^2}$, and again obtain the Posthumous formula:

$$\lambda = \frac{942 r_a^2 H}{pU_a} \qquad (7.55)$$

This formula plays as important a role for the regimes of tangential oscillation of the magnetron as the Barkhausen formula does for the retarding-field system and the klystron, or the Okabe formula for the radial oscillations of the magnetron. The Posthumous formula may be obtained by various methods, of which we have demonstrated the two simplest and physically clearest here and in section 3.2.

The proportional relationship between λ and H obtained in this case does not in the least contradict the inversely proportional

relationship between the same quantities which obtains in the regime of first-order oscillations. This is not hard to understand if we analyze the role of H as the flight factor in both cases. In the case of first-order oscillations, an increase in H reduces the transit time spent by the electron on its path, and consequently shortens the oscillation period. In the case of higher-order oscillations, however, an increase in H leads to a reduction in the rotational velocity of the electronic rotor, which is naturally accompanied by an increase in the oscillation period. It must nevertheless be remarked that the most general relation of the Barkhausen type for all "flight" processes is satisfied both for radial and tangential oscillations. And in fact:

(a) First-order oscillations (radial):

$$\lambda = \frac{C_0}{H}, \text{ and since } H = H_k = \frac{6.72}{r_a} U_a, \text{ then}$$

$$\lambda\sqrt{U_a} = \frac{C_0 r_a}{6.72} = \text{const.}$$

(b) Higher-order oscillations (tangential). For them usually

$$H > H_k; \text{ let us put } H = kH_k, \text{ where } k > 1.$$

Then

$$H = kH_k = k\,\frac{6.72}{r_a} U_a^{1/2}$$

or, by substitution in the Posthumous formula, we get

$$\lambda\sqrt{U_a} = \frac{6330}{p} r_a k = \text{const.} \qquad (7.56)$$

A very vivid idead of the relation between U_a, H and under the regime of higher-order electronic oscillations may be obtained if we

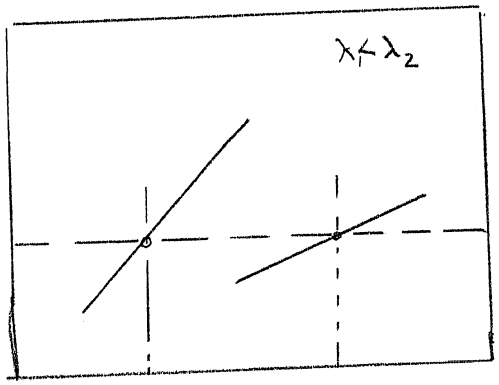

Figure 7.47

transform formula (7.56) into

$$U_a = \frac{1}{\lambda^2 G} k^2, \qquad (7.57)$$

where $G = p^2/(6330)^2 r_a^2$ is the geometric constant of the tube in question. "Straight iso-wave lines" may be plotted in coordinates U_a, k^2, on the basis of equation (7.57) and these may then be used for computation. A verification of relation (7.57), undertaken by the author and I. I. Vasserman [8] yielded the following results. If expression (7.57) is presented in the form

$$\frac{\lambda}{k} = \frac{1}{\sqrt{U_a G}} \qquad (7.58)$$

the ratio λ/k might be expected to remain constant at constant U_a and varying H for the given tube. Experiment showed that as k increases, the ratio λ/k asymptotically approaches the value calculated from formula (7.58). We illustrate this by Figure 7.48,

which gives the curves $\frac{1}{\sqrt{G}} = f(k)$ for 8-, 16- and 20-segment magnetrons, at constant U_a of 500 volts and identical r_a = 0.5 cm, alongside of the calculated values (the straight broken lines).

The analysis presented assumes that any two contiguous segments at any given instant shall be opposite in sign to each other. This condition is automatically satisfied where the anode

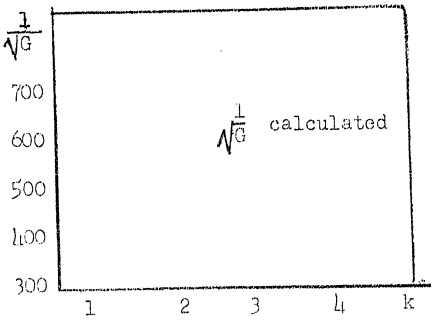

Figure 7.48

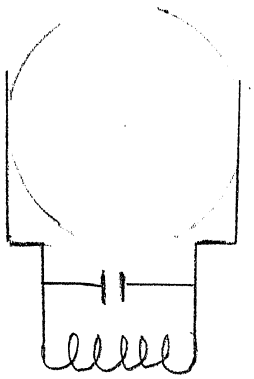

Figure 7.49

of the magnetron has an even number of segments, of which half are connected to one pole of the oscillatory circuit and half to the other, as shown, e.g. by Figure 7.49 for the four-segment magnetron. The distribution of potential along the perimeter of the anode may

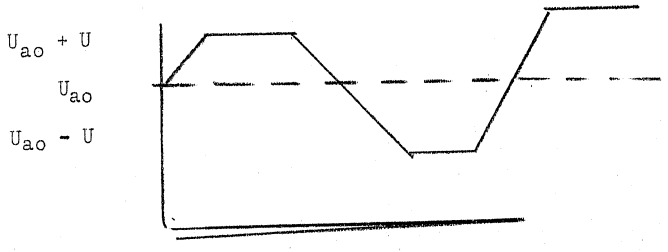

Figure 7.50

here be represented by the broken line of Figure 7.50, and may be expanded into a Fourier series; by virtue of symmetry, this series will have only uneven harmonics. This means that oscillations corresponding to the types ±p; ±3p; ±5p;..... may be excited in a magnetron with 2p anodes. The first of these terms is the most important, and by confininf ourselves to it we may write the following expression for the distribution of potential along the anode perimeter:

$$U_a = U_o + CU_1 \sin p\theta e^{i\omega t} \qquad (7.59)$$

where U_o is the DC voltage and $\pm U_1 e^{i\omega t}$ is the oscillatory voltage on the anodes. The coefficient C is obtained from the expansion of the curve in Figure 7.50 into a Fourier series. It is near unity as is shown by its calculation for the extreme cases:

Very narrow anodes: $\alpha = 0; \quad \beta = \frac{\pi}{n}; \quad C = \frac{8}{\pi^2} \approx 0.8$

Very broad anodes: $\alpha = \frac{\pi}{n}; \quad \beta = 0; \quad C = \frac{4}{\pi} \approx 1.28$

The second term of formula (7.59) may be expanded into two imaginary exponential series, which are symbolized by the decomposition of an oscillation, into two opposing rotations, which is usual in many common practices for many theories. This gives us the following expression for the distribution of alternating potential along the anode perimeter:

$$CU_1 \sin p\theta e^{i \quad t} = \frac{CU_1}{2i} [e^{i(\omega t + n\theta)} - e^{i(\omega t - n\theta)}] \qquad (7.60)$$

The same amplitude of the alternating anode voltage corresponds to both rotations, but the density of currents $I_{(n)}$ and $I_{(-n)}$ are different. It follows from this that the magnetron may be represented as a system of two parallel impedances $Z_{(+n)}$ and $Z_{(-n)}$;

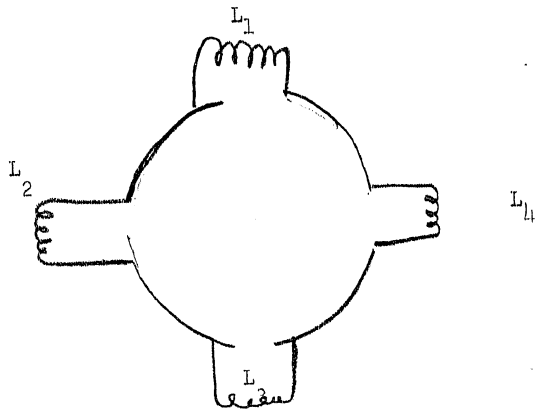

Figure 7.51

the resultant impedance Z is represented

$$\frac{1}{Z} = \frac{1}{Z_{(+n)}} + \frac{1}{Z_{(-n)}} \qquad (7.61)$$

The situation is a little different in the case of the multi-circuit ("multicell") magnetron schematically represented in Figure 7.51. Here all the circuits L_1C_1 .... L_4C_4 are identical and one anode may lead its neighbor by a phase angle less than π . The single condition is that the first anode (arbitrary assignment!) must be reached again, after a full revolution, at phase 0 or $2n\pi$. In other words, in a magnetron with 2p anodes, the total phase shift after a full revolution must be 2π , 4π ,..., $2p\pi$, which gives us the following possible values for the phase angle between two adjoining anodes:

$$\Phi = \frac{\pi}{p}, \quad \frac{2\pi}{p}, \quad \cdots \quad \frac{p-1}{p}\pi, \pi$$

In view of this the arrangement represented in Figure 7.51 may be operated at frequencies corresponding to the types of os-

cillation:

$$n' = 1, 2, \ldots, p - 1, p.$$

It is hard to provide for the origination of any one type of oscillation in this case, and to eliminate the possibility of spontaneous establishment of a regime, the anode segments in the multicell magnetrons in technical use are consecutively connected by short conductors, thus imposing compulsory phasing on all anodes and circuits participating in the process.

However, the multi-circuit schematic of Figure 7.51 affords greater opportunities than the single-circuit design of Figure 7.49. And, in fact, a magnetron with an odd number of anodes may be excited under a multi-circuit system and polyphase UHF alternating currents may, accordingly, be obtained, as has been shown experimentally in a number of projects [21, 22]. Oscillations take place in polyphase systems under the same conditions as in the ordinary slotted magnetrons. The proportionality between and H also holds, and only the synchronization conditions must naturally be formulated somewhat differently on account of the off number of segments.

7.5 "DYNATRONIC" OSCILLATIONS IN THE MAGNETRON

The meaning of the term "dynatronic" oscillations has already been explained in the foregoing discussion. We once again emphasize the very inept choice of this term. but unfortunately the other terms suggested for this phenomenon likewise leave too much to be wished. Thus, the oscillations obtained, on account of the static falling characteristic, in a circuit connected to a slotted magnetron, are sometimes called "circuit oscillations". However, the so-called

"electronic oscillations" are excited in a certain circuit only when there is a peculiar mechanism of energy exchange between that circuit and the electron stream. The term "convection oscillations" has also been proposed. While we recognize that this term corresponds somewhat better to reality (the "convection" of electrons between anodes), we still prefer the term "dynatronic" oscillations, since it contains a direct reference to the presence of a static falling characteristic. It is in essence the latter that determines this phenomenon.

First of all we must note that no sharp line of demarcation can be drawn between the electronic oscillations we have been describing and the "dynatronic". If we plot the excitability of a slotted magnetron, characterized, for instance, by the maximum attenuation of the circuit at which oscillation still occurs, as a function of the order n of the oscillations, we get the graph of Figure 7.52. It will be seen from it that for small values of n (n 1 - 4) the frequency of theoscillations excited corresponds with fair precision to the integer values of n. Discrete excitation regions correspond to n = 1 and n = 2, but these are not observed in all tubes. For two-segment magnetrons there is no region n = 2, while this region appears only seldom in four-segment tubes. The region n = 3 can occur only for tubes with a number of segments divisible by 3. For values of n = 4, as may be seen from Figure 7.52, excitability is obtained for any value of n, which need not be a whole number. At this point the negative resistance produced by the motion of electrons through fields approximating stationary ones, commences to operate. The flight factors rededе to the secondary level of importance, while the static falling characteristic

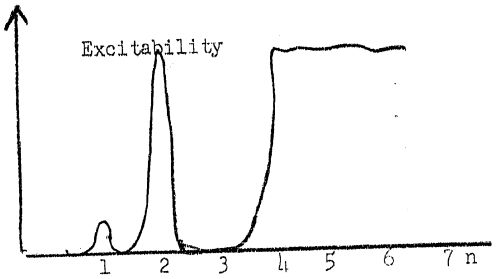

Figure 7.52

may be considered the fundamental element that determines the oscillatory possibility of the system. The continuous transition from the higher-order electronic oscillations to the "dynatronic" may also be very clearly illustrated by Figure 7.53, which shows the curves of equal efficiency on the plane λ - H for four-segment tubes. The following circumstance, which is easy to see from this diagram, is very characteristic and worthy of attention: the maximum values of the efficiency correspond to those regions of higher order electronic oscillation that have low values of n, and then, after a certain "gap", the efficiency once more increases on account of the purely "dynatronic" oscillations.

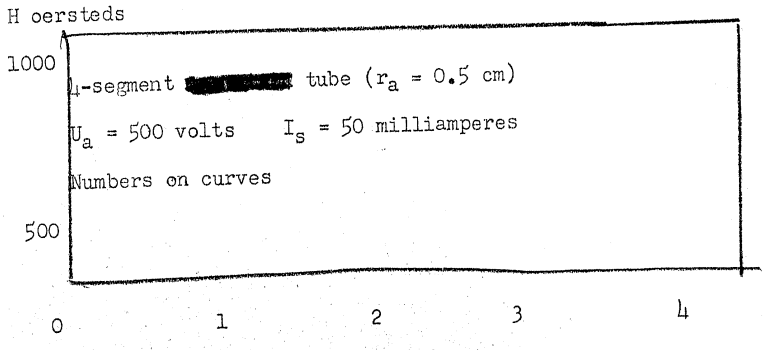

Figure 7.3

This fact indicates: (a) the very favorable action of the synchronization of alternating field and electron-motion that manifests itself at relatively low values of n; and (b) the existence of a certain "transitional" regime, under which the synchronizing factors still play a part, but where the main course of excitation is apparently the static negative resistance.

Study of the dynatronic oscillations reduces to two basic stages:

(a) proof of the existence of static negative resistance and calculation of the static characteristics; and (b) analysis of the oscillations of a system with an assigned characteristic. The problem posed by the first stage may be considered solved, on the basis of the data in section 7.3, for the material therein set forth proves the presence of the static falling characteristic in certain slotted-magnetron regimes. In the second stage, the ordinary radiotechnical methods may be applied, which allow us to bring the theory of "dynatronic" oscillations almost up to the theory of ordinary oscillator tubes.

Let us now set up the differential equations of oscillation for the magnetron oscillator for which the skeleton diagram and operating circuit are given in Figure 7.54 [23]. We denote the currents in the branches of the circuit by I_1 and I_2, and the currents in the segments of the anode by i_1 and i_2; and may write the following conditions:

$$I_1 = -C\frac{dU}{dt} - i_1$$
$$I_2 = -C\frac{dU}{dt} + i_2 \qquad (7.62)$$

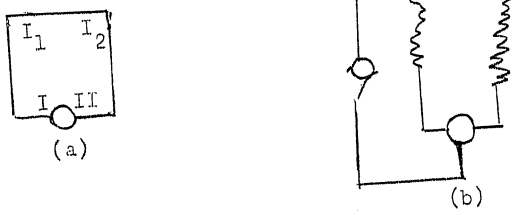

Figure 7.54

Here C is the total capacity of the circuit, including the intersegment capacity, and U is the intersegment potential difference. If L_1, R_1 and L_2, R_2 are the values of the inductance and active resistance of the respective branches of the circuit, then obviously

$$U = R_1 I_1 + L_1 \frac{dI_1}{dt} + R_2 I_2 + L_2 \frac{dI_2}{dt} \qquad (7.63)$$

Substituting the values of I_1 and I_2 from (7.62), and assuming, by virtue of the symmetry of the circuit diagram, that $R_1 = R_2 = R/2$, and that $L_1 = L_2 = L/2$, we obtain the following equation:

$$\frac{d^2U}{dt^2} + \frac{R}{L} \frac{dU}{dt} + \frac{6l}{LC} U + \frac{R}{2LC}(i_1 - i_2) + \frac{1}{2C} \frac{d(i_1 - i_2)}{dt} = 0. \qquad (7.64)$$

The question of the condition for the self-excitation of the system may be solved if we only know how $(i_1 - i_2)$ and U are interrelated, i.e. if we know the equation of the diversity characteristic of the magnetron. Slutskin [23] has proposed the following third-degree equation for the two-segment magnetron:

$$i_1 - i_2 = \frac{-3}{2} \cdot \frac{I_m}{U_m} U + \frac{1}{2} (I_m/U_m)U^3 \qquad (7.65)$$

which reproduces fairly well the characteristics that have been experimentally observed. Here I_m and U_m are the maxima of the diversity current and potential difference U between the segments. Denoting the mean value of the slope of the diversity characteristic by $S = I_m/U_m$, and making use of the equation of the characteristic, we may transform equation (7.64) and find the condition for self-excitation of the circuit in the form:

$$\frac{R}{L} - \frac{3}{4} \frac{S}{C} \leqslant 0 \qquad (7.66)$$

or, since $\frac{L}{RC} = Z$, then

$$S \geqslant \frac{4}{3} \cdot \frac{1}{z}$$

Since the value of S is directly connected with that of the negative resistance $\bar{R}$ in the magnetron: $S = 1/R$ the value of $\bar{R}$ must therefore satisfy the condition

$$\bar{R} \leqslant \frac{3}{4} z. \qquad (7.67)$$

If the intersegment potential difference $U = U_o \cos \quad t$, then the oscillatory power is expressed as follows:

$$P_{osc} = \frac{3}{8} \frac{I_m}{U_m} U_o - \frac{3}{32} \frac{I_m}{U_m^3} U_o^4 \qquad (7.68)$$

In the case of the regime being established it is equal to the power consumed by the circuit

$$P_k = \frac{U_o^2}{2Z}.$$

Whence we may find the amplitude of the oscillation established:

$$U_o = 2U_m \sqrt{1 - \frac{U_m}{\frac{3}{4} I_m Z}} \qquad (7.69)$$

At the same time the efficiency may be expressed as

$$\eta = \frac{1}{3} \frac{U_m I_m}{U_a I_a} \qquad (7.70)$$

I_a here represents the mean value of the emission current when the system is oscillating. The value of U_m must be selected by changing the magnetic field, as illustrated by Figure 7.55, where the straight broken line defines by its slope the mean negative resistance of a magnetron oscillating under the optimum regime.

But the characteristic expressed by the third-degree equation of (7.65) gives a description of the phenomena only in first approximation. The next approximation is given by a fifth-degree equation of form

$$i_1 - i_2 = aU + bU^3 + cU^5,$$

which in expanded form may be represented as

$$i_1 - i_2 = S_o U - (2S_o U_m + \frac{5}{2} I_m) \frac{U^3}{U_m^3} + (\frac{3}{2} I_m + S_o U_m) \frac{U^5}{U_m^5} \qquad (7.71)$$

where S_o is the transconductance of the characteristic at the origin of coordinates. For $H > H_k$, when the falling sector of the characteristic commences at a certain finite ΔU (cf. section 7.3), we may set $S_o = 0$ and bring (7.71) to take the form

$$i_1 - i_2 = \frac{-5}{2} I_m \frac{U^3}{U_m^3} + \frac{3}{2} I_m \frac{U^5}{U_m^5} \qquad (7.72)$$

which reproduces the actual course of the diversity characteristic for $H > H_k$ better than the third-degree equation. The introduction of fifth degree terms into the equation of the characteristic is also dictated by the need for taking account of the phenomenon of elongation observed in two- and four-segment magnetrons when the oscillation regime varies smoothly. If S_o , the value of the transconductance S_o of the diversity characteristic at the origin of coordinates is employed, we obtain a condition for self-excitation that does not depend on the shape of the characteristic:

$$S_o \frac{2}{Z} \qquad (7.73)$$

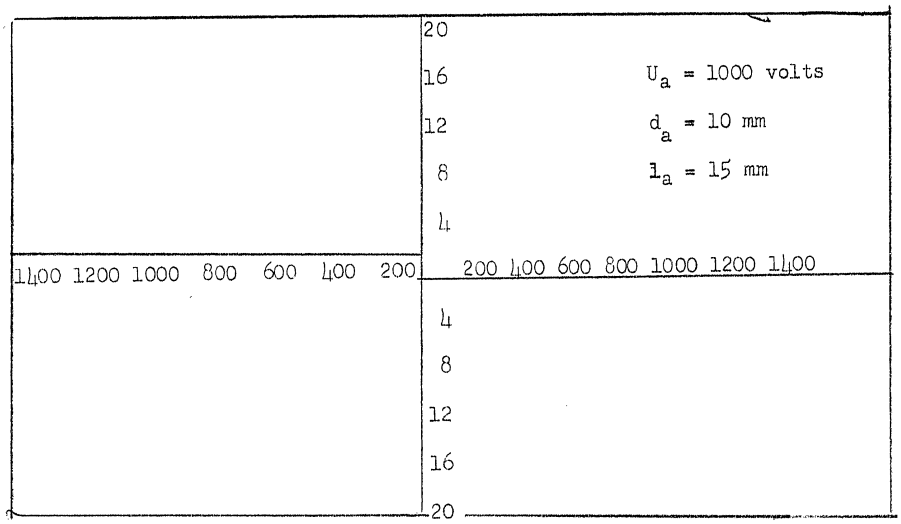

Figure 7.55

The magnitudes of the amplitude established, the optimum amplitude, the oscillatory power and the efficiency for a magnetron described by a fifth-degree characteristic are expressed as follows:

$$U_o = U_m\sqrt{1 \pm \sqrt{1 - \frac{32}{15}\frac{U_m}{I_m Z}}}$$

(± denotes the existence of two stable values for the amplitude)

$$U_{opt} = \sqrt{\frac{6}{5}}\, U_{m_{opt}} = \frac{9}{20}\sqrt{\frac{6}{5}}\; I_m Z$$

$$P_{osc_{max}} = 0.27\, I_m U_{m_{opt}} \qquad (7.74)$$

$$\eta = 0.27\,\frac{I_m U_m}{I_a U_a}\,.$$

Thus, a magnetron operating under a "dynatronic oscillation" regime and manifesting static negative resistance is in many ways similar to the ordinary oscillator tube, and all that has been worked out for the study of the latter may be fully utilized for the former. Further development of this theme would lead us outside the scope of the present exposition. On questions concerning calculations for the magnetron oscillator and various technical details, the reader is referred to Chapter 6 of my book Decimeter and Centimeter Waves, 1939.

7.6 THE "ASYMMETRIC REGIME OF THE MAGNETRON

In taking static characteristics of the magnetron we must contend with parasitic [dikiy] oscillations, which sometimes show up in the most unexpected regimes, for instance at $H \approx 4H_k$ and $\Delta U \lesssim (0.5 - 0.8)U_a$. Over a number of years the so-called "asymmetric" regime of magnetrons of various types has been systematically studied in our laboratory. This term must be taken to denote the operation of a magnetron at constant potential difference ΔU_o applied between the segments. In addition to U_a, H and I_{em}, which are the ordinary parameters of the regime, ΔU_o is here introduced as a

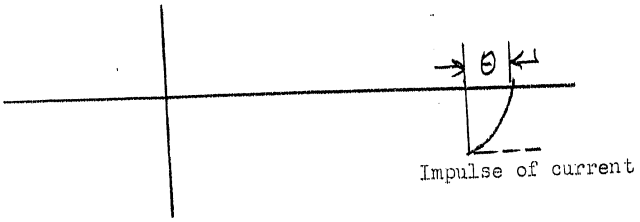

Figure 7.56

new parameter that characterizes the electrostatic asymmetry of the system. The role of this parameter may, to a certain extent, be compared to that of the constant grid displacement in the ordinary oscillator tube. Recalling Figures 7.24 and 7.25, which showed the analogy between the schematics of the magnetron and the ordinary oscillator tube, we may get some idea of the action of the factor of electrostatic asymmetry ΔU from Figure 7.56. From looking at the static characteristics of the magnetron for $H \quad H_k$ we may expect the excitation of oscillation to be facilitated when symmetry is disturbed by displacing the point of rest by U_o, along the axis of abscissae with respect to the various parts of the characteristic. If the characteristic is conceived as consisting in first approximation of rectilinear segments, the operation of the magnetron may be represented as follows (Figure 7.56). Here $\Delta U = \Delta U_o + \Delta U_m \cos \omega t$; $\Delta U_1 = \Delta U_o + \Delta U_m \cos \theta$, where θ plays the part of the angle of cut-off. If the characteristic of the type plotted is symmetric with respect to the origin of coordinates, then under the condition $2 \Delta U_o = \Delta U_m (1 - \cos\theta)$, the oscillator operation becomes one-sided, impulses of Δi of only a single sigh occur in the circuit. This may have certain advantages with respect to increasing the simplicity of the relations obtained and making the ordinary theory of the triode oscillator more applicable. The role of ΔU_o as one of the factors of the regime has been studied for all regions of magnetron oscillation

by the author and A. N. Sus [26], N. I. Grachev [24, 27], and Vasserman [28]. The following is a brief resume of their results:

(a) The role of electrostatic asymmetry under regimes of "dynatronic" oscillations (applicable to two- and four-segment magnetrons) was for fairly long waves ($\lambda \gtrsim 200$ cm) so as to exclude the influence of the slight factors as far as possible. The typical pattern corresponding to considerable values of H ($H \lessapprox 2H_k$) is shown in Figure 7.57, in which are plotted the branches of the diversity characteristic Δi and the curve of oscillation intensity in relation to ΔU_o, the constant potential difference between the segments. The latter discloses several oscillation re-

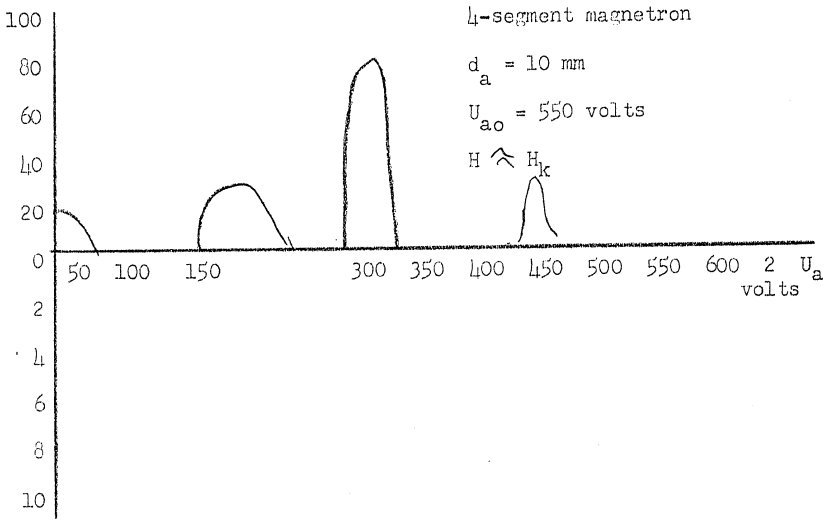

Figure 7.57

gions: the most intense oscillation corresponds to Region A, which is located along the steepest part of the slope of the falling characteristic. Region B, which has a somewhat lesser intensity

lies along the gently sloping part of the characteristic, and, finally, Region C corresponds to the ordinary "symmetrical" oscillations of the magnetron, which are observed when uniform potential is applied to all segments of the anode. At other values of H, of course, there is a different pattern of distribution for the Regions. A typical "working diagram for the asymmetric regime" and pattern of the oscillation regions on the plane H -ΔU_o has the form shown in Figure 7.58. In all oscillation regions the wavelength is determined by the circuit.

Thus, the introduction of electrostatic asymmetry into the regions of dynatronic oscillations may lead under certain conditions to increasing the oscillatory power of the magnetron.

(b) Under the regime of first-order electronic oscillations the role of the factor ΔU_o was studied in magnetron tubes with 2 to 20 segments, and the following conclusions drawn. Variation of ΔU_o within the range 0 - U_a has no practical effect on the frequency generated, but at $\Delta U_o \approx 0.6 U_{ao}$ leads to the formation of a fairly diffuse maximum of intensity, which is well expressed in the four-segment tube. With increasing number of segments this maximum is displaced towards higher values of ΔU_o and becomes still more diffuse. Electrostatic asymmetry apparently acts as a peculiar selective factor for first-order electronic oscillations, and its action may be likened to that of the additional field of lateral plates [bokovaya plastina].

(c) Under the regime of higher-order electronic oscillations, variations of ΔU_o (0 - U_{ao}) and H (H_k - $5H_k$) are obtained in a very broad region when the oscillating circuit is appropriately

tuned. If H is held constant, then with only the factor ΔU_o varying, wavelength is observed to remain almost constant (with some tendency to fall as ΔU_o increases), but the maximum of oscillation intensity is more sharply expressed than in the preceding case, and is reached in the region where ΔU_o varies from 0.2 U_{ao} to 0.6 U_{ao} [29].

In summing up this chapter, the following must be noted. The magnetron is one of the most important devices for generating microwaves. It unquestionably takes the first place in obtaining the shortest waves of the highest power. But the physical processes that accompany magnetron operation, especially under the regime of higher-order electronic oscillations, are very complex. While the magnetron in general obeys the fundamental relations that characterize the operation of generators of electronic oscillations (within the meaning of the definition given in the Introduction) it also manifests peculiarities which hamper considerably the investigation by the general methods that yield a relatively simple

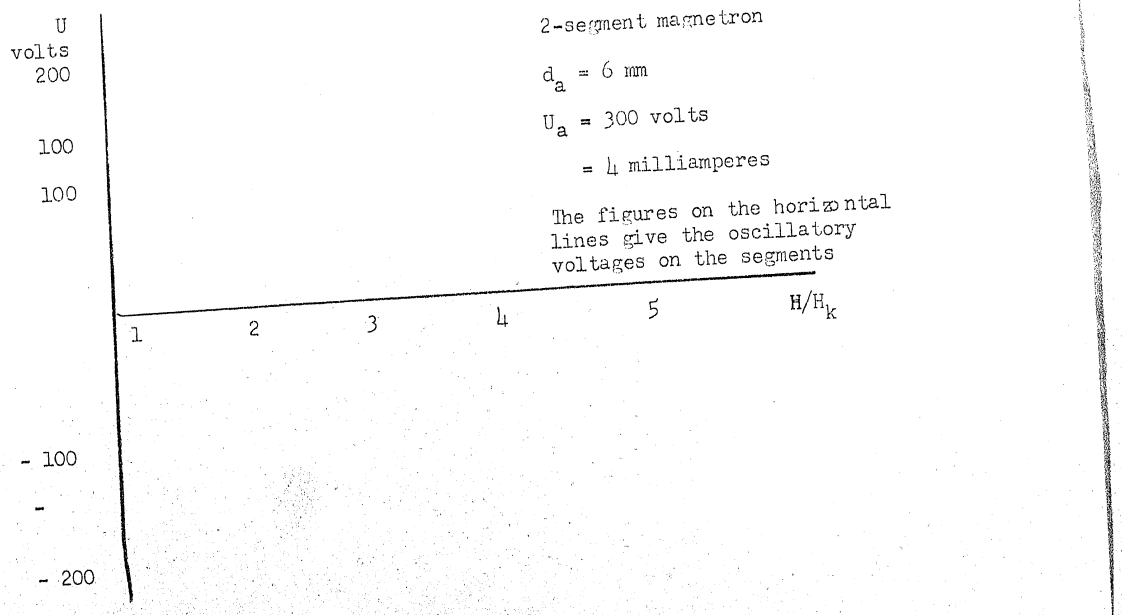

physical pattern for the operation of other oscillators. These peculiarities are connected with the presence of the magnetic field as the element that determines electron dynamics, with the resultant great diversity of the processes of excitation and the significant part played by the space charge. In connection with this a considerable number of basic factors still remain almost untouched on the physical side. Such factors include, for example, the actual character of the electron-trajectories (especially the question of the existence of outgoing and returning electron streams at $H \gtrsim H_k$), the "tangential mechanism" of higher-order electronic oscillations, the magnitude and role of the ring-currents, and other details of the processes in the magnetron. The systematic and consistent application of the general theory of the dynamic control of electron streams to the tangential processes in the magnetron has apparently been able to deepen considerably our knowledge of them.

BIBLIOGRAPHY OF CHAPTER VII

1. Teoriya magnetrona (Theory of Magnetron). Collection edited by V. C. Lukoshkov, Sov. Radio, 1946.
2. S. Ya. Braude, ZhTF, X, 217, 1940.
3. S. Ya. Braude, ZhTF, XV, 107, 1945.
4. G. Kilgore, PIRE, 24, 1140, 1936.
5. M. Grechowa, Techn. Phys. USSR, II, No 6, 1935; III, No 7, 1936.
6. V. I. Kalinin, Detsimetrovyye i Tsentimetrovyye Volny (Decimeter and Centimeter Waves), Chapter V, 1939.
7. Blewett and Ramo, Phys. Rev. 57, 635, 1940. Journal Appl. Phys. 12, 856, 1941.
8. V. Kalinin and I. Vasserman, IAN, ser. fiz. X, 1946, No 1.
9. V. Lukoshkov, IEST, No 10, 46, 1940.
10. A. Nedzvetskiy, Sborn. trud. KISI (collection of transactions of KISI) I, 45, 1941.
11. J. Groszkowski and S. Ryiko, Hochfrequenz u. Elektriz. 47, 55, 1936.
12. Lukoshkov and IL'inski, ZhTF, VIII, 1996, 1938.
13. Katsman and Rubina, ZhTF, IX, 499, 1939.
14. O. Groos, Einfuhr. Theorie u. Techn. d. Dezimeterwellen, 1937.
15. H. Zuhrt, Hochfreq. u. Elektriz. 48, 91, 1936.
16. Grinberg and Lukoshkov, ZhTF, V, 1426, 1935.
17. I. Brenev, ZhTF, VI, 302, 1936; VI, 637, 1936.
18. J. Groszkowski, PIRE 24, 1041, 1936.
19. V. I. Kalinin and G. M. Gershteyn, DAN, LXI, No 4, 1946.
20. G. M. Gershteyn, Radiotekhnika, No 2, 1946
21. I. Muller, Hochfreq, u. Elektriz. 48, 155, 1936.
22. N. A. Kuz'min, Vozbuzhdeniye elektron. koleb. ultravisokikh chastot v mnogofaznikh sistemakh (The Excitation of Electronic Oscillations of Ultra-High Frequency in Polyphase

Systems). Dissertation, SGY, SGU, 1941.

23. A. Slutskin, ZhTF, V, 632, 1935.

24. N. E. Grachev, Uch. Zap. KPI, 7, 89, 1943.

25. A. Chernets, ZhTF, VI, vyp. 7, 1941.

26. V. Kalinin and A. Sus, Elektrosvyaz (Electric Communications) No 5, 1939.

27. N. I. Grachev, Issledovaniye asimmetrichnogo rezhima rasreznogo magnetrona (An Investigation into Asymmetric Regime of the Slotted Magnetron), Dissertation, SGU, 1941.

28. I. I. Vasserman, Issledovaniye mnogosegmentnokh magnetronov (An Investigation of Multisegment Magnetrons), Dissertation, SGU-LGU, 1944-1945.

29. V. Kalinin, ZhTF, XVI, vyp 5, 1946, 577-592.